

Electronic Thesis and Dissertation Repository

10-17-2019 11:00 AM

Strains in Regions of the Brain Modelled from Female Youth Soccer Players Performing Purposeful Headers in Season

Wayne Allison
The University of Western Ontario

Supervisor
James, Dickey
The University of Western Ontario

Graduate Program in Kinesiology
A thesis submitted in partial fulfillment of the requirements for the degree in Master of Science
© Wayne Allison 2019

Follow this and additional works at: <https://ir.lib.uwo.ca/etd>



Part of the [Biomechanics Commons](#)

Recommended Citation

Allison, Wayne, "Strains in Regions of the Brain Modelled from Female Youth Soccer Players Performing Purposeful Headers in Season" (2019). *Electronic Thesis and Dissertation Repository*. 6740.
<https://ir.lib.uwo.ca/etd/6740>

This Dissertation/Thesis is brought to you for free and open access by Scholarship@Western. It has been accepted for inclusion in Electronic Thesis and Dissertation Repository by an authorized administrator of Scholarship@Western. For more information, please contact wlsadmin@uwo.ca.

Abstract

Soccer is the world's most popular sport, and intentional heading of the ball is exclusive to it. Head impacts in youth players are riskier than adults as their brains are developing. Finite element models can quantify parameters, like strains within regions of the brain, that are otherwise difficult to assess. The purpose of this study was to examine the relationship between head kinematics collected by wireless head impact sensors and brain strains in regions of interest related to concussion. As well, we assessed head impact strains in regions of interest related to concussion for headers from various game scenarios. In conclusion, the findings of this thesis showed that maximum principal strain increases in relation to linear acceleration and angular velocity, though the strength of relationships ranged between the kinematic parameters and the different regions of the brain. As well, game scenarios are important to the magnitude of max strains.

Keywords

Finite Element Modelling, Concussion, Maximum Principal Strain, Youth, Soccer, Angular Velocity, Linear Acceleration, Corpus Callosum, Thalamus, Brain Stem, Game Scenario, Headers, Head Impacts

Summary for Lay Audience

Soccer is one of the world's most popular sports, and has over 265 million people worldwide play. Heading the ball is exclusive to the game and helps players to maintain control and keep the ball from the opposing team. In younger soccer players, exposure to head impacts is potentially more at risk for a concussion as the brain is continuing to grow and develop until the age of 30. Tracking the forces with wireless accelerometers acting on the head during play offers insight into what is occurring in head impacts. To follow up, computer models calculate a plethora of equations designed with precise anatomical accuracy to recreate impacts based on this data. This creates a simulation of the head impact that offers more information that is available from the sensors alone such as internal forces acting on the brain.

The purpose of this study was to examine the relationship in forces imposed on the head collected by wireless head impact sensors to strains of the brain occurring in various regions of interest that are related to concussion. As well, to assess the various game scenarios head impact strains in regions of interest related to concussion. This thesis observed increased levels of max principal strain at specific regions of interest in the brain compared to a single concussion case resulting from purposeful headers. As well, linear accelerations and angular velocities were both related to increased strains occurring in the brain following head impacts. In conclusion, the findings of this thesis showed increased maximum principal strain in relation to linear acceleration and angular velocity. As well, game scenarios are important to the magnitude of max strains.

Based on the findings of this study it is shown that FEM models can provide important insights into the risks associated with purposeful headers, and that ROIs related to concussion warrant further examination.

Co-Authorship Statement

The work described in this thesis was performed by the author as well as contributions from the following:

All field research and data collection of the head impacts was collected and shared by Alexandra Harris.

All finite element modelling simulations were performed with the assistance of Kewei Bian.

Acknowledgments

To my supervisor, Dr. Jim Dickey. You have taught me more than I ever imagined during this experience. Thank you for indulging me to let my mind run wild in pursuit of scientific experience. As well, thank you for being a teacher and mentor of the highest quality.

To Kewei Bian, thank you for aiding me throughout this process and always making yourself available whenever I had questions.

To Dr. Haojie Mao, thank you for helping to set the foundation for this thesis with your unique expertise and for offering clarification whenever I was unsure.

To Alexandra Harriss, thank you for sharing with me your field research and helping to guide me through my questions as they arose.

To Jeff Brooks, thank you for always assisting me whenever I had questions or needed help.

To my lab mates in the Joint Biomechanics lab, thank you for making every lab meeting an event and for always being willing to help and offer insight.

To my loving wife Megan and daughter Aubrey, thank you both for always being supportive and understanding. You both are the largest influences in everything I do and I am so grateful to have you both. Your love and support mean everything and keeps me going!

To my loving family, thank you for indulging me to talk about what I do and listening. All of your love and support keeps me grounded.

Table of Contents

Abstract.....	i
Summary for Lay Audience.....	ii
Co-Authorship Statement.....	iii
Acknowledgments.....	iv
Table of Contents.....	v
List of Tables.....	ix
List of Figures.....	xi
Chapter 1.....	1
1 Introduction.....	1
1.1 Prevalence of Head Injury in Sports.....	1
1.2 Occurrence of Concussion in Soccer.....	2
1.3 Anatomical Regions of Interest Relating to mTBI.....	4
1.4 Finite Element Modelling of the Head.....	6
Chapter 2.....	10
2 Purpose Statement and Hypothesis.....	10
2.1 Purpose Statement.....	10
Chapter 3.....	11
3 Methods.....	11
3.1 Participants.....	11
3.2 Instrumentation.....	11
3.3 Video Analysis Protocol.....	14
3.4 Impact Selection.....	16
3.4.1 Concussion Case.....	16
3.5 Data Analysis.....	16

3.6	Finite Element Modelling	17
3.7	Post Simulation Analysis	18
3.8	Statistical Analysis.....	20
4	Results	22
4.1	Head impacts.....	22
4.2	Game Scenarios	24
4.3	Relationship between the peak linear acceleration and maximum principal strain	26
4.3.1	Relationship between the peak linear acceleration and MPS in the corpus callosum	26
4.3.2	Relationship between the peak linear acceleration and MPS in the thalamus	31
4.3.3	Relationship between the peak linear acceleration and MPS in the brain stem.....	36
4.4	Relationship between Angular Velocity and Maximum Principal Strain.....	39
4.4.1	Relationship between the peak angular velocity and MPS in the corpus callosum	39
4.4.2	Relationship between the peak angular velocity and MPS in the thalamus	44
4.4.3	Relationship between the peak angular velocity and MPS in the brain stem	49
4.5	Maximum Principal Strains for Headers from Different Game Scenarios	52
4.5.1	Corpus Callosum.....	52
4.5.2	Thalamus.....	54
4.5.3	Brain Stem	56
5	Discussion	58
5.1	Head Impacts	58
5.2	Game scenarios	60
5.3	Correlations between head impact kinematics and APMPS.....	61

5.4 Association between APMPS and concussion.....	62
5.5 Limitations	66
5.5.1 Wireless Sensors	66
5.5.2 Maximum Principal Strain.....	66
5.5.3 Collection Periods and Type of Head Impacts	67
5.5.4 The Single Concussion Case.....	67
5.5.5 Number of Variables Assessed.....	68
5.5.6 Size of Regions of Interest.....	68
6 Conclusion	69
References.....	70
Appendices.....	85
Appendix A	85
Appendix B	86
Appendix C	96
Appendix D.....	107
Curriculum Vitae	108

List of Tables

Table 1 Classification of the contexts for the different types of purposeful headers.	15
Table 2. Brain regions, and the regions of interest within each of the brain regions, that were examined during the simulations.	20
Table 3. Number, and percentage, of head impacts in the sample pool (n=110) and the full data set (n=434), broken down by player age.	22
Table 4. Description of the number of players in the youth soccer data set and number of players that were included in the simulations, for each of the three age groups.	23
Table 5. Number, and percentages, of headers in each of the game scenarios, in the sample pool (n=110) and the total pool (n=434), as well as the average and standard deviation of the peak linear accelerations and angular velocities recorded using the wireless devices. The maximum linear acceleration and angular acceleration represent the individual header with the largest values recorded in that game scenario. All values are based on the sample pool of 110 head impacts.....	25
Table 6. Correlations (r) and coefficients of determination (r^2) between APMPS and linear acceleration for each of the ROIs in the CC.	26
Table 7. Correlations (r) and coefficients of determination (r^2) between APMPS and linear acceleration for each of the ROIs in the thalamus.	31
Table 8. Correlations (r) and coefficients of determination (r^2) between APMPS and linear acceleration for each of the ROIs in the brain stem.....	36
Table 9. Correlations (r) and coefficients of determination (r^2) between APMPS and angular velocity for each of the ROIs in the CC.....	39
Table 10. Correlations (r) and coefficients of determination (r^2) between APMPS and angular velocity for each of the ROIs in the thalamus.....	44

Table 11. Correlations (r) and coefficients of determination (r^2) between APMPS and angular velocity for each of the ROIs in the brain stem 49

List of Figures

Figure 1. Headband on player during game, device was secured in compartment below nuchal line, outlined in yellow for improved visibility..... 12

Figure 2. Size of the GFT2 device size compared to a quarter. The coordinate system of the devices is shown in red with +Z directed downwards. Adapted from Campbell (2016) 13

Figure 3. Example of time series plot illustrating the Maximum Principal Strain versus time. The peak strains of each of the nine elements from the 3x3 layout are highlighted in red. The average peak maximum principal strain (APMPS) was calculated as the average of these nine peaks. 19

Figure 4. Relationship between the peak linear acceleration and resulting maximum principal strain (MPS) in the genu of the corpus callosum on the left side. The dotted line represents the line of best fit. The single concussion case is represented with the red circle..... 27

Figure 5. Relationship between the peak linear acceleration and resulting maximum principal strain (MPS) in the genu of the corpus callosum on the right side. The dotted line represents the line of best fit. The single concussion case is represented with the red circle..... 28

Figure 6. Relationship between the peak linear acceleration and resulting maximum principal strain (MPS) in the splenium of the corpus callosum on the left side. The dotted line represents the line of best fit. The single concussion case is represented with the red circle. 29

Figure 7. Relationship between the peak linear acceleration and resulting maximum principal strain (MPS) in the splenium of the corpus callosum on the right side. The dotted line represents the line of best fit. The single concussion case is represented with the red circle. 30

Figure 8. Relationship between the peak linear acceleration and resulting maximum principal strain (MPS) in the posterior thalamus on the left side. The dotted line represents the line of best fit. The single concussion case is represented with the red circle. 32

Figure 9. Relationship between the peak linear acceleration and resulting maximum principal strain (MPS) in the posterior thalamus on the right side. The dotted line represents the line of best fit. The single concussion case is represented with the red circle. 33

Figure 10. Relationship between the peak linear acceleration and resulting maximum principal strain (MPS) in the anterior thalamus on the left side. The dotted line represents the line of best fit. The single concussion case is represented with the red circle..... 34

Figure 11. Relationship between the peak linear acceleration and resulting maximum principal strain (MPS) in the anterior thalamus on the right side. The dotted line represents the line of best fit. The single concussion case is represented with the red circle..... 35

Figure 12. Relationship between the peak linear acceleration and resulting maximum principal strain (MPS) in the lateral posterior brain stem on the left side. The dotted line represents the line of best fit. The single concussion case is represented with the red circle. 37

Figure 13. Relationship between the peak linear acceleration and resulting maximum principal strain (MPS) in the lateral posterior brain stem on the right side. The dotted line represents the line of best fit. The single concussion case is represented with the red circle. 38

Figure 14. Relationship between the peak angular velocity and resulting maximum principal strain (MPS) in the genu of the corpus callosum on the left side. The dotted line represents the line of best fit. The single concussion case is represented with the red circle..... 40

Figure 15. Relationship between the peak angular velocity and resulting maximum principal strain (MPS) in the genu of the corpus callosum on the right side. The dotted line represents the line of best fit. The single concussion case is represented with the red circle..... 41

Figure 16. Relationship between the peak angular velocity and resulting maximum principal strain (MPS) in the splenium of the corpus callosum on the left side. The dotted line represents the line of best fit. The single concussion case is represented with the red circle. 42

Figure 17. Relationship between the peak angular velocity and resulting maximum principal strain (MPS) in the splenium of the corpus callosum on the right side. The dotted line represents the line of best fit. The single concussion case is represented with the red circle. 43

Figure 18. Relationship between the peak angular velocity and resulting maximum principal strain (MPS) in the posterior thalamus on the left side. The dotted line represents the line of best fit. The single concussion case is represented with the red circle. 45

Figure 19. Relationship between the peak angular velocity and resulting maximum principal strain (MPS) in the posterior thalamus on the right side. The dotted line represents the line of best fit. The single concussion case is represented with the red circle. 46

Figure 20. Relationship between the peak angular velocity and resulting maximum principal strain (MPS) in the anterior thalamus on the left side. The dotted line represents the line of best fit. The single concussion case is represented with the red circle. 47

Figure 21. Relationship between the peak angular velocity and resulting maximum principal strain (MPS) in the anterior thalamus on the right side. The dotted line represents the line of best fit. The single concussion case is represented with the red circle. 48

Figure 22. Relationship between the peak angular velocity and resulting maximum principal strain (MPS) in the lateral posterior brain stem on the left side. The dotted line represents the line of best fit. The single concussion case is represented with the red circle. 50

Figure 23. Relationship between the peak angular velocity and resulting maximum principal strain (MPS) in the lateral posterior brain stem on the right side. The dotted line represents the line of best fit. The single concussion case is represented with the red circle. 51

Figure 24. Box and whisker plots showing the average peak of the maximum principal strain (MPS) at the ROIs of the corpus callosum for the various game scenarios. Boxes represent the 25th – 75th quartile ranges and line within each box represents the median. The whiskers represent the 95% CI. The dotted line represents the MPS for the single concussion case.... 53

Figure 25. Box and whisker plots showing the average peak of the maximum principal strain (MPS) at the ROIs of the thalamus for the various game scenarios. Boxes represent the 25th – 75th quartile ranges and line within each box represents the median. The whiskers represent the 95% CI. The dotted line represents the MPS for the single concussion case. 55

Figure 26. Box and whisker plots showing the average peak of the maximum principal strain (MPS) at the ROIs of the lateral posterior brain stem for the various game scenarios. Boxes represent the 25th – 75th quartile ranges and line within each box represents the median. The whiskers represent the 95% CI. The dotted line represents the MPS for the single concussion case..... 57

Chapter 1

1 Introduction

The increased prevalence of concussions, and the growing awareness of long-term consequences of head impacts, has motivated research into the nature of the underlying brain injury. In relation to sport, a concussion has been defined as a brain injury that is representative of a traumatic brain injury with complex pathophysiological changes affecting the brain induced by biomechanical forces (McCrory et al., 2017). A sport related concussion (SRC) can occur in any sport as a result of incidental contact in both non-contact [e.g. competitive cheer] or contact sports [e.g. football] (Bretzin et al., 2018). SRC may produce rapid onset of symptoms which in turn can have neurological functional changes as well as neuropathological changes (McCrory et al., 2017). In National College Athletic Association (NCAA) Division I football players increased rates of incidence for concussion were observed following the 2010 NCAA concussion management policy (Houck et al., 2016). The rate of incidence preceding this policy increased from 0.99 to 1.39 concussions per 1000 athletic exposures (practice and games) following its implementation (Houck et al., 2016). In a position statement (2019) by the American Medical Society for Sports Medicine analyzing 19 different studies involving both contact and non-contact sports, there were 6,293 concussions were recorded in 239,564 athletes. These athletes ranged from grade 8 to college, across all 19 studies it was found that an average of 2.6% were concussed per season (Harmon et al., 2019).

1.1 Prevalence of Head Injury in Sports

Over a 15 year (1988-2004) time period across 16 sports with male and female representation, data was collected on injury and exposures. The three sports with the highest rates of concussion per 1000 athletic exposures were women's ice hockey (0.91), men's spring football (0.54), and women's soccer (0.41) (Hootman, Dick, & Agel, 2007).

More recently in NCAA athletes spanning from 2009 – 2014, men’s wrestling (10.92), men’s ice hockey (7.91), woman’s ice hockey (7.50), men’s football (6.71), women’s soccer (6.31), had the five highest rates of concussion per 1,000 athletic exposures across 25 different sports (Zuckerman et al., 2015). The Michigan High School Athletic Association consisting of nearly 200,000 student athletes in the 2015-2016 school year, found that the three highest sports with SRC were football (46.1%), women’s basketball (11.6%), and women’s soccer (9.5%) (Bretzin et al., 2018). Football, hockey and soccer are consistently identified as sports with the greatest rate of SRC (Bretzin et al., 2018; Fraser, Grooms, Guskiewicz, & Kerr, 2017; Houck et al., 2016; Wasserman, Kerr, Zuckerman, & Covassin, 2016; Zuckerman et al., 2015). Of these, women’s soccer stands out due to the high incidence of concussions. This is because incidental contact between players may result in fouls effectively discouraging players from initiating contact (NCAA 2018). This is a contrast to other non-contact sports, such as basketball, which do not penalize this type of accidental contact.

1.2 Occurrence of Concussion in Soccer

Soccer is the world’s most popular sport with over 265 million players playing professionally and as amateurs (Rodrigues, Lasmar, & Caramelli, 2016). In soccer, intentional head contact with the ball when it is airborne is a part of the game. The number of headers that players perform depends on their position and play style. In amateur soccer players, the number of moderate to severe central nervous system (CNS) symptoms correlated with the number of head impacts received during the previous two weeks (Stewart et al., 2017). Furthermore, players who experienced one unintentional impact in the preceding two weeks had nearly three times the risk of experiencing concussive CNS symptoms compared to players that only experienced intentional head impact (Stewart et al., 2017). This further illustrates that exposure to a lifetime of head impacts may have negative ramifications that can begin during adolescence for athletes.

Over seven million high school student athletes and 480,000 playing in NCAA each academic year (NCAA, 2019). Approximately 388,000 and 27,600 women participate in women's Soccer in high school and the NCAA respectively, encompassing two different age ranges in adolescents and young adults (NCAA, 2019). The NCAA started reporting all injury and exposure data in 1982 with the end goal of injury prevention. Between 2009-2014 concussions comprised 6.2% of all the injuries reported by the NCAA-ISP (Zuckerman et al., 2015). Women's soccer contributed the third highest number of SRC (8.1%) behind only Football (36.1%) and men's Ice Hockey (13.4%) per the NCAA-ISP between 2009-2014 (Wasserman et al., 2016). Women's soccer had 6.31 concussions per 10,000 athletic exposures (Zuckerman et al., 2015). Ball contact accounts for 33.8% SRC in women's soccer (Zuckerman et al., 2015). Ball contact resulting in SRC is the second largest (27.3%) ball related injury in women's soccer behind only sprains (38.5%) across 11 different sports from data gathered from the NCASS-ISP (Fraser et al., 2017). To address concussions in sport, addressing head impacts in adolescents is necessary as this is an important time in development, as well when the foundation for sports is created (Alosco & Stern, 2019; Lebel, Walker, Leemans, Phillips, & Beaulieu, 2008).

Various factors can make an athlete vulnerable to concussion. For example, in terms of athletes age, younger athletes are more vulnerable as they are in a crucial stage of cognitive development (Lebel et al., 2008). Head to body mass ratios, growth spurts and changing body mass all affect the momentum of young athletes, in conjunction with the developing brain (Buzzini & Guskiewicz, 2006). An online injury surveillance reporting system showed rates of concussion in US high school athletes had risen over a 10 year span that ended following the 2014 season (Comstock, Currie, Pierpoint, Grubenhoff, & Fields, 2015). This matched the trend that had been observed in NCAA athletes over a similar time period coinciding with the 2010 NCAA concussion management policy (Houck et al., 2016). As well, rates of concussion due to heading have significantly increased ($p = 0.03$) amount among females over this period of time (Comstock et al., 2015). Furthermore, research has shown that the frequency of heading increases with age in soccer across different age groups (U13, U14, U15), and is

independent of position (Harriss, Johnson, Walton, & Dickey, 2019b). The neurological development and physical maturation of adolescent athletes are at a critical stages as the brain and body are both in the midst of physiological changes (Lebel et al., 2008; Lenroot & Giedd, 2006; Luders, Thompson, & Toga, 2010).

1.3 Anatomical Regions of Interest Relating to mTBI

The human brain is continuously developing from birth through adulthood (Lebel et al., 2008). In early childhood, the brain grows rapidly, approaching its peak mass (80-90%) around the age of five (Dekaban & Sadowsky, 1978). Following the brains early development, the overall growth slows down, and the brain's white matter (WM) then becomes increasingly myelinated with age, increasing connectivity (Iwasaki et al., 1997). These changes in WM may be well represented with diffuse tensor imaging (DTI) (Basser, Mattiello, & LeBihan, 1994; Le Bihan, 2003). DTI, through fractional anisotropy (FA) and mean diffusivity (MD), quantifies the diffusion of water diffusing in an region, and net displacement of water in a region respectively (Lebel et al., 2008). This is an effective method of evaluating the function of the neural networks of the brain, which can become impaired during concussion. A systematic review on imaging of youth (aged 5-18) with diagnosed mild traumatic brain injury (mTBI) revealed there was a trend that when there was a mTBI present FA values increased and MD values decreased compared to healthy controls (Schmidt et al., 2018). Increases in FA post-concussion in adolescents are believed to be associated with tissue damage associated with structural damage to the axons (Virji-Babul et al., 2013). Therefore the fiber tracts communicating information throughout the brain being susceptible during development warrant further research.

The corpus callosum (CC) is the largest white matter structure in the brain. It connects the left and right hemispheres transversely, functionally connecting to the contralateral sides within the homologous cortical regions (Kiernan & Rajakumar, 2013). The number of fibers within the CC is determined in utero, increases in myelination of the fibers with

age at the CC affects the size (Lebel et al., 2008; Luders et al., 2010). When connection is impaired, as can be seen in agenesis of the CC, there is decreased processing speed and reduced capacity for higher level thinking (Hinkley et al., 2012). CC impairment can affect behavior and development such as attention deficit hyperactivity disorder (ADHD), bipolar disorder, alien hand syndrome, and autism (van der Knaap & van der Ham, 2011). During a concussion, similar effects can be seen acutely and in conjunction with changes in FA and MD affecting white matter (Borich, Maken, Boyd, & Virji-Babul, 2013). Interestingly, this study also identified that these changes are also correlated with declines in subjective concussion testing scores. The CC's central anatomical location and vast array of connections are important for segueing information. Forces reaching the CC transmit throughout via anatomical and direct neural connections .

The thalamus is one of the most important regions within the brain. This structure is responsible for receiving and transmitting sensory and motor information and is the major subcortical sensori-motor relay (Stiles & Jernigan, 2010). The thalamus receives information from sensory receptors such as the retina and relays it to the sensorimotor regions of the neocortex (Stiles & Jernigan, 2010). The thalamus is located within the forebrain, adjacent to the CC. It has numerous neural connections to the CC, including the spinothalamic tract (Kiernan & Rajakumar, 2013). Thalamic volume and processing speeds in cognitive tests are impaired in professional fighters who are exposed to a large magnitude of head impacts (Bernick et al., 2015). Retired NFL players had decreased thalamus volume compared to healthy age matched controls that negatively correlated with age began playing tackle football and total number of years playing (Schultz et al., 2018). As well, in individuals who have suffered mild traumatic brain injuries had higher resting thalamic state network activation and decreased symmetry between sides compared to healthy controls (Tang et al., 2011). The developments in the thalamus that can be observed either following a professional athletes careers or from sustaining a concussion show the thalamus' importance in being assessed further in head impacts.

The brain stem is an integral region of the brain that connects the brain to the periphery of the body. It is composed of the midbrain, pons and medulla oblongata (Kiernan &

Rajakumar, 2013). As well, the reticular activating system (RAS) of the brain stem linked with loss of consciousness (LOC) is functionally and anatomically connecting the thalamus to the brain stem (Delano-Wood et al., 2015). Diffuse axonal injuries (DAI) are one of the most common causes of deformation based injuries of the brain stem and other white matter regions with direction potentially playing a significant role in concussion (Giordano & Kleiven, 2014; Sidaros et al., 2008). Damage to the brain stem is regarded to be incompatible with life due to the fundamental functions that it performs, such as respiration and cardiovascular regulation (Bernat et al., 2010; Giordano & Kleiven, 2014). Impacts in football to the front of the head produce higher strains in the brain stem (Beckwith et al., 2018). As well, frontal oblique impacts to the head had the greatest MPS in the brain stem in simulations that incorporated a football helmet in the Global Human Body Models Consortium (GHBMC) head model (Darling, Muthuswamy, & Rajan, 2016).

1.4 Finite Element Modelling of the Head

Modeling studies have predicted the strains in different regions of the brain during simulations of the head impacts that led to concussions or were non-injuries (Beckwith et al., 2018; Miller, Pinkerton, et al., 2019; Patton, McIntosh, & Kleiven, 2013; Pellman, Viano, Tucker, Casson, Waeckerle, 2003). The maximum principal strain (MPS) in several regions is larger in concussion impacts vs non injury impacts in computer simulations of Australian football and rugby players (Patton et al., 2013). The CC, thalamus, and WM experienced the greatest relative differences in MPS in concussion cases vs non injuries and MPS was the best predictor of injury severity in impacts in these regions (Patton et al., 2013). As well, MPS was seen to be highest in the cerebrum followed by the brain stem and CC relative to other regions within the brain in simulations of helmeted impacts using two different finite element models (FEM) (Beckwith et al., 2018). Furthermore, oblique frontal impacts simulations experienced nearly double MPS than coronal impacts for simulated impacts at the brain stem (Darling et al., 2016).

FEM of the head allows a unique way of evaluating the mechanics of the head that can enable robust analysis of the entire complex system (Mao, Gao, Cao, Genthikatti, & Yang, 2013). FEM creates an estimation of an event through a computational simulation. For a head model this is possible through the recreation of the human anatomy to replicate a scenario based on data input. Both video recordings and head-mounted impact sensors yield data that can be used as boundaries for simulation (Campbell et al., 2016; Cortes et al., 2017; Mao et al., 2013; Pellman et al., 2003). FEM uses mathematical equations to calculate the stresses and strains for the model components based on the model's geometry, material properties and boundary conditions (Mao et al., 2013). The simulation responses, such as maximum principal strains, can be validated against human cadavers (Mao et al., 2013).

At its core, the concept of FEM solves complicated problems by finding solutions to subsets of problems. FEM is suited to situations that have several material compositions and complex loading conditions (e.g. impact sports) (Yang, 2018). This is refined when applying physiological and anatomical features to establish appropriate responses to the simulated impact (Yang, 2018). The number of elements affects the resolution of a simulation, more elements allows more information at the cost of computational processing power and time. The analysis in FEM is based on a continuum, the solution of one element's equations affecting the adjacent elements, resulting in a ripple effect (Yang, 2018).

The mesh for FEM consists geometrical polygons comprised of nodes connected by elements. The nodes represent specific locations in the model and are the links that connect and compose the overall structure. In contrast, elements represent information regarding the material properties of the mesh such that displacement of the nodes results in stresses and strains in the elements. It is imperative that the nodes are situated to capture the relevant anatomy in sufficient detail, and that the elements adequately describe the mechanical properties of the structures. The number of elements changes the

precision of the overall structure, increasing accordingly. Albeit this comes at the cost of time requiring vast quantities of computational processing power.

Computer simulations of football impacts using a head and neck model found that early onset muscle activation resulted in decreased rotational velocities (Jin et al., 2017). As well, research has shown that neck strength is an important factor in effectively reducing the magnitude of head accelerations in deliberate use during soccer heading (Gutierrez, Conte, & Lightbourne, 2014). Several studies have used wireless sensors attached to the head to obtain information in regards to linear accelerations, angular velocities and number of impacts during athletic exposures (E. M. Hanlon & Bir, 2012; Harriss, Johnson, Walton, & Dickey, 2019a; Press & Rowson, 2017). This information may allow objective assessments of the head impacts when used providing valuable information when a concussion occurs. FEM allows for the recreation of head impacts offering insight regarding the immediate impact using data collected from sensors.

The internal responses of the brain to external perturbations, such as accelerations are of interest because of their influence regarding concussions. Internally the brain undergoes deformations due to accelerations caused by head impacts resulting in a domino effect that penetrates the layers of the brain that may be observed in simulations (King, Yang, Zhang, Hardy, & Viano, 2003; Kleiven, 2007; Patton et al., 2013; Patton, McIntosh, & Kleiven, 2015; Rowson & Duma, 2013; Takhounts, Craig, Moorhouse, McFadden, & Hasija, 2013; Vianno & Lovsund, 1999). Several studies have attempted to predict concussion outcomes from linear and angular accelerations measured with wireless sensors (Rowson & Duma, 2013; Zhang, Yang, & King, 2004). Studies that have used FEM to look at the internal effects following a simulated impact have found that strain, strain rate, as well as products of strain and strain rate to be effective predictors of concussion (King et al., 2003; Kleiven, 2007; Patton et al., 2013, 2015; Takhounts et al., 2013; Zhang et al., 2004). These studies have focused on deep brain structures such as the CC, thalamus, brainstem; all of which anatomically connected (King et al., 2003; Kleiven, 2007; Patton et al., 2013, 2015; Takhounts et al., 2013; Zhang et al., 2004). The effect of excessive strain within the brain has been used as a strong predictor for mild

traumatic brain injuries (mTBI) as well as its derivatives and byproducts (King et al., 2003; Kleiven, 2007; Patton et al., 2013, 2015; Takhounts et al., 2013). MPS exceeding 0.21 at the corpus callosum may be used as a predictor for concussion at 50% probability of a concussion (50POC) (Kleiven, 2007). In contrast, an average strain rate of 84 s^{-1} with the brainstem and a product of strain and strain rate of 36 s^{-1} , was found on average in brain injuries (King et al., 2003).

Chapter 2

2 Purpose Statement and Hypothesis

2.1 Purpose Statement

There are two purposes to this study that will be addressed by analyzing the maximum principal strain in several brain regions during purposeful head impacts performed by female youth soccer players. This will be accomplished by drawing upon a set of previously recorded head kinematics from purposeful headers performed during soccer games, and recreating (simulations) them using finite element model. The first purpose was to assess the relationship between individual kinematic variables and the maximum principal strain in purposeful headers in soccer. The second purpose was to compare the maximum principal strain for the headers from different game scenarios, and to compare them to a concussion case.

Hypotheses

- 1) There will be strong relationships between linear and angular head kinematics and the resulting strains in the various regions of interest in the brain that are related to concussion
- 2) In concussions, the maximum principal strains in the various regions of interest in the brain that are related to concussion will be larger than strains during purposeful headers

Chapter 3

3 Methods

3.1 Participants

This study is based on head impact data previously collected from a convenience sample of 36 female youth soccer players from the Ontario Player Developmental League (OPDL) (Harriss et al., 2019a). The players in that study had an average age of 13.4 (SD = 0.9) years, height of 1.60 (SD = 0.10) m, and a mass of 50.6 (SD = 8.7) kg. The players participated in weekly practices and games. Kinematics from head impacts in games and practices were collected using wireless sensors; video recordings were also captured during games to characterize the game scenario such as type of purposeful header. Ethics approval was granted by the Western University's Health Science Research Ethics Board (HSREB protocol 107948). Written informed consent was obtained from players parents prior to participating in this study.

3.2 Instrumentation

Each participant in the field study (Harriss et al., 2019a) was equipped with a wireless device (GForce Tracker (GFT2), Artaflex Inc., Markham, Ontario, Canada) that was secured in a custom neoprene headband (Figure 1). The headbands were positioned below the nuchal line, which is consistent with other studies (Caccese, Lamond, Buckley, & Kaminski, 2016; Gutierrez et al., 2014). The GFT2 contains both a tri-axial linear accelerometer and a tri-axial gyroscope allowing for wireless collection of these data during head impacts (Figure 2). The impact location is calculated by the device according to the azimuth and elevation angles and then classified as front, back, left, right, top or

bottom (Campbell et al., 2016). The devices were preset to record impacts that exceeded the minimum threshold of 7 g on any axis. Pilot testing revealed that purposeful headers may result in head accelerations as low as 8 g, and accordingly the devices were set to record impacts that exceeded 7 g on any axis. This is consistent with other studies that measured collegiate women's [6 g minimum with header] and U14 youth soccer wireless head impacts [4.5 g with header and 5 g non header] (E. Hanlon & Bir, 2010; Press & Rowson, 2017).



Figure 1. Headband on player during game, device was secured in compartment below nuchal line, outlined in yellow for improved visibility

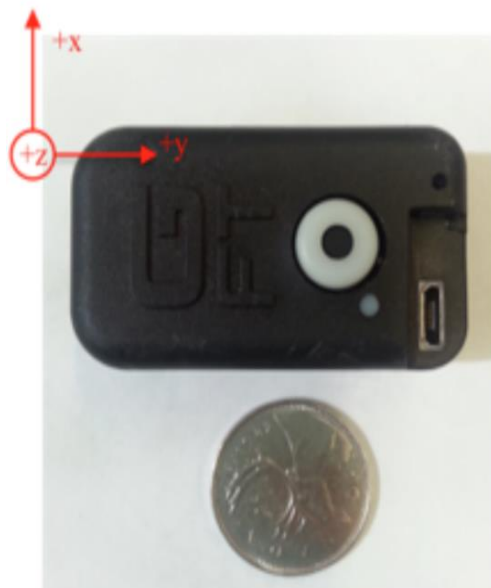


Figure 2. Size of the GFT2 device size compared to a quarter. The coordinate system of the devices is shown in red with +Z directed downwards. Adapted from Campbell (2016)

GFT2 devices recorded time stamps when head impacts exceeded the user-defined threshold and saved data for 40 ms, starting 8 ms prior, through to 32 ms following the threshold. This duration is consistent with other wireless sensors that have been used to measure head impacts in soccer (E. M. Hanlon & Bir, 2012). The tri-axial linear accelerometer signals were filtered through a 300 Hz low-pass anti-aliasing filter and sampled at 3000 Hz. The tri-axial rotational velocity signals were filtered with a low pass anti-aliasing filter and sampled at 800 Hz.

All collected data were stored on the device's on-board memory during games. Following each game, head impact data were uploaded to the GFT's internet server software through a laptop network connected by micro USB to the GFT2. The head impacts were further processed on the internet server to calculate resultant linear accelerations and rotational velocities calculated for each impact.

The impact data was downloaded from the GFT Server to match with video analysis described below. Individual player files contained a summary page that included the time stamp for each head impact, peak linear acceleration (gForce), impact location, Head Injury Criteria (HIC), resultant rotation velocity ($^{\circ}/s$), azimuth and elevation. For each impact the time series data for the linear accelerations and angular velocities were stored in files that could be downloaded. Raw data was extracted and used for further analysis.

3.3 Video Analysis Protocol

In the field study a total of 60 regular season games (20 games per team) were recorded using a Canon Vixia HD camera that mounted to a telescoping system (EVS25, Endzone Video Systems, Sealy, Texas, United States). Game video was uploaded to a video analysis software program (dba HUDL, Agile Sports Technologies Inc., Lincoln, Nebraska, United States). An appointed researcher matched each purposeful header from the video with the associated impact recorded by the GFT sensor. One rater was deemed appropriate for this analysis based on previous work (Harriss, Walton, & Dickey, 2018). The appointed researcher also categorized heading events by game scenario (Table 1).

Table 1 Classification of the contexts for the different types of purposeful headers.

Header Context	Description of purposeful headers
Pass Air	Ball was kicked into the air by a player prior to header
Drop Kick	Header performed following goalie dropping the ball from hands and kicking it prior to touching the ground within own goal crease
Deflection	Ball was deflected off another player or legal body location prior to header occurring
Throw	Header performed following a player throwing the ball in from the sideline
Corner	Header performed following a stationary kick taken from the corner of the field after the ball crossed behind the goal line by the defending team
Free Kick	Header performed following a stationary kick awarded following a foul at spot of foul by the opposing team, may be taken across active playing field
Goal Kick	Header performed following a kick taken from the six-yard box after the ball has gone over the goal line by the attacking team.

3.4 Impact Selection

All confirmed impacts identified through video analysis were compiled and ranked in descending order of peak resultant linear acceleration. As well, impacts were also ranked based on peak rotational velocity. The ranked percentiles for these variables were averaged to determine a neutral valuation of the head impacts accounting for both variables. Following this, 110 head impacts were evenly selected, representing the spectrum of head impacts. Both the maximum and minimum cases were included to ensure that the full range of verified head impacts were included. As well, the data set included one head impact that resulted in a concussion. This case was included for comparison. This concussion impact occurred during a practice.

3.4.1 Concussion Case

A single concussion case occurred in the field study, during a practice. The concussion occurred in a 14 year old player performing a crossing drill which would emulate a corner kick heading situation in game context. In terms of other head impact exposures for this player, they had 3 head impacts represented in the 110 simulated cases, and 5 head impacts within the entire field study's 434 head impacts. Details about the kinematics and MPS for the full set of impacts for this participant are presented in Appendix A.

3.5 Data Analysis

FEM simulations were driven using linear accelerations and angular velocities collected by the GFT2 Devices for the set of impacts described above. Linear acceleration values were converted from the g to mm/s^2 , and all angular velocities were converted from $^\circ/\text{s}$ to rads/s . Each simulation of an impact was based on the 40 ms time series of linear

acceleration and angular velocity data. The boundary conditions for the simulation were set based on the phenomena as described the linear acceleration and angular velocity of the head impacts.

3.6 Finite Element Modelling

The Global Human Body Models Consortium (GHBMC) head model was used for the simulations (Mao et al., 2013). The GHBMC is a highly detailed model of the head that has been validated against 35 experimental cases (Mao et al., 2013). The GHBMC model contains elements representing the skin surface, skull and facial bones, sinuses, cerebrum, cerebellum, lateral ventricles, corpus callosum, thalamus, and brainstem as well as white matter (Mao et al., 2013). This head model is independent of neck musculature and acts autonomously within the model in space based on the boundaries set prior to simulation.

There is no validated model for youths, therefore, similar to previous research (Jiang et al., 2014), the model used in the present study was scaled to represent the age of the population. The model in this study was scaled to 88% of the GHBMC head model to represent a 13 year old female's head. This was determined by using previous literature of sex volume differences reported from 6 studies (Giedd, 2004; Giedd, Raznahan, Mills, & Lenroot, 2012; Gur, 2002; Gur, et al., 1999; Hanlon & Bir, 2012; Ostby et al., 2009). This was done by scaling the model to 0.9583 of the original length, resulting in the desired volume reduction, similar to other studies (Jiang et al., 2014; Roth, Raul, & Willinger, 2008). This model contains 270, 552 elements with several variations of shell shapes. Specific details are presented in other literature (Mao et al., 2013).

The simulations were run using commercially available software LS-DYNA (Livermore Software Technology Co., Livermore, CA) using an 8-core processor. The boundary conditions of the simulations were defined according to the time series data collected by

the wireless sensors for each head impact case. In specific, the linear acceleration and angular velocity data collected for each purposeful header determined the kinematics of the center of mass of the head.

Based upon each elements stiffness and other properties, the LS-DYNA program estimates the displacement of each node throughout the mesh of the model. These deformations across the mesh are calculated on a continuum with adjacent elements. The effects are calculated across each time point, these calculations then may be quantified via further processing in LS-DYNA PrePost.

3.7 Post Simulation Analysis

Regions of interest (ROIs) (Table 2) were selected based on previous research that highlighted regions effected during mTBI with imaging techniques (Banks et al., 2016; Borich et al., 2013; Delano-Wood et al., 2015). The genu and splenium of the CC were selected as DTI imaging revealed disruptions in white matter integrity in children with concussions (Van Beek, Ghesquière, Lagae, & De Smedt, 2015). The thalamus was selected as it has vast connections throughout the brain, and makes key contributions to the integration and assimilation of sensory and motor information (Stiles & Jernigan, 2010). Thirdly, the brain stem was selected due to its involvement in motor activity (Kiernan & Rajakumar, 2013), and the observation that standing balance is often impaired in concussed athletes (Guskiewicz, Ross, & Marshall, 2001). We specifically selected the middle and inferior cerebellar peduncles on the dorsal aspect of the brain stem.

The size of each ROI was 9 elements in a 3x3 layout on the superficial surface as previously performed in FEM literature (Claeson & Barocas, 2017). This layout was done

to mitigate the volatility from individual elements. The selected ROIs were from anatomical locations within the model: the CC, thalamus, and brain stem. Each ROI was assessed on the left and right side of the brain. Within each ROI, the MPS in the elements was calculated using LS-PrePost (V2.4). Using a custom LabVIEW program, the peak MPS of each element over the time series from a ROI (Figure 3) was extracted. These values were averaged to yield a peak MPS value for the entire ROI, and has been termed the average peak maximum principal strain (APMPS).

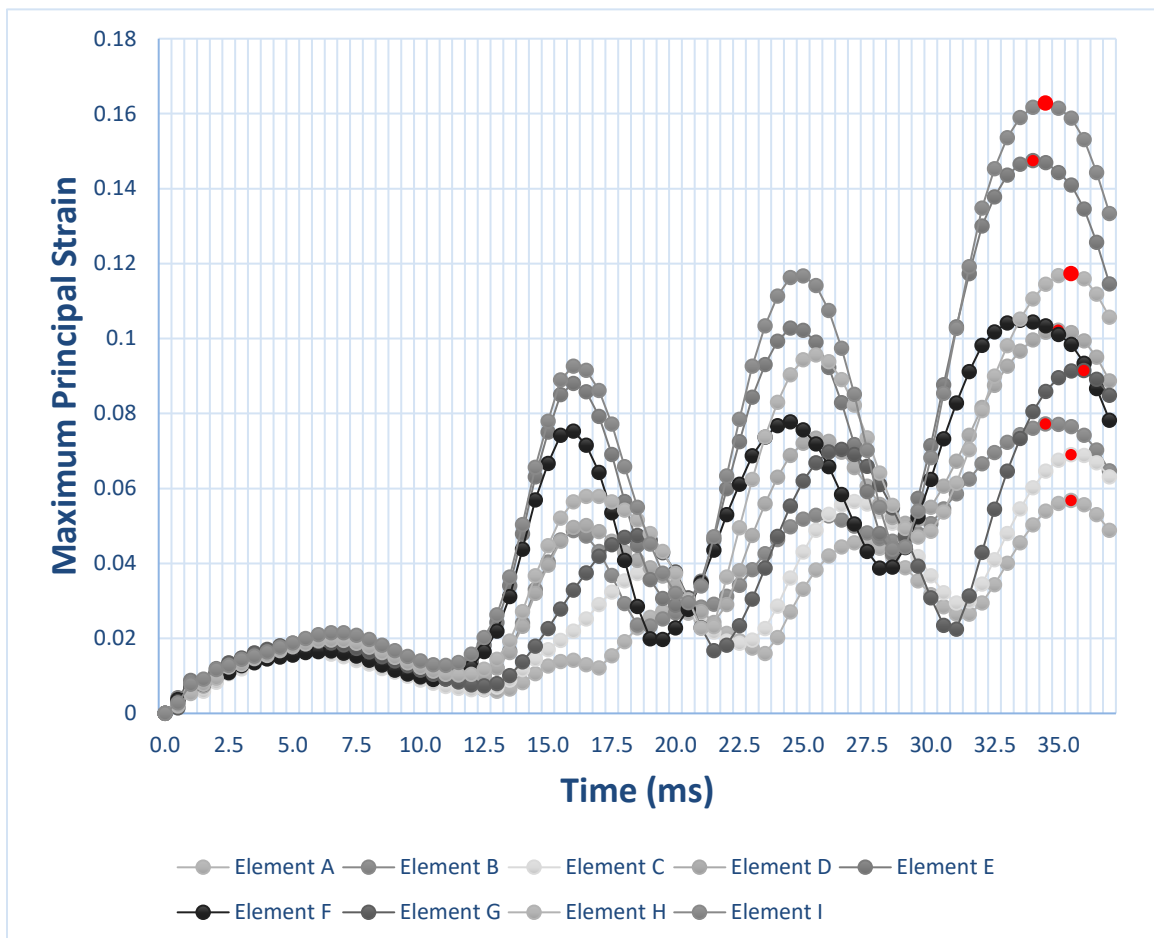


Figure 3. Example of time series plot illustrating the Maximum Principal Strain versus time. The peak strains of each of the nine elements from the 3x3 layout are highlighted in red. The average peak maximum principal strain (APMPS) was calculated as the average of these nine peaks.

Table 2. Brain regions, and the regions of interest within each of the brain regions, that were examined during the simulations.

<i>Brain Region</i>	<i>Region of Interest</i>
<i>Corpus Callosum</i>	Genu of corpus callosum
	Splenium of corpus callosum
<i>Thalamus</i>	Posterior thalamus
	Lateral anterior thalamus
<i>Brain Stem</i>	Lateral posterior brain stem (dorsal pons)

3.8 Statistical Analysis

A Chi-squared analysis was performed to evaluate whether the proportion of head impacts for the different age groups in the sample of 110 simulations were representative of the percentages in the total pool. A separate Chi-squared analysis was performed to evaluate whether the proportion of head impacts for the different game scenarios in the sample of 110 simulations were representative of the percentages in the total pool.

Analyses were performed to evaluate whether the strains in various ROIs for the headers in different game scenarios were significantly different than the single concussion case. In specific, the APMPS for the single concussion case was compared against the mean and 95% CI for various game scenarios, for each of the different ROIs. Box and whisker plots were used with the whiskers in the plots indicating the 95% CI of each game scenario. The difference in APMPS between the concussion and the headers in the various game scenarios were regarded as statistically significant if it fell outside the

bounds of the confidence intervals for the APMPS for various game scenarios (Prel, Hommel, Röhrig, & Blettner, 2009).

Pearson product-moment correlations were calculated to evaluate the strength of the relationship between average peak MPS (APMPS) and peak angular velocity, and between APMPS and peak linear acceleration within each of the ROI's. Thresholds for describing the strength of the correlation was based off of recommendations within the literature (Mukaka, 2013). The correlation coefficient (r) values in the range of 0 – 0.3 were considered negligible, 0.3 – 0.5 low, 0.5 – 0.7 moderate, 0.7 – 0.9 high, and 0.9 – 1.0 very high.

Chapter 4

4 Results

4.1 Head impacts

From a total of 60 games played in the OPDL, 434 purposeful headers were measured with wireless sensors and confirmed with video analysis. From this sample pool, 110 impacts were selected for FEM analysis. The frequency distribution of head impacts by age is presented in Table 3. The proportion of head impacts in each of the age groups in the sample used for simulations was not significantly different than the percentages in the total pool (Chi-square = 1.893, $p=0.3881$). This indicates that the distribution of impacts in the sample pool for the different age groups was representative of the total pool.

Table 3. Number, and percentage, of head impacts in the sample pool (n=110) and the full data set (n=434), broken down by player age.

<i>Age (Years)</i>	<i>Number (percentage) of head impacts in the sample pool</i>	<i>Number (percentage) of head impacts in the total pool</i>
<i>13</i>	35 (31.8%)	113 (26.0%)
<i>14</i>	47 (42.7%)	214 (49.3%)
<i>15</i>	28 (25.5%)	107 (24.7%)
<i>Total</i>	110 (100%)	434 (100%)

Not all players who performed purposeful headers were included in the set of simulated purposeful headers (Table 4). As well, it happened that the head impacts from certain players in each age group were represented at a higher frequency than other players- 3 players represented 27.3% of all simulations.

Table 4. Description of the number of players in the youth soccer data set and number of players that were included in the simulations, for each of the three age groups.

<i>Age (Years)</i>	<i>13</i>	<i>14</i>	<i>15</i>	<i>Total</i>
<i># of Players in Field Study</i>	10	16	8	34
<i># of Players Represented in FE Analysis</i>	9	10	8	27
<i># of Players Not Represented in FE Analysis</i>	1	6	0	7
<i>Mean Headers per Player in FE Analysis</i>	3.9	4.7	3.5	4.1
<i>Peak Frequency of Headers by a single player in FE Analysis</i>	8	9	11	11

4.2 Game Scenarios

The characteristics of the head impacts for the different game scenarios are listed in Table 5. The proportion of head impacts in each of the different game scenarios in the sample used for simulations was not significantly different than the percentages in the total pool (Chi-square = 3.984, $p = 0.6788$). This indicates that the distribution of impacts in the sample pool for the different game scenarios was representative of the total pool.

The most common game scenario was a pass through the air. On average corner kicks produced larger linear accelerations and angular velocities compared to other game scenarios. Both the largest linear acceleration and angular velocity occurred in passes through the air.

Head impacts resulting from a pass through the air, corner kick, goal kick and free kick all had larger average linear accelerations than the sample pool average. As well, head impacts resulting from a pass through the air, corner kick, goal kick and free kick all had larger average angular velocities than the sample pool average. On average, the corner kick had the largest linear acceleration and angular velocity compared to the other kicks. On average, the angular velocity for head impacts from corner kicks were nearly 50% higher than the next highest game scenario.

Table 5. Number, and percentages, of headers in each of the game scenarios, in the sample pool (n=110) and the total pool (n=434), as well as the average and standard deviation of the peak linear accelerations and angular velocities recorded using the wireless devices. The maximum linear acceleration and angular acceleration represent the individual header with the largest values recorded in that game scenario. All values are based on the sample pool of 110 head impacts.

<i>Game Scenario</i>	<i>Number (percent) in the sample pool</i>	<i>Number (percent) in the total pool</i>	<i>Peak resultant linear Acceleration (m/s²)</i>	<i>Peak resultant angular velocity (rads/s)</i>
<i>Pass Air</i>	47 (42.7)	179 (41.2)	198.14 ± 114.51	21.35 ± 12.02
<i>Throw</i>	39 (35.5)	129 (29.7)	159.44 ± 48.22	15.66 ± 9.28
<i>Deflection</i>	10 (9.1)	43 (9.9)	128.27 ± 53.04	12.59 ± 12.28
<i>Drop Kick</i>	7 (6.4)	35 (8.1)	162.13 ± 99.12	17.26 ± 12.35
<i>Corner</i>	3 (2.7)	12 (2.8)	288.50 ± 43.64	33.56 ± 11.03
<i>Goal Kick</i>	2 (1.8)	16 (3.7)	243.47 ± 96.21	22.39 ± 1.99
<i>Free Kick</i>	2 (1.8)	20 (4.6)	224.56 ± 158.28	18.94 ± 10.97
<i>Total</i>	110 (100)	434 (100)	179.55 ± 91.98	18.58 ± 11.46

4.3 Relationship between the peak linear acceleration and maximum principal strain

4.3.1 Relationship between the peak linear acceleration and MPS in the corpus callosum

There were low correlations between the linear acceleration and APMPS for all of the ROIs of the CC (Table 5). Between 1.1 and 2.6% of the variance in APMPS was explained by the linear acceleration, showing a low contribution. There was a weak relationship between linear acceleration and APMPS for all of the ROIs within the CC (Figures 3-6). These data are broken down by age and presented in Appendix B

Table 6. Correlations (r) and coefficients of determination (r^2) between APMPS and linear acceleration for each of the ROIs in the CC.

<i>Region of Interest</i>	<i>r</i>	<i>r²</i>
<i>Left Genu of CC</i>	0.1034	0.0107
<i>Right Genu of CC</i>	0.1597	0.0255
<i>Left Splenium of CC</i>	0.0755	0.0057
<i>Right Splenium of CC</i>	0.1281	0.0164

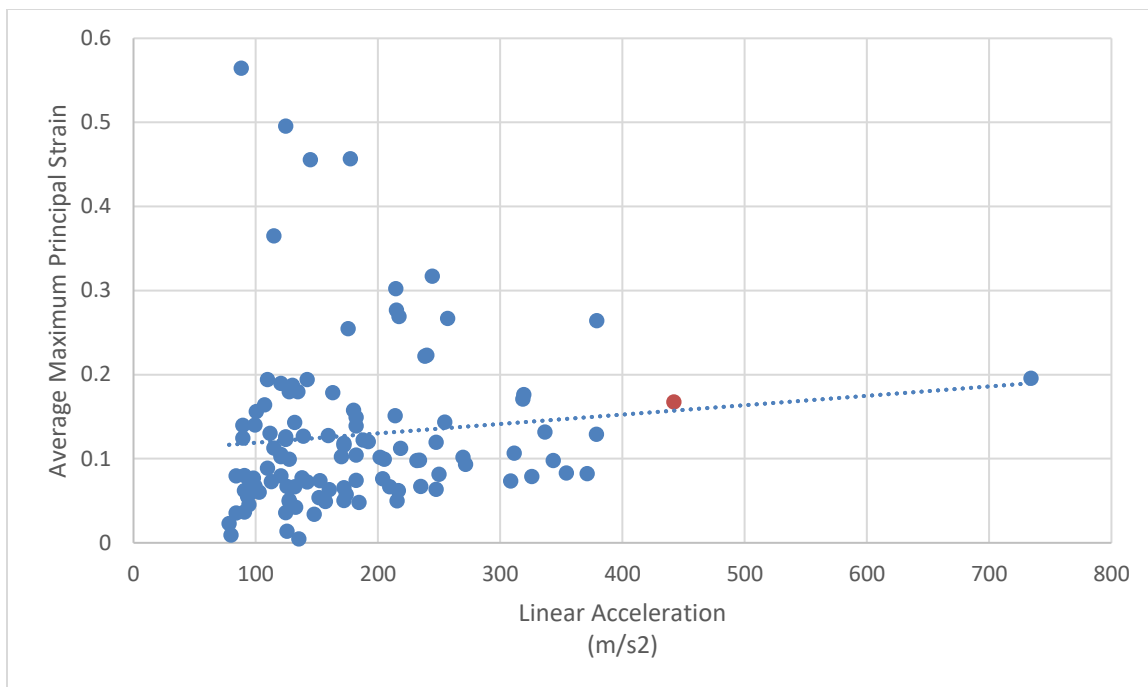


Figure 4. Relationship between the peak linear acceleration and resulting maximum principal strain (MPS) in the genu of the corpus callosum on the left side. The dotted line represents the line of best fit. The single concussion case is represented with the red circle.

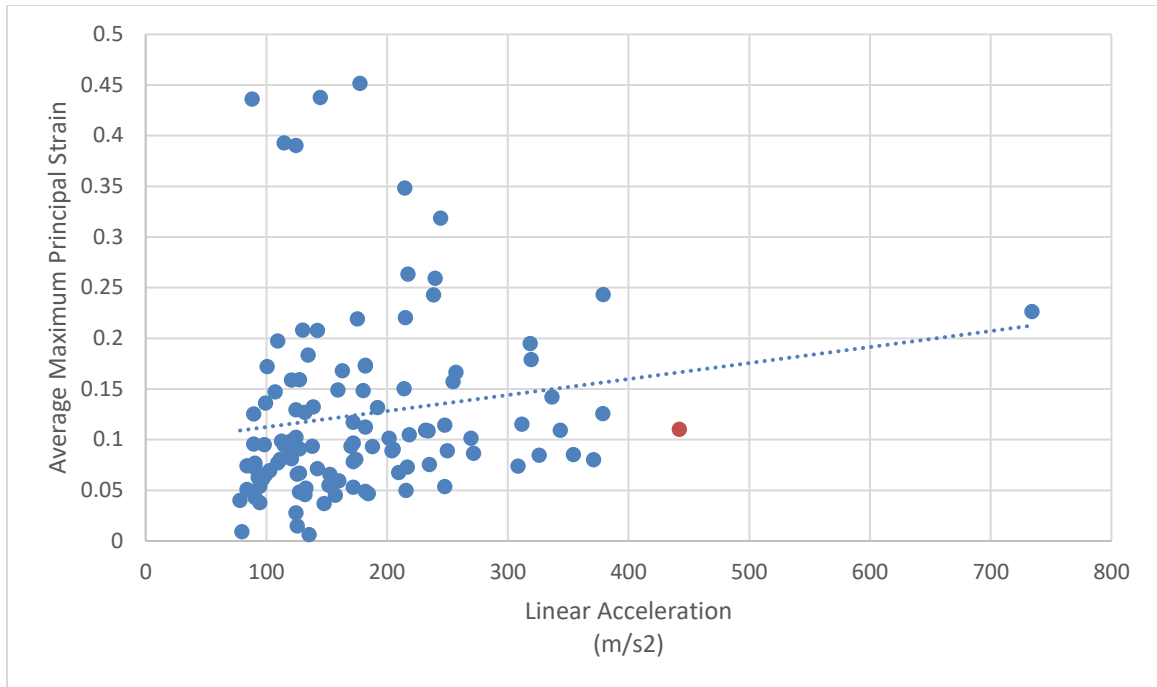


Figure 5. Relationship between the peak linear acceleration and resulting maximum principal strain (MPS) in the genu of the corpus callosum on the right side. The dotted line represents the line of best fit. The single concussion case is represented with the red circle.

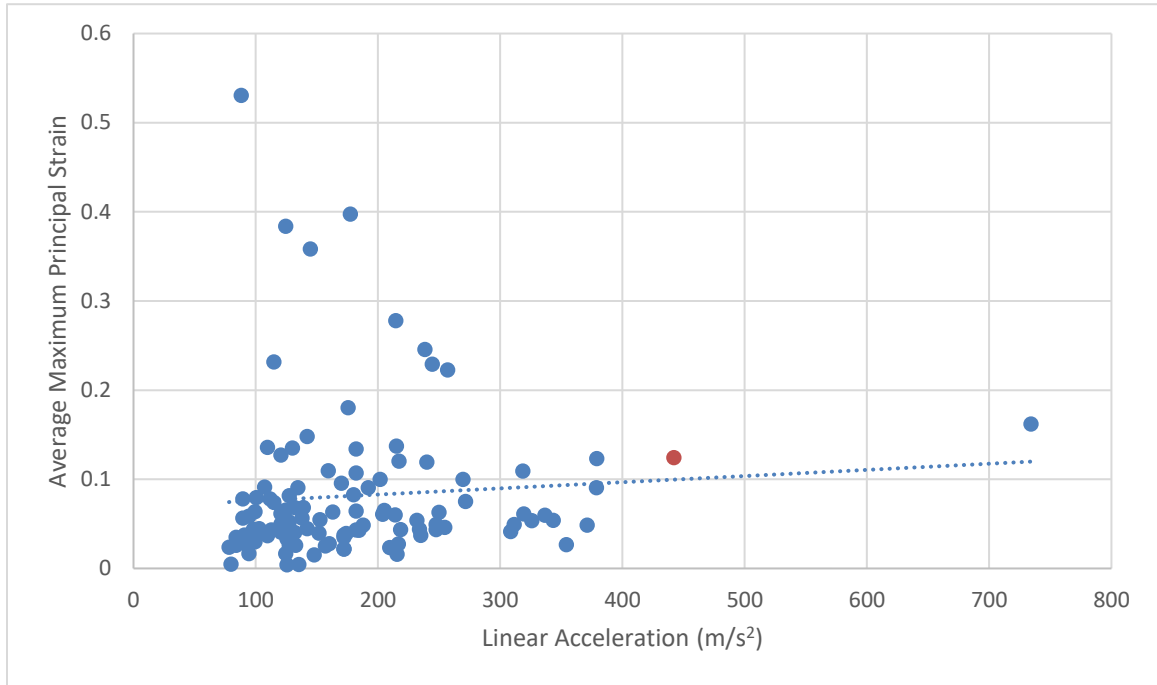


Figure 6. Relationship between the peak linear acceleration and resulting maximum principal strain (MPS) in the splenium of the corpus callosum on the left side. The dotted line represents the line of best fit. The single concussion case is represented with the red circle.

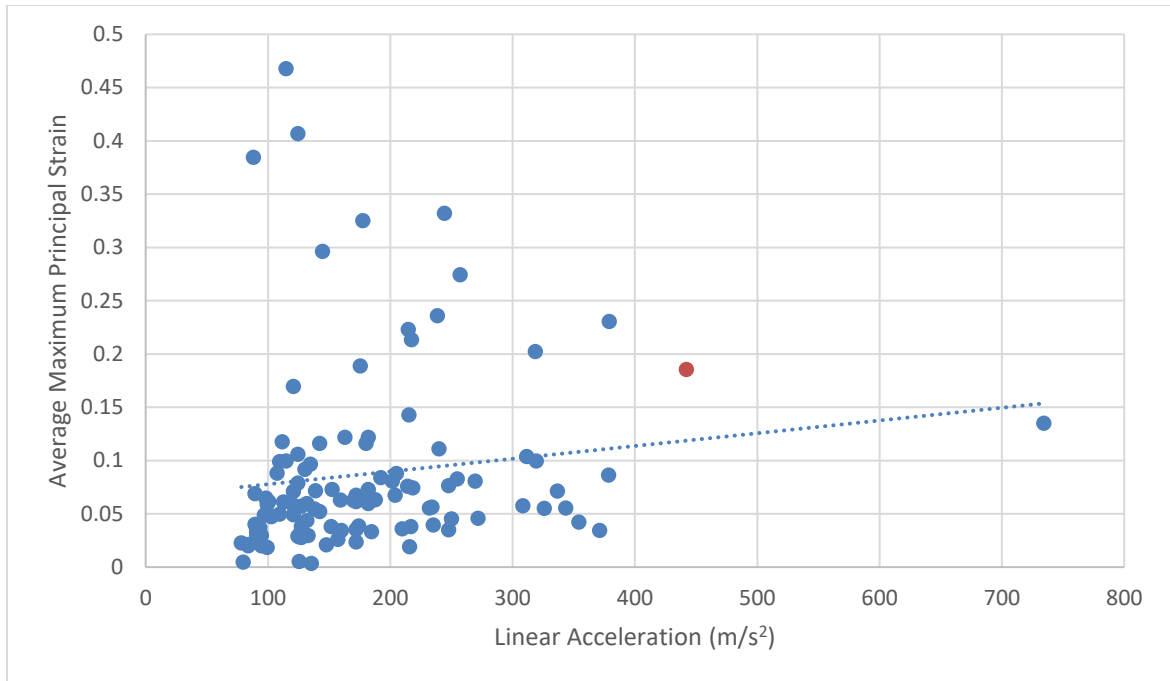


Figure 7. Relationship between the peak linear acceleration and resulting maximum principal strain (MPS) in the splenium of the corpus callosum on the right side. The dotted line represents the line of best fit. The single concussion case is represented with the red circle.

4.3.2 Relationship between the peak linear acceleration and MPS in the thalamus

There were low correlations between the linear acceleration and APMPS for all of the ROIs of the thalamus (Table 6). Between 1.4 and 4.7% of the variance in APMPS was explained by the linear acceleration, showing a low contribution. There was a weak relationship between linear acceleration and APMPS for all of the ROIs within the thalamus (Figures 7-10). These data are broken down by age and presented in Appendix B

Table 7. Correlations (r) and coefficients of determination (r^2) between APMPS and linear acceleration for each of the ROIs in the thalamus.

<i>Region of Interest</i>	<i>r</i>	<i>r²</i>
<i>Left Posterior Thalamus</i>	0.1175	0.0138
<i>Right Posterior Thalamus</i>	0.2159	0.0466
<i>Left Anterior Thalamus</i>	0.1493	0.0223
<i>Right Anterior Thalamus</i>	0.1330	0.0177

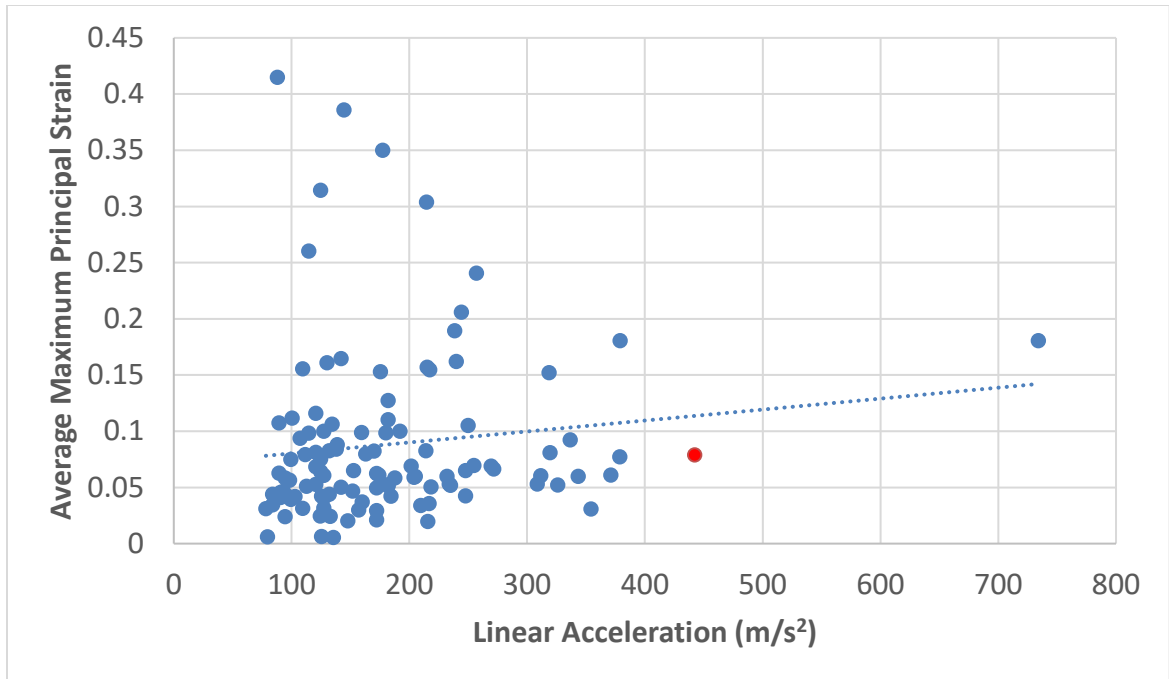


Figure 8. Relationship between the peak linear acceleration and resulting maximum principal strain (MPS) in the posterior thalamus on the left side. The dotted line represents the line of best fit. The single concussion case is represented with the red circle.

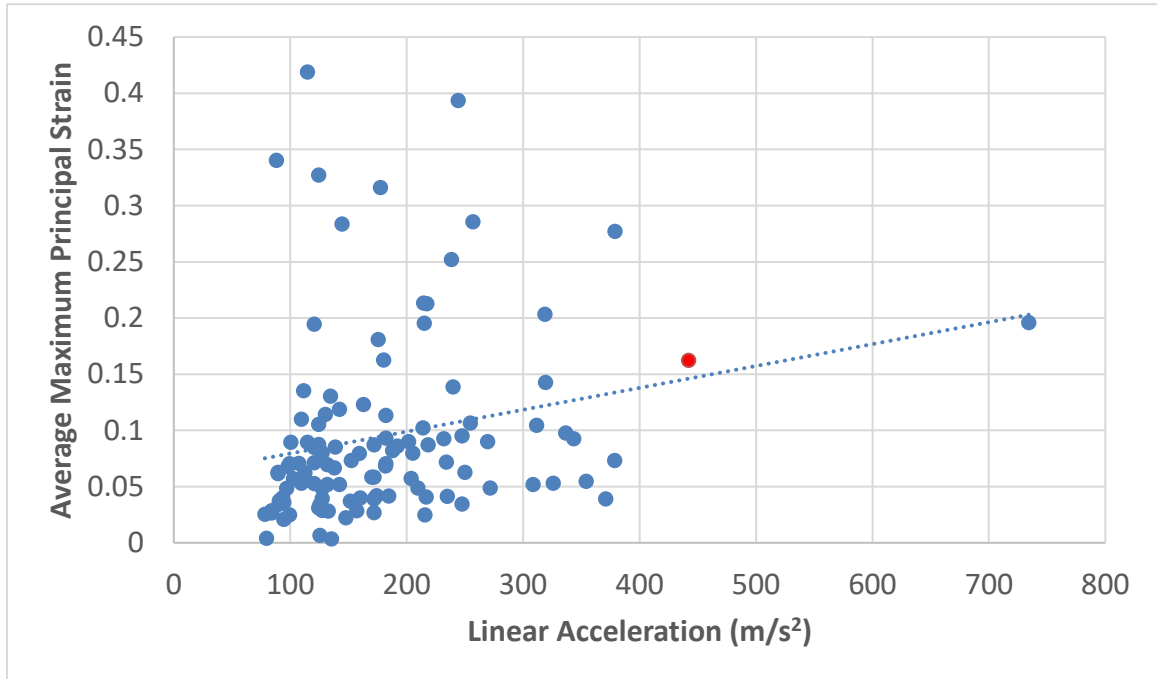


Figure 9. Relationship between the peak linear acceleration and resulting maximum principal strain (MPS) in the posterior thalamus on the right side. The dotted line represents the line of best fit. The single concussion case is represented with the red circle.

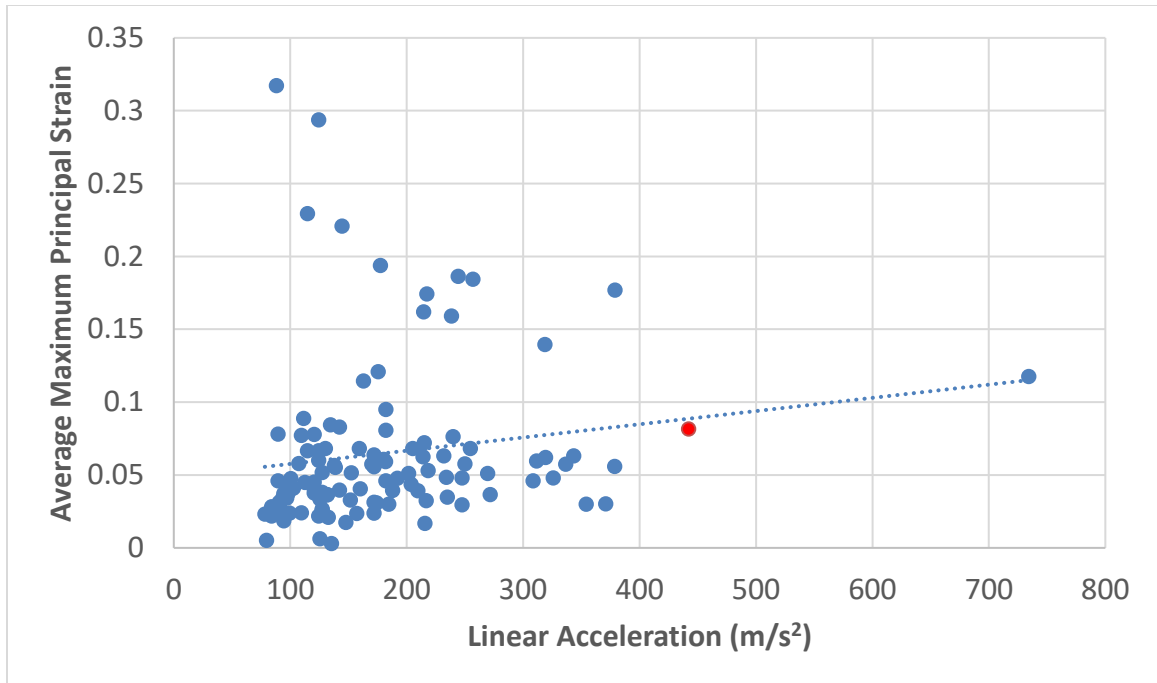


Figure 10. Relationship between the peak linear acceleration and resulting maximum principal strain (MPS) in the anterior thalamus on the left side. The dotted line represents the line of best fit. The single concussion case is represented with the red circle.

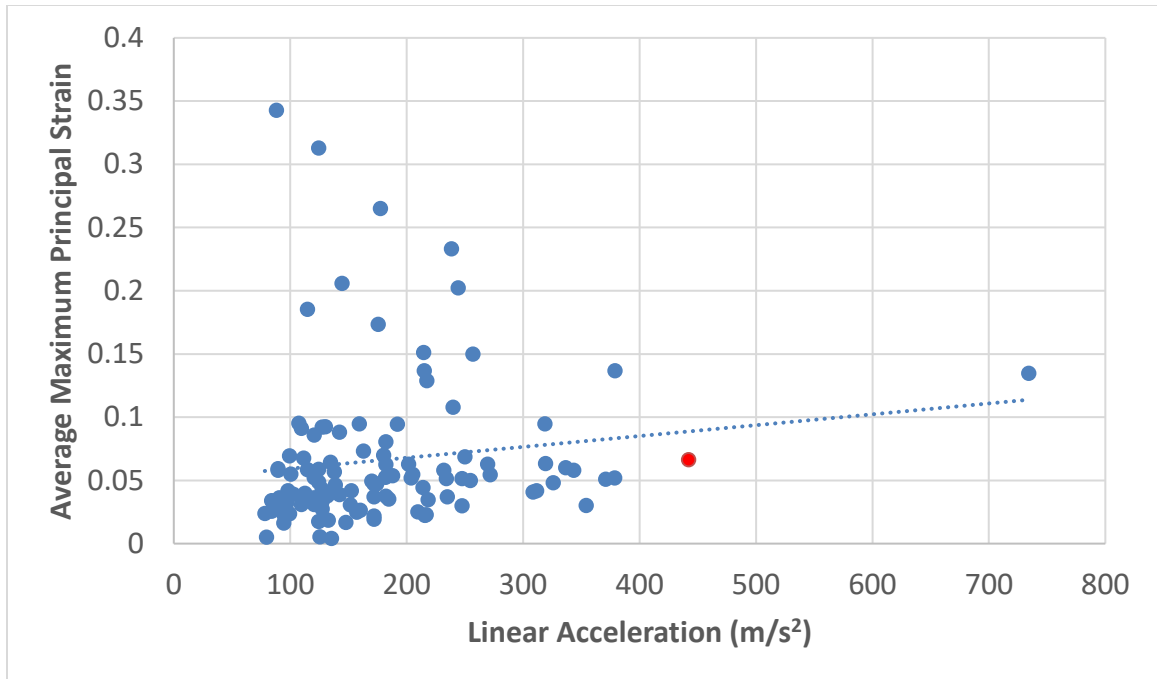


Figure 11. Relationship between the peak linear acceleration and resulting maximum principal strain (MPS) in the anterior thalamus on the right side. The dotted line represents the line of best fit. The single concussion case is represented with the red circle.

4.3.3 Relationship between the peak linear acceleration and MPS in the brain stem

There were low correlations between the linear acceleration and APMPS for both of the ROIs of the brain stem (Table 7). Between 9.2 and 11.0% of the variance in APMPS was explained by the linear acceleration, showing a low contribution. There was a weak relationship between linear acceleration and APMPS for both of the ROIs within the brain stem (Figures 11-12). These data are broken down by age and presented in Appendix B

Table 8. Correlations (r) and coefficients of determination (r^2) between APMPS and linear acceleration for each of the ROIs in the brain stem

<i>Region of Interest</i>	<i>r</i>	<i>r²</i>
<i>Left Posterior Brain Stem</i>	0.3314	0.1098
<i>Right Posterior Brain Stem</i>	0.3025	0.0915

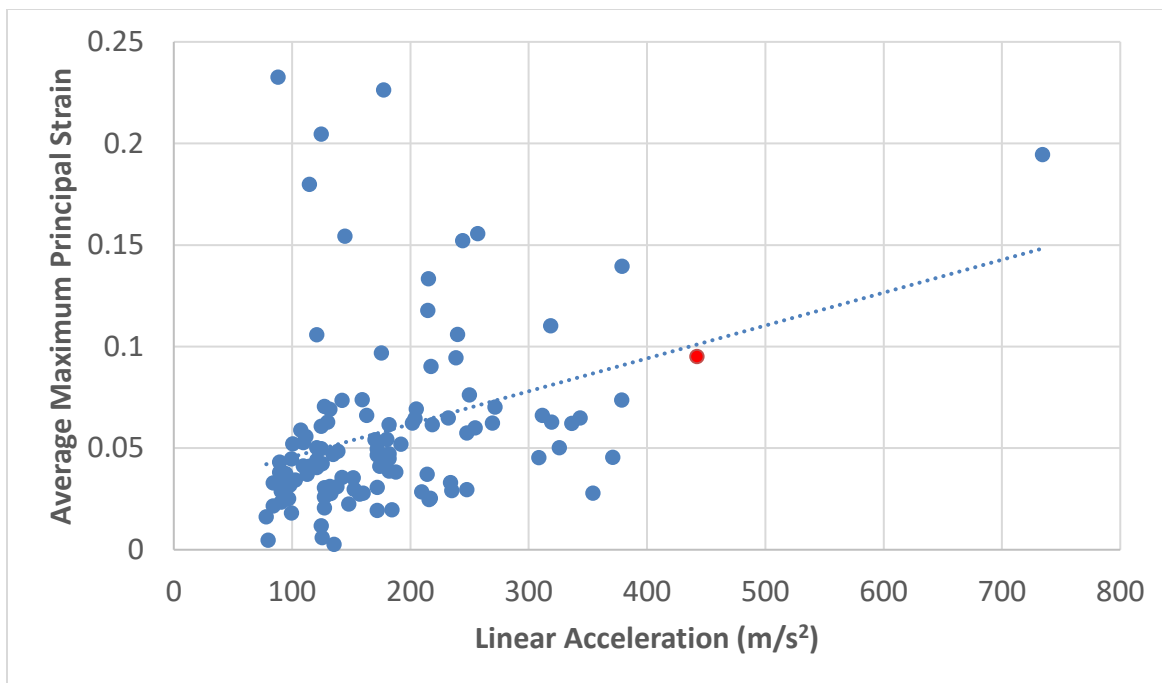


Figure 12. Relationship between the peak linear acceleration and resulting maximum principal strain (MPS) in the lateral posterior brain stem on the left side. The dotted line represents the line of best fit. The single concussion case is represented with the red circle.

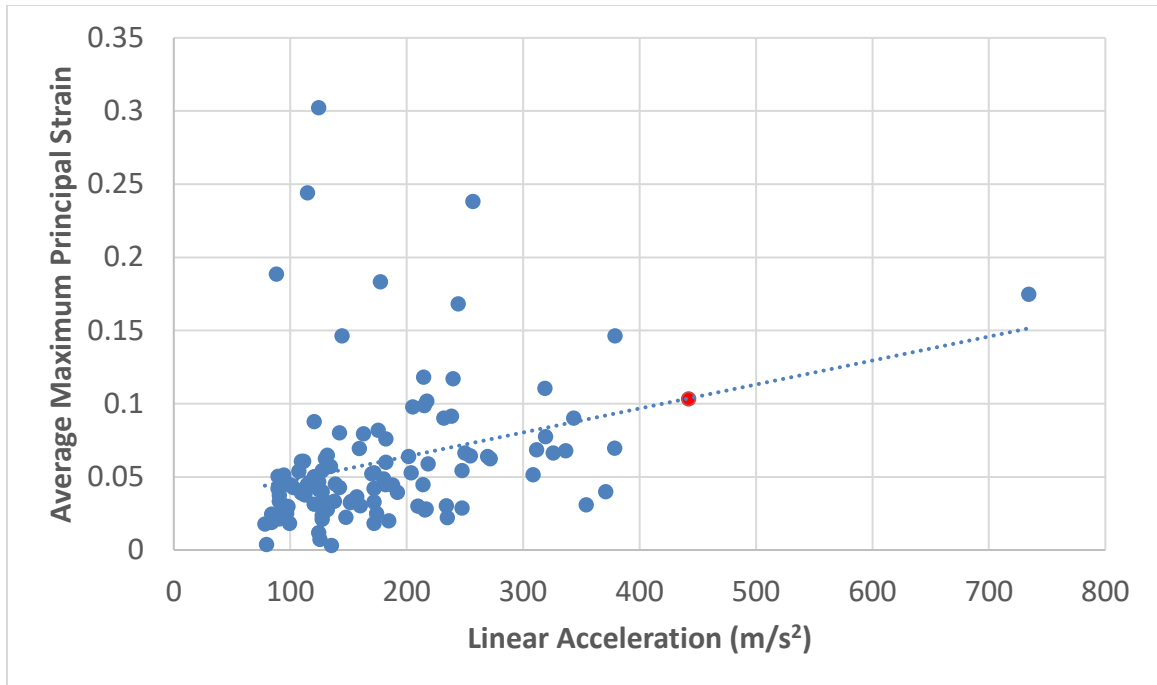


Figure 13. Relationship between the peak linear acceleration and resulting maximum principal strain (MPS) in the lateral posterior brain stem on the right side. The dotted line represents the line of best fit. The single concussion case is represented with the red circle.

4.4 Relationship between Angular Velocity and Maximum Principal Strain

4.4.1 Relationship between the peak angular velocity and MPS in the corpus callosum

There were high correlations between the angular velocity and APMPS for all of the ROIs of the (Table 8). Between 57.4 and 68.2% of the variance in APMPS was explained by the angular velocity. This illustrated a large contribution of the angular velocity to the APMPS. There was a strong relationship between angular velocity and APMPS for all of the ROIs within the CC (Figures 13-16). These data are broken down by age and presented in appendix C.

Table 9. Correlations (r) and coefficients of determination (r^2) between APMPS and angular velocity for each of the ROIs in the CC.

<i>Region of Interest</i>	<i>r value</i>	<i>r² value</i>
<i>Left Genu of CC</i>	0.8068	0.651
<i>Right Genu of CC</i>	0.7828	0.6127
<i>Left Splenium of CC</i>	0.7579	0.5744
<i>Right Splenium of CC</i>	0.8261	0.6824

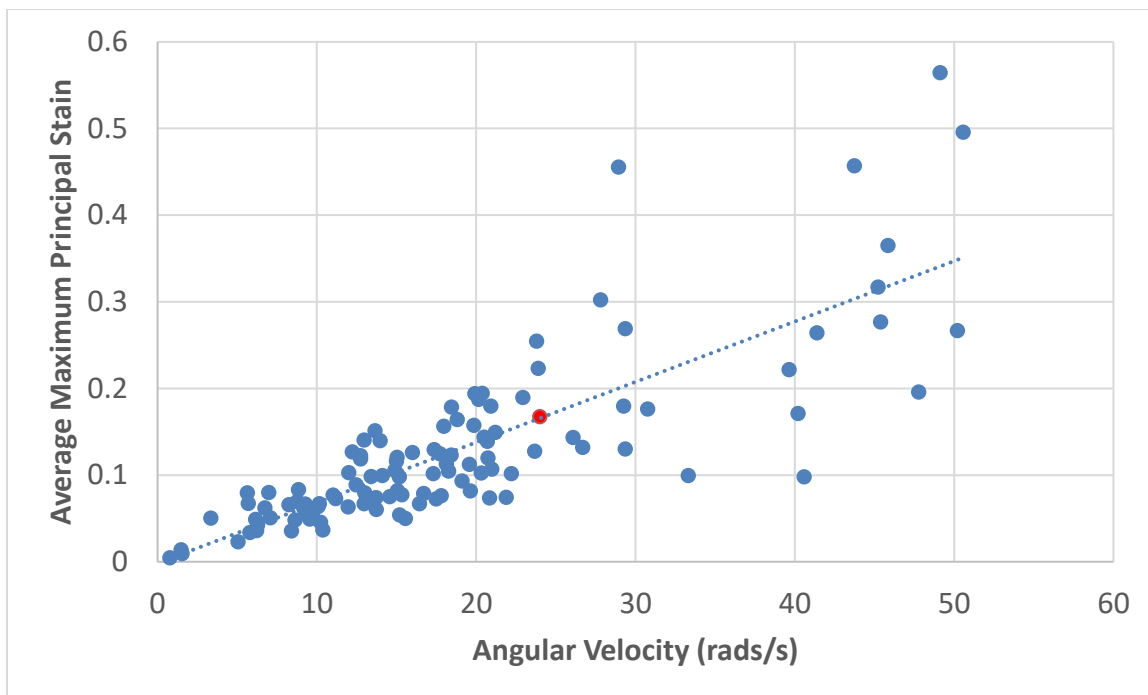


Figure 14. Relationship between the peak angular velocity and resulting maximum principal strain (MPS) in the genu of the corpus callosum on the left side. The dotted line represents the line of best fit. The single concussion case is represented with the red circle.

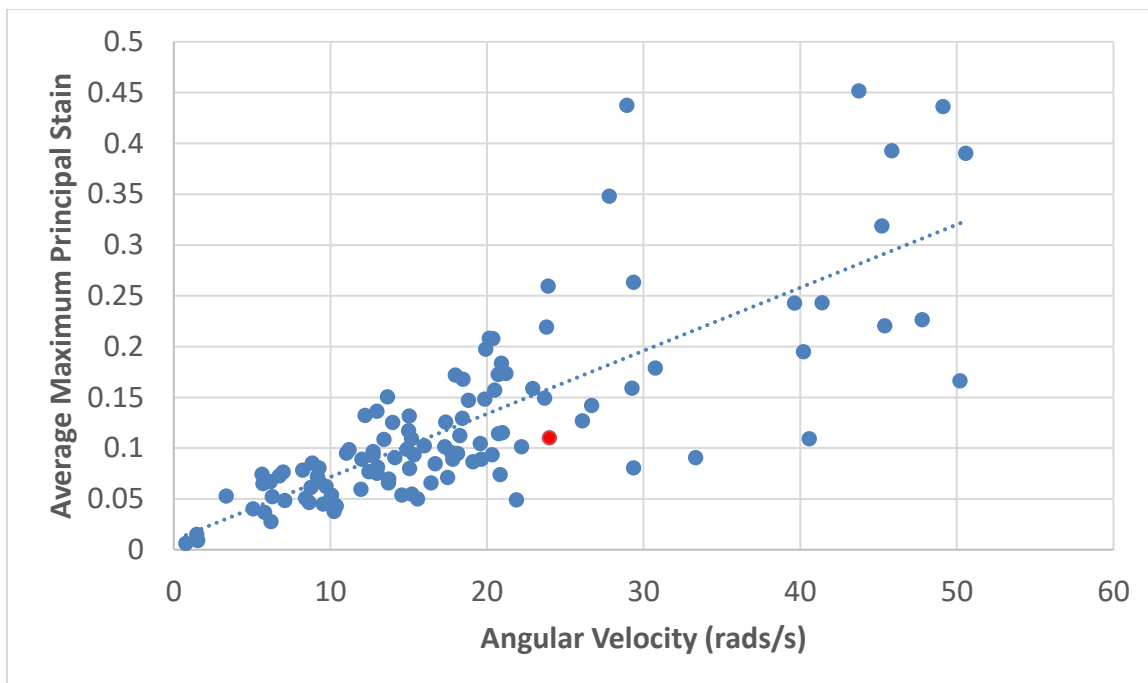


Figure 15. Relationship between the peak angular velocity and resulting maximum principal strain (MPS) in the genu of the corpus callosum on the right side. The dotted line represents the line of best fit. The single concussion case is represented with the red circle.

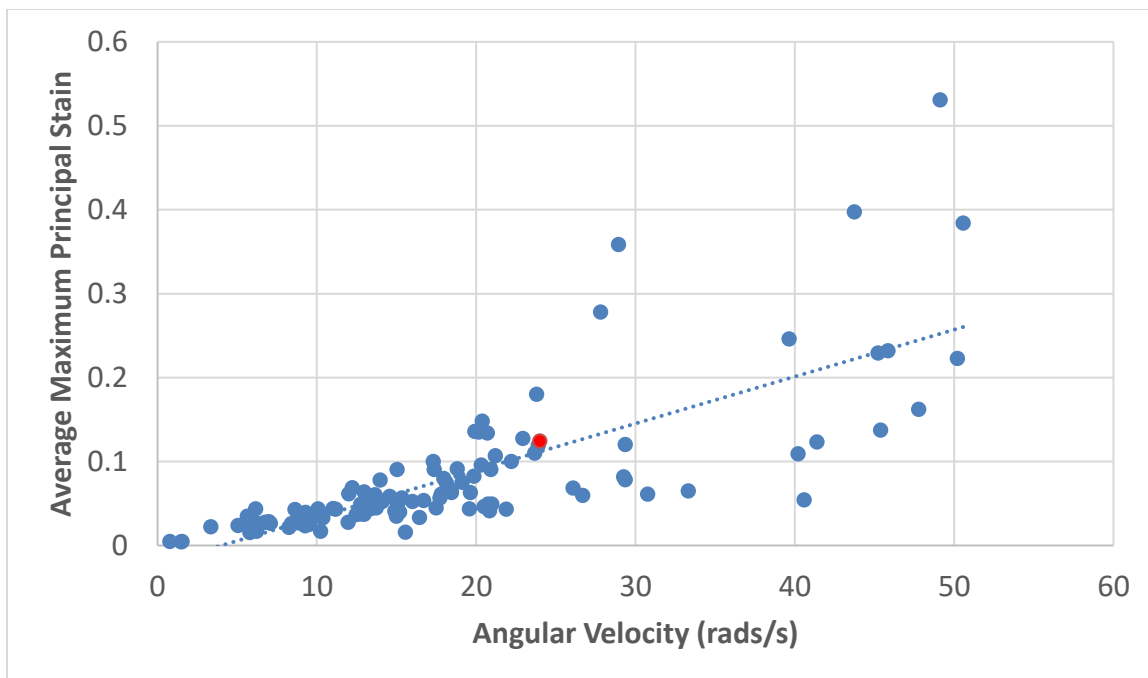


Figure 16. Relationship between the peak angular velocity and resulting maximum principal strain (MPS) in the splenium of the corpus callosum on the left side. The dotted line represents the line of best fit. The single concussion case is represented with the red circle.

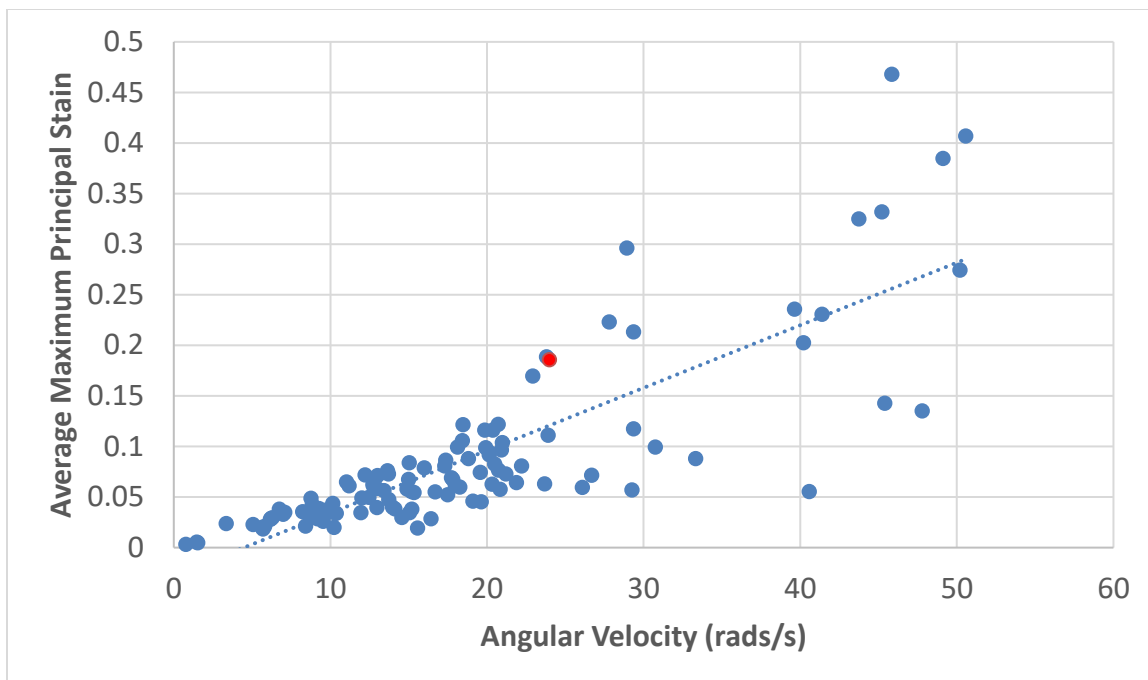


Figure 17. Relationship between the peak angular velocity and resulting maximum principal strain (MPS) in the splenium of the corpus callosum on the right side. The dotted line represents the line of best fit. The single concussion case is represented with the red circle.

4.4.2 Relationship between the peak angular velocity and MPS in the thalamus

There were high correlations between the angular velocity and APMPS for all of the ROIs of the thalamus (Table 9). Between 61.0% and 75.2% of the variance in APMPS was explained by the angular velocity. This illustrated a large contribution of the angular velocity to the APMPS. There was a strong relationship between angular velocity and APMPS for all of the ROIs within the thalamus (Figures 17-20). These data are broken down by age and presented in Appendix C.

Table 10. Correlations (r) and coefficients of determination (r^2) between APMPS and angular velocity for each of the ROIs in the thalamus

<i>Region of Interest</i>	<i>r</i>	<i>r²</i>
<i>Left Posterior Thalamus</i>	0.7812	0.6102
<i>Right Posterior Thalamus</i>	0.8672	0.752
<i>Left Anterior Thalamus</i>	0.8268	0.6836
<i>Right Anterior Thalamus</i>	0.8167	0.667

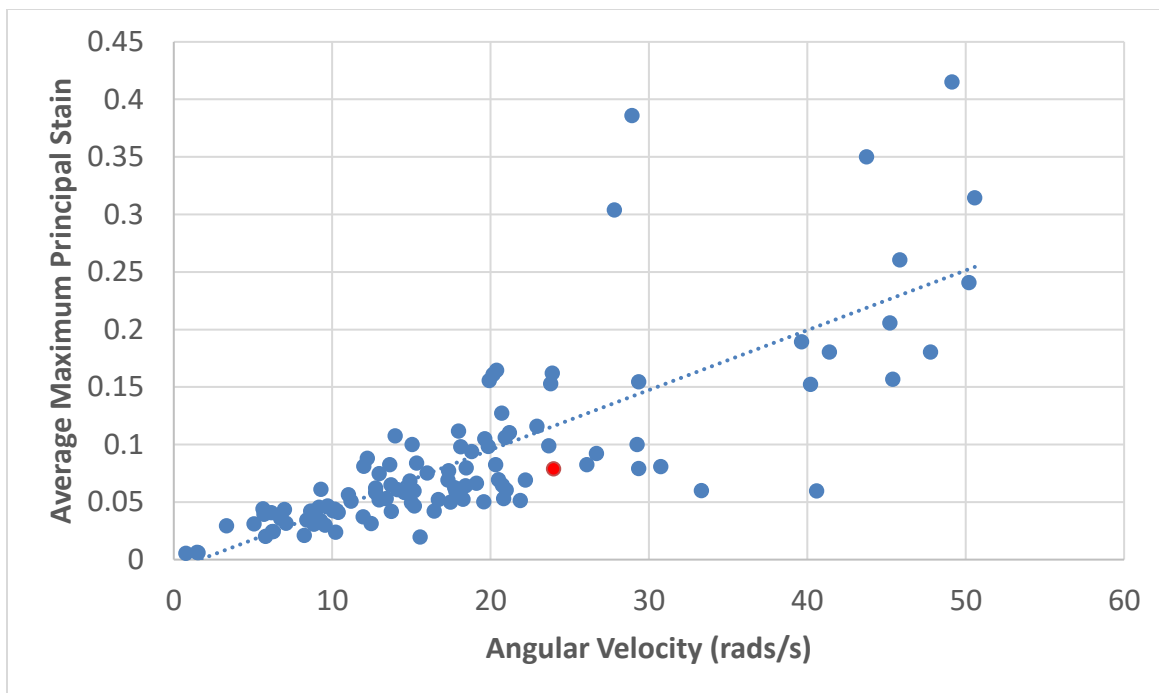


Figure 18. Relationship between the peak angular velocity and resulting maximum principal strain (MPS) in the posterior thalamus on the left side. The dotted line represents the line of best fit. The single concussion case is represented with the red circle.

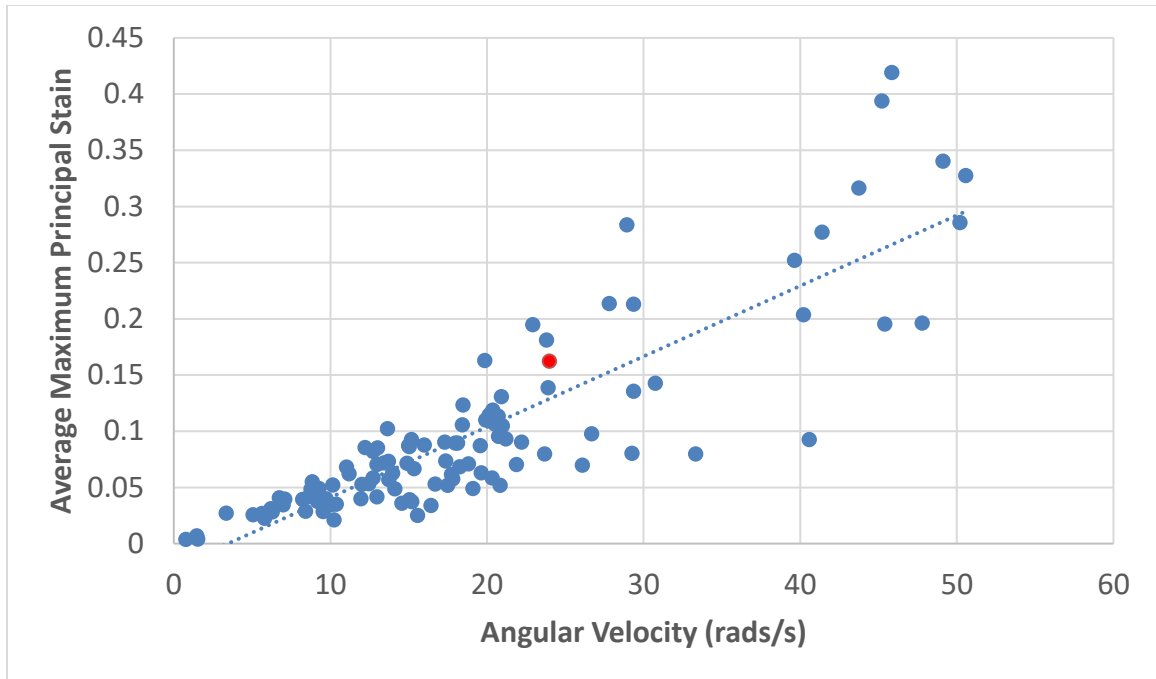


Figure 19. Relationship between the peak angular velocity and resulting maximum principal strain (MPS) in the posterior thalamus on the right side. The dotted line represents the line of best fit. The single concussion case is represented with the red circle.

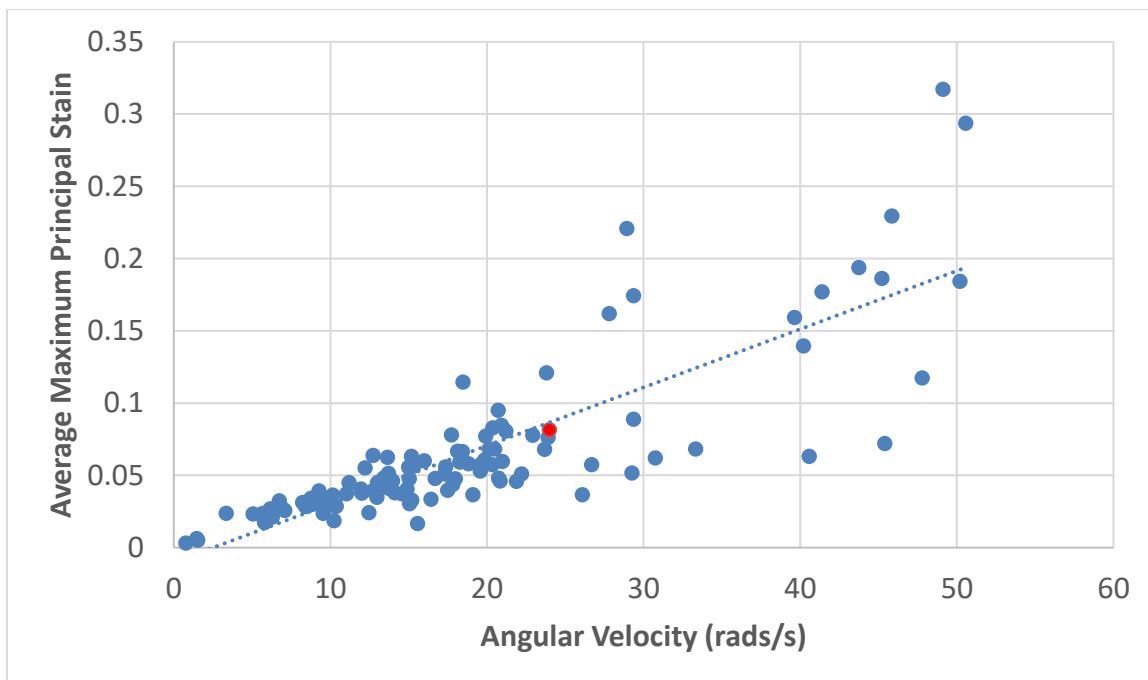


Figure 20. Relationship between the peak angular velocity and resulting maximum principal strain (MPS) in the anterior thalamus on the left side. The dotted line represents the line of best fit. The single concussion case is represented with the red circle.

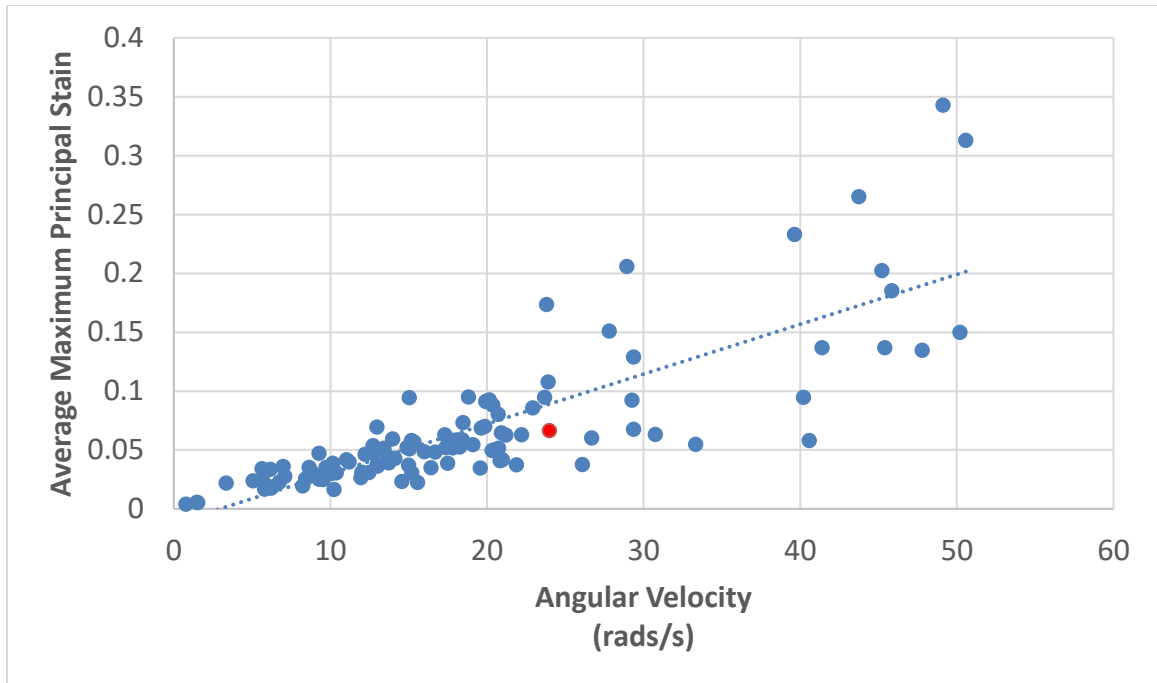


Figure 21. Relationship between the peak angular velocity and resulting maximum principal strain (MPS) in the anterior thalamus on the right side. The dotted line represents the line of best fit. The single concussion case is represented with the red circle.

4.4.3 Relationship between the peak angular velocity and MPS in the brain stem

There were high correlations between the angular velocity and APMPS for both of the ROIs of the brain stem (Table 10). Between 79.0% and 80.5% of the variance in APMPS was explained by the angular velocity. This illustrated a large contribution of the angular velocity to the APMPS. There was a strong relationship between angular velocity and APMPS for all of the ROIs within the CC (Figures 21-22). These data are broken down by age and presented in Appendix C.

Table 11. Correlations (r) and coefficients of determination (r^2) between APMPS and angular velocity for each of the ROIs in the brain stem

<i>Region of Interest</i>	<i>r</i>	<i>r²</i>
<i>Left Posterior Brain Stem</i>	0.8970	0.8046
<i>Right Posterior Brain Stem</i>	0.8889	0.7901

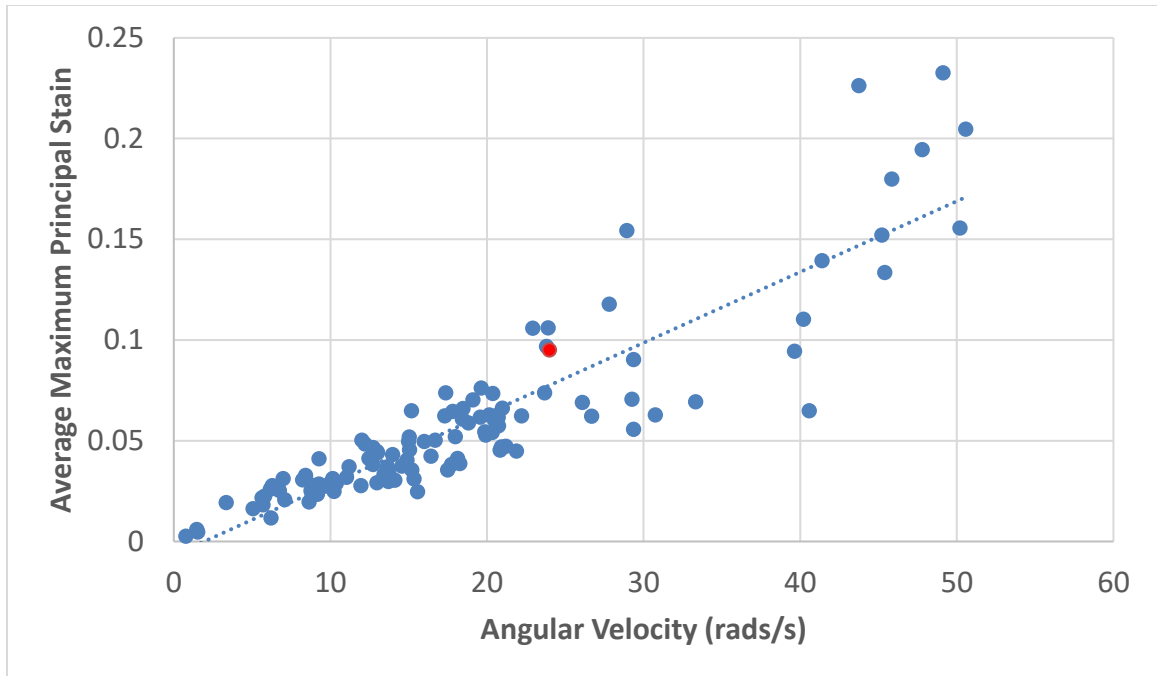


Figure 22. Relationship between the peak angular velocity and resulting maximum principal strain (MPS) in the lateral posterior brain stem on the left side. The dotted line represents the line of best fit. The single concussion case is represented with the red circle.

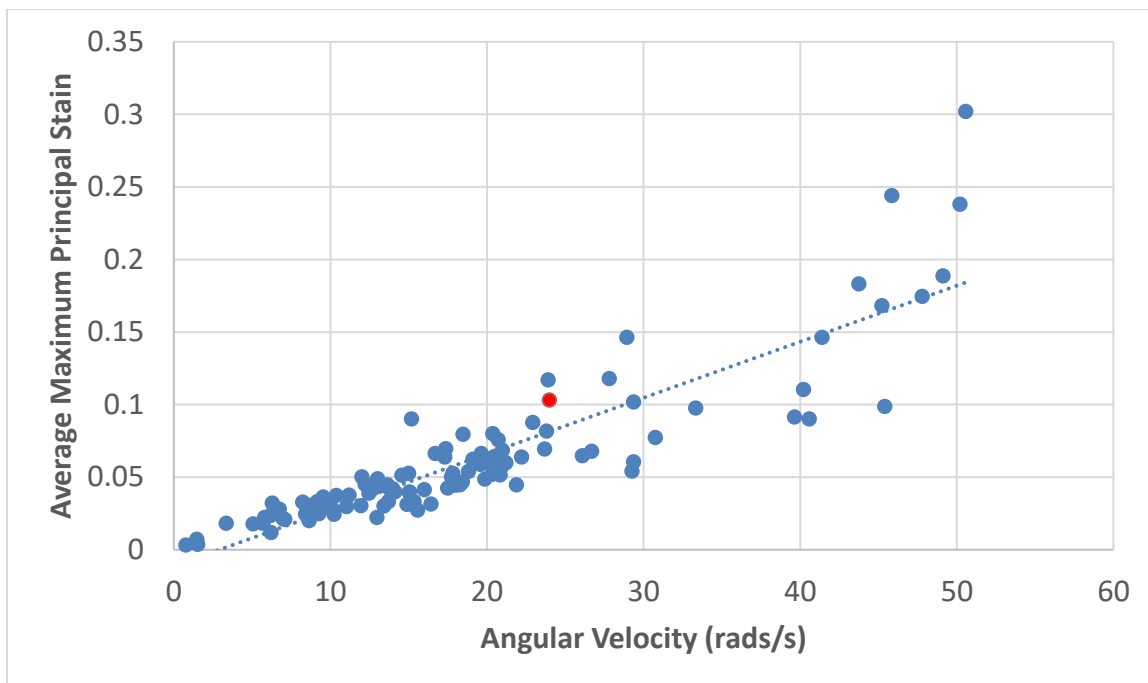


Figure 23. Relationship between the peak angular velocity and resulting maximum principal strain (MPS) in the lateral posterior brain stem on the right side. The dotted line represents the line of best fit. The single concussion case is represented with the red circle.

4.5 Maximum Principal Strains for Headers from Different Game Scenarios

The APMPSs for a single concussion case for each of the ROIs were compared to each of the game scenario's head impacts to provide some indication of the risk of concussion for each game scenario. Furthermore, more detailed results differentiating the purposeful headers by age are presented in Appendix D.

4.5.1 Corpus Callosum

In the genu of the CC, on the left side there was statistically significant differences between the APMPS in the concussion case compared to the head impacts resulting from deflection, free kick and throw ins (Figure 23 – upper left panel). On the right side, none of the game scenarios were significantly different than the concussion case (Figure 23 – upper right panel).

In the splenium of the CC, on the left side, there were statistically significant differences in APMPS from head impacts occurring in deflection, dropkicks, free kicks and throw in scenarios compared to the concussion case (Figure 23 – lower left panel). On the right side, there were significant differences between deflection, drop kicks, passes through the air, free shots and throw in scenarios compared to the concussion (Figure 23 – lower right panel).

For this region, the right side of the splenium of the CC experienced the highest APMPS during the concussion case (0.1856). Interestingly, the other three regions in the CC were

at or below 0.1676. As well, the posterior right thalamus region had the most scenarios that were significantly different than the concussion case.

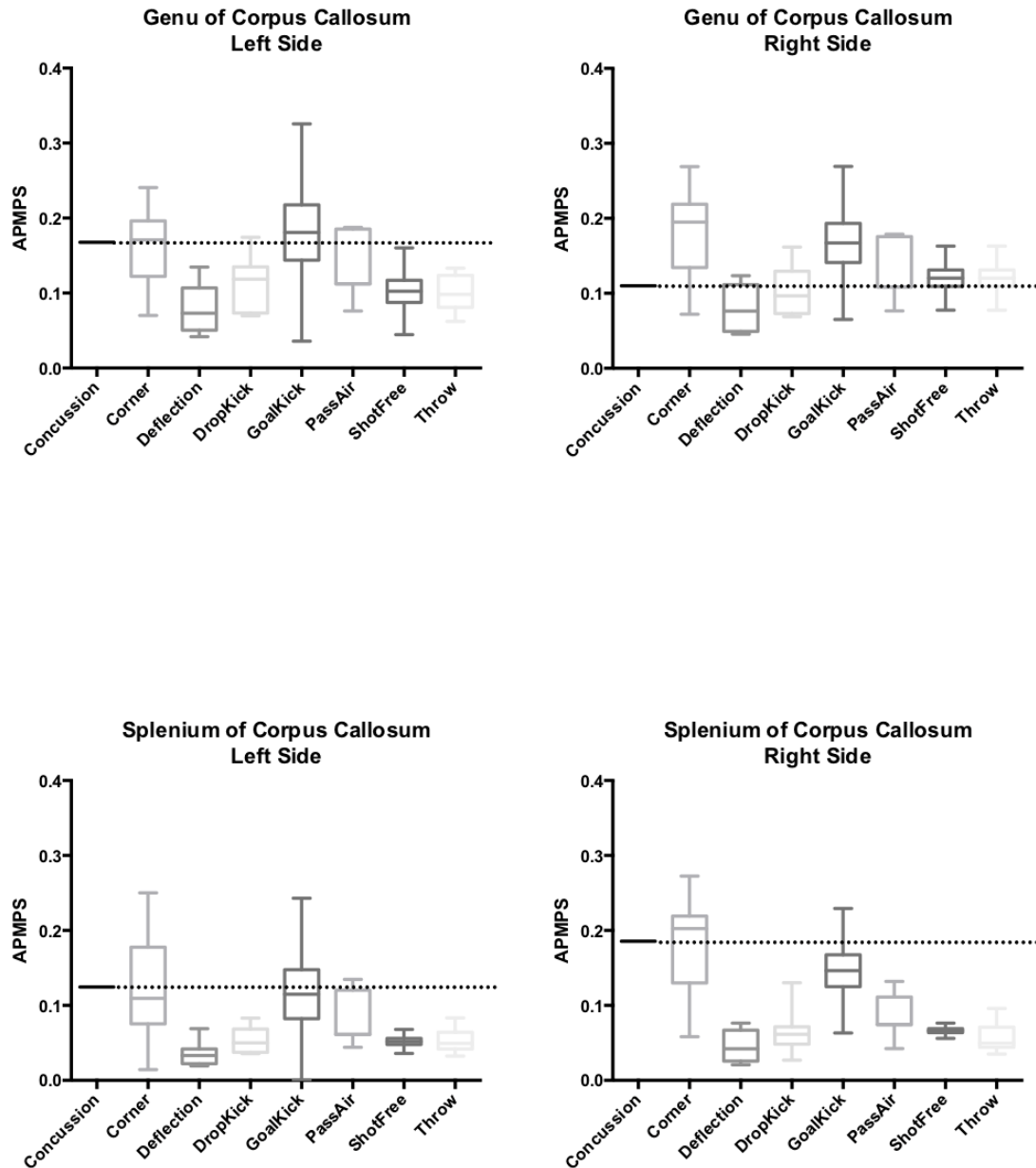


Figure 24. Box and whisker plots showing the average peak of the maximum principal strain (MPS) at the ROIs of the corpus callosum for the various game scenarios. Boxes represent the 25th – 75th quartile ranges and line within each box represents the median. The whiskers represent the 95% CI. The dotted line represents the MPS for the single concussion case.

4.5.2 Thalamus

In the posterior region thalamus on the left side (Figure 24 – upper left panel) there were no statistically significant differences in APMPS between the concussion case and the head impacts from the various game scenarios. However, on the right side (Figure 24 – upper right panel) there were statistical significant differences between the concussion case and the head impacts from deflections, dropkicks, passes through the air, free kicks and throw ins.

In the anterior thalamus on the left side (Figure 24 – lower left panel) there were statistically significant differences in APMPS between the concussion case and several game scenarios (deflections, free kicks, and throw ins). On the right side (Figure 24 – lower right panel), none of the game scenarios were significantly different than the concussion case.

For this region, the right posterior thalamus region experienced the highest APMPS during the concussion case (0.1625). Interestingly, the other three regions in the thalamus were at or below 0.0816. As well, the posterior right thalamus region had the most scenarios that were significantly different than the concussion case.

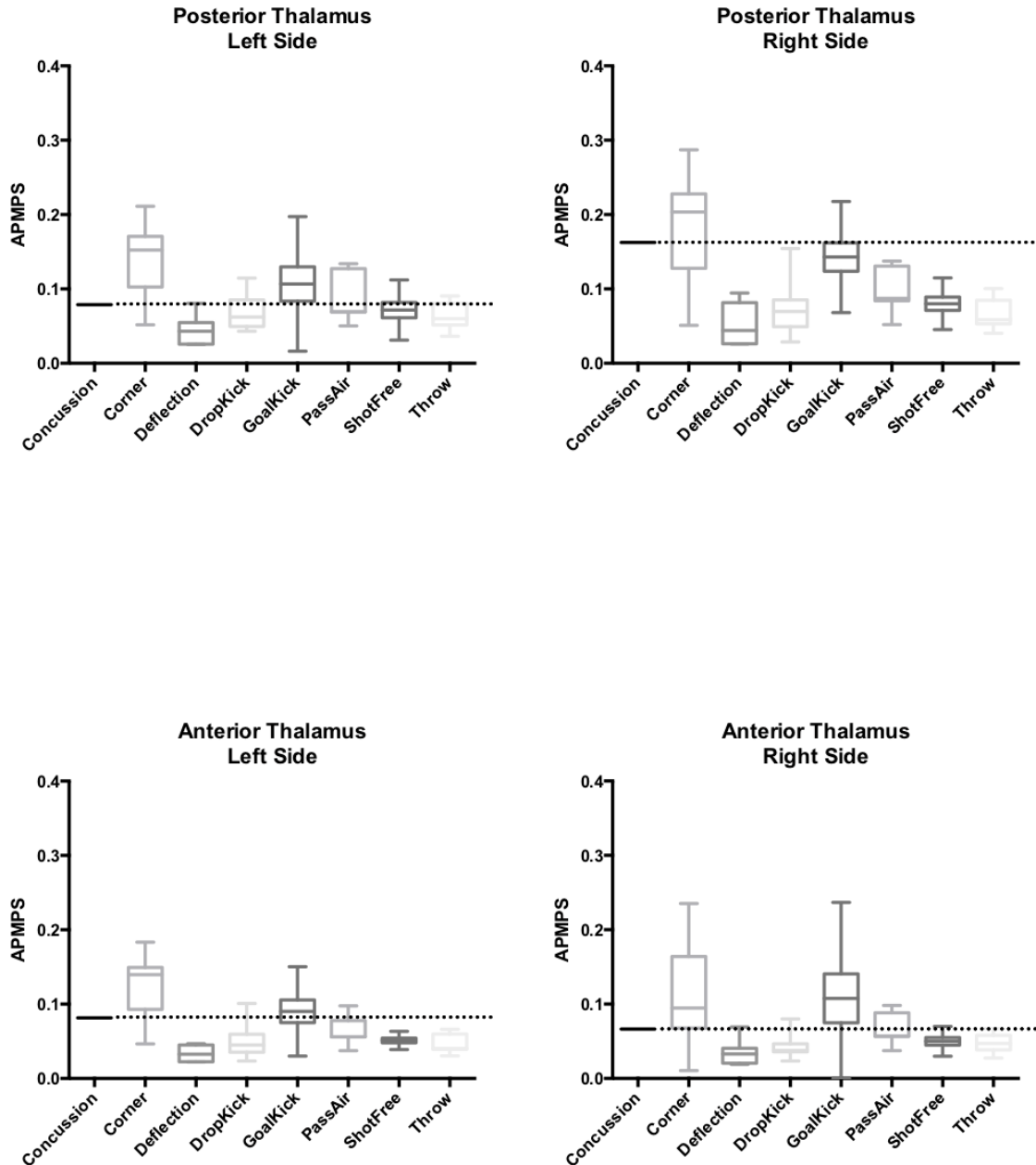


Figure 25. Box and whisker plots showing the average peak of the maximum principal strain (MPS) at the ROIs of the thalamus for the various game scenarios. Boxes represent the 25th – 75th quartile ranges and line within each box represents the median. The whiskers represent the 95% CI. The dotted line represents the MPS for the single concussion case.

4.5.3 Brain Stem

In the lateral posterior region of the brain stem on the left side, there were statistically significant differences between headers in individual game scenarios compared to the concussion case for deflections, dropkicks, passes through the air, free kicks and throw ins (Figure 25 – left panel). In the lateral posterior region of the brain stem on the right side there were statistically significant differences between headers in individual game scenarios compared to the concussion case for deflections, dropkicks, goal kicks, passes through the air, free kicks and throw ins (Figure 25 – right panel).

Of interest is the fact that, even with independent game scenarios by regions being assessed, the corner kick was the only game scenario with MPSs that were not significantly different than the concussion case. Across all scenarios with head impacts the brain stem was effected to a statistically significant level across most scenarios.

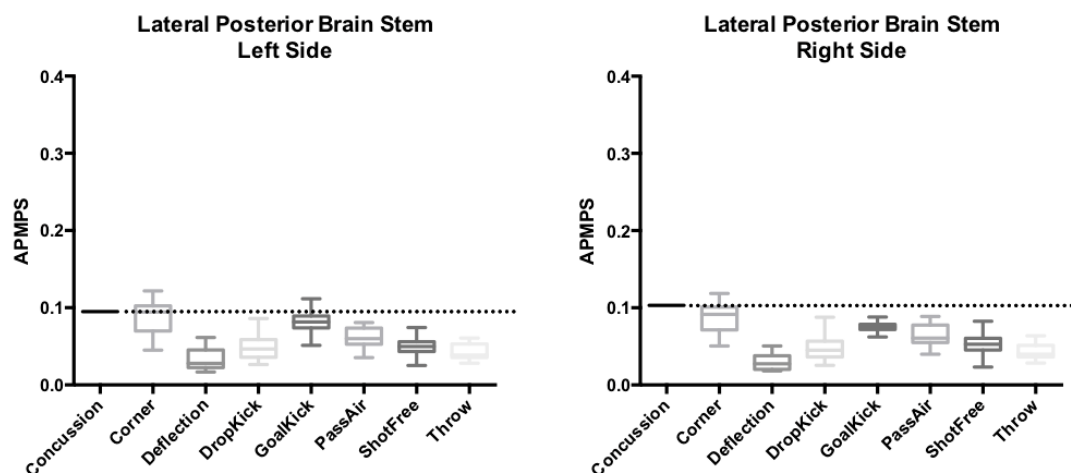


Figure 26. Box and whisker plots showing the average peak of the maximum principal strain (MPS) at the ROIs of the lateral posterior brain stem for the various game scenarios. Boxes represent the 25th – 75th quartile ranges and line within each box represents the median. The whiskers represent the 95% CI. The dotted line represents the MPS for the single concussion case.

5 Discussion

This study evaluated the MPS of specific regions of interest in the brain during purposeful head impacts recreated using FEM, compared to a single concussion case, and compared to thresholds for concussion. The FEM simulations were based on representative headers performed during female youth soccer games. The magnitude of the head impacts was quantified using kinematics captured using wireless sensors. These head kinematics were used to drive the simulations. The nature of the head impacts was captured from video recordings of games, enabling detailed reporting of the MPSs for different game scenarios.

It was hypothesized that there will be strong relationships between linear and angular head kinematics and that the APMPS at the various ROI related to concussion. In brief, we observed larger correlations between the MPS of the various ROI related to concussion and angular velocity than linear acceleration. It was also hypothesized that game scenarios where a header occurred would have a lesser magnitude of maximum principal strain compared to the concussion case in the various regions of interest compared to the purposeful headers. In brief, we observed that corner kicks produced sizable MPS throughout the ROIs and that the brain stem is a particularly susceptible region compared to a concussion case. These findings will be discussed in detail below.

5.1 Head Impacts

Soccer heading occurs frequently within the rules, and increases with age in female youth soccer players (Harriss et al., 2019b). As well, heading is performed with greater frequency in games over practices at the high school and collegiate levels (McCuen et al., 2015). Based on recollection, adult amateur soccer players performed a median of approximately 24 headers in a two week period (Stewart et al., 2018). This study

identified that an increased number of headers in these 2 week windows was associated with poorer scores on psychomotor speed, and attention tasks. Similarly, prolonged exposure to repetitive head impacts, as seen in professional American football and professional Association football, has been associated with neurological deficits later in life in the form of reduced brain volume (Schultz et al., 2018) and chronic traumatic encephalopathy (Ling et al., 2017; Schultz et al., 2018).

Previous research has used wireless sensors to collect data about head impacts in soccer in adolescent athletes (Caccese et al., 2016; Gutierrez et al., 2014; E. M. Hanlon & Bir, 2012; Harriss et al., 2019b; Miller, Pinkerton, et al., 2019). Most of these studies used video analysis to confirm the impacts (Caccese et al., 2016; E. M. Hanlon & Bir, 2012; Harriss et al., 2019b; Miller, Pinkerton, et al., 2019). This is necessary as wireless sensors typically overestimate the number of head impacts. For example, one study of lacrosse reported that 65% of head impacts recorded with GFT devices were bona fide head impacts verified by video (Cortes et al., 2017). In this same study, only 32% of head impacts recorded with X-Patch sensors were bona fide head impacts. Video confirmation was used in this thesis to ensure sensor recordings were representative of purposeful headers.

In addition to false-positive recordings, the accuracy of kinematic measures made by wireless sensors has also been questioned. Research verifying the xPatch observed large errors in linear and angular accelerations (approximately 50% RSME) compared to accelerations of a Hybrid III headform (McCuen et al., 2015). Campbell and colleagues (Campbell et al., 2016) assessed the accuracy of GFT device measures in football helmets and found strong correlations between both the linear acceleration ($r = 0.82$) and the rotational velocity ($r = 0.94$) against impacts using a Hybrid III dummy. In this same study, GFT devices had 14% mean average percent error after a correction algorithm was applied for the specific helmet type. This reduced error compared to other wireless sensors legitimizes the use GFT wireless sensors for the present study.

In research quantifying head impacts in youth soccer, Miller and colleagues (2019) report that the median linear acceleration (9.4 g) from headers in soccer games was lesser than that reported in this study (16.1 g). This may be due to the low volume of game impacts in that study (n=13) compared to this study (n=110). Previous research with a larger number of header impacts (n=47) in female youth soccer players reported an average peak linear acceleration of 20.4 g (E. M. Hanlon & Bir, 2012), which compares more favorably to the present study's findings (18.3 g). The average and median angular velocities for headers were considerably higher in this study (18.58 and 16.12 rads/s respectfully) compared to other research (3.8 and 4.1 rads/s respectively; (Miller, Pinkerton, et al., 2019)). This difference may be due to the different sensing approaches, as the research performed by Miller and colleagues (2019) was performed with wireless sensors attached to mouthpieces. The measures in this study reflect those found in other literature that utilize a similar wireless sensor placement (E. M. Hanlon & Bir, 2012).

5.2 Game scenarios

In terms of proportions of impacts, the sample pool in this study was representative of the total pool as it matched the distributions of the various game scenarios and the different player ages. The proportion of headers from the various scenarios that we observed in this study was similar to previous research by Miller and colleagues (2019). Miller and colleagues (2019) observed that passes through the air and throw ins were the most frequent headers, which compares well with the present study.

In terms of impact magnitudes, Miller and colleagues (2019) found the peak average linear accelerations and angular velocities came from long kick scenarios. In the present study this was the equivalent to the corner kick and pass through air scenario and supports the corner kicks high linear accelerations and angular velocities observed.

5.3 Correlations between head impact kinematics and APMPS

Pellman and colleagues (2003) used video analysis of impacts in professional football to recreate impacts using Hybrid III dummies. These impacts assessed head impacts of both the striking player and the struck player. The findings indicated that linear acceleration was the primary reason for concussions. This is in contrast to the findings of this study, as we found that there was a weak correlation between linear acceleration and MPS in the various regions of interest in the brain that are related to concussion. As well, the low coefficients of determination for each of these relationships indicates that the linear accelerations recorded by the wireless sensors only explain a minority of the variance in APMPS. Accordingly, it appears that linear acceleration recordings from head impact sensors may not be useful surrogate measures for strains within certain ROIs of the brain.

Furthermore, Pellman and colleagues (2003) found that there was negligible between the angular velocity and injury risk. This is in opposition to the findings in this thesis. We found that the angular velocity was highly correlated with APMPS. This is important as MPS has been shown to be associated with concussion, and has been used by several studies to establish a threshold for probability of concussion (Giordano & Kleiven, 2014; Kleiven, 2007). The high coefficient of determination for the relationship between angular velocity and APMPS shows that a large amount of variance is explained by angular velocity. Accordingly, it appears that angular velocity recordings from head impact sensors may be useful surrogate measures for strains within certain ROIs of the brain.

Due to the uncertain reliability of the relationship between these two different kinematic measures and MPS within certain ROIs of the brain, it is recommended that researchers use caution when utilizing data from head impact sensors.

5.4 Association between APMPS and concussion.

The CC is located centrally within the brain, contains an abundance of connections transversely connecting both hemispheres of the brain, and is susceptible to damage during head impacts. For example, in cases of adolescents with diagnosed concussions, the CC has shown changes in DTI biomarkers (FA and MD; E. A. Wilde et al., 2008). The CC is sensitive to disruption of the fiber tracks in concussion, as evidenced by the DTI biomarkers' fluctuations. This region is particularly relevant to youths as the fiber tracts are undergoing progressive myelination into adulthood (Lebel & Beaulieu, 2011; McAllister et al., 2012). These changes in the global CC structure are also evident within specific regions of the CC. For example, DTI studies have shown statistically significant differences between FA and MD measures at the CC's genu and splenium in patients with moderate traumatic brain injuries compared to healthy controls (Kumar et al., 2010). This is also supported by the significant elevation in FA values within the genu of the CC in a SRC group compared to healthy control (Borich et al., 2013). We observed that the CC experienced the highest APMPS across all of the ROIs evaluated within this thesis. As well, the concussion case had the highest APMPS value within the splenium of the CC ROI on the right side. Indicating that the CC might have been the area of the brain that was injured in this particular concussion.

The thalamus has been highlighted as a region that plays a role in the recovery from mTBI (Munivenkatappa, Devi, Shukla, & Rajeswaran, 2016). Thalamic volumes are decreased in boxers and MMA fighters (Bernick et al., 2015), but are increased, in parallel with increases in cognitive test scores, in patients recovering following mTBI (Munivenkatappa et al., 2016). The fighters had significant decreases in brain volume and decreased processing speeds that were proportional to their head impact exposure (0.3 and 0.19% per fight respectively). Furthermore, in retired NFL football players, the amount of years playing football was negatively correlated with thalamic volume (Schultz et al., 2018).

In one study that utilized FEM to recreate football impacts used ROIs in the thalamus to distinguish between concussive impacts that led to LOC compared to those with no LOC (Cournoyer & Hoshizaki, 2019). MPS values for shoulder and head impacts were 0.21 and 0.38 respectively for impacts resulting in LOC. These values are of interest in our study as purposeful headers involve voluntary impacts of the head, and therefore secondary contact is not relevant. In regards to all sampled impacts, corner and goal kicks were the only game scenarios with APMPS at or above the 0.21 LOC threshold observed by Cournoyer and Hoshizaki (2019). Interestingly, the concussion case did not reach this injury threshold value for any of the ROIs in the thalamus.

We observed that the ROIs in the brain stem had the highest positive correlations between APMPS and angular velocity ($r > 0.85$). These correlations were higher than between the linear acceleration and APMPS in the brain stem ($r > 0.3$). In contrast, Cournoyer & Hoshizaki (2019) observed that impact velocity, peak linear and rotational acceleration were all significantly greater in the LOC group than the no LOC group. A FEM study recreated football impacts based off of two different conditions: oblique frontal impact, and a crown impact (Darling et al., 2016). In the oblique frontal impact, the MPS at the brain stem was nearly double (0.089) that of the impact to the crown (0.045). This impact location is noticeably similar to that of a purposeful header performed with proper technique. This highlights that purposeful heading in soccer places large strain on the brain stem. This is highlighted in this study in two ways. We observed the larger correlations between the MPS in the brainstem and the linear acceleration and angular velocity compared to the other brain regions. We also observed that the MPSs in the brainstem in the concussion case was significantly higher than most game scenarios. This reinforces that increased strains in the brain stem may related to increased risk of concussion, as observed by others (Cournoyer & Hoshizaki, 2019).

Giordano and Kleiven (2014) evaluated whether axonal strain was a predictor of TBI compared to strain-based measures such as MPS. They simulated concussion head

impacts and non-injurious head impacts, and evaluated several brain regions including the CC, thalamus and brain stem. The differences in APMPS between the concussion and the headers in the various game scenarios were statistically significant ($p = 0.01$) except the CC ($p = 0.062$). All strain-based measures were good predictors of mTBI. Of note, Giordano and Kleiven (2014) observed that the best predictor of concussion with MPS was in the brain stem. This is consistent with the current study as the brain stem was subjected to significantly less MPS in the purposeful headers compared to the concussion case (except in the case of corner, and goal kick (left side only)).

Furthermore, a number of studies have established concussion thresholds based on the strain-based measures. Giordano and Kleiven (2014) determined that the 50POC MPS values within the CC, thalamus and brain stem were 0.1177, 0.1199, and 0.1264 respectively. Similarly, Beckwith and colleagues (2018) identified that concussive head impacts had median MPS values of 0.13 and 0.14 for the CC and brain stem respectively. The relative consistency of these thresholds indicates a level of internal validity.

In the present study, the APMPS in the single concussion case was compared to the various kick types. Based on Giordano and Kleiven's (2014) thresholds, the MPS threshold for 50POC was surpassed in three of the four ROIs in the CC; the right side of the genu of the CC was the sole exception. Somewhat similarly, two of the four ROI's surpassed the threshold for concussion in the CC as described by Beckwith and colleagues (2018).

In this thesis, the APMPS surpassed Giordano and Kleiven's 50POC threshold in only the right posterior thalamus ROI. Furthermore, in comparing the MPS in the brain stem during the concussion case to Beckwith and colleagues' threshold, our concussion case was equal to median concussion MPS value in the right ROI. However, neither regions in the brain stem reached the 50POC threshold for Giordano and Kleivan's threshold. This

is interesting, as the concussion case had a statistically significant greater MPS in the both brain stem regions than most kick types (corner and goal kick excepted).

Considering all of the regions of interest, the brainstem ROIs were the only regions in which the strains in the concussion case were significantly larger than the strains for most of the game scenarios. Presumably this indicates that the brainstem might have been the area of the brain that was injured in this particular concussion. Of interest is the fact that the corner kick was the only game scenario that had strains that were not significantly different than the concussion case. The lowest peak 95% CIs for corner kicks were within the brain stem. Across all scenarios the brain stem was effected to a statistically significant level across most scenarios. This also is of interest because the brain stem is increasingly effected in oblique frontal impacts as shown by Darling and colleagues (2016).

In terms of risk of injury from heading, one study has suggested that players should limit the number of goal kick headers to reduce their head impact exposure (Caccese et al., 2016). We observed that the strains in goal kick headers were large, and therefore it seems reasonable to consider reducing headers from goal kicks as a means of reducing head impact exposure. However, we noted that the strains in the headers off of corner kicks were consistently as large or larger than goal kicks, and therefore strategies to reduce head impact exposures should also target corner kicks for their large magnitude strains. Finally, in terms of the magnitude of head impact exposure, it is important to realize that both goal kicks and corner kicks represent a relatively small fraction of the overall number of purposeful headers in our group of female youth soccer players (less than 4% each). Accordingly, considering cumulative head impact exposure, it would be important to target reductions in other forms of purposeful headers as well.

5.5 Limitations

5.5.1 Wireless Sensors

The nature of the raw data collected by the GFT2 sensors was a limitation. This is because they do not measure angular accelerations which review papers indicate is associated with DAI (Miller, Urban, et al., 2019). Although it is possible to numerically differentiate angular velocity signals to calculate angular accelerations, that was not done in this study. As well, the 40 ms time window measuring impacts is appropriate for measuring peak accelerations, and has been used routinely with wireless head impact sensors (E. M. Hanlon & Bir, 2012). Other studies have also performed FEM simulations based on a 40 ms window length (Beckwith et al., 2018). However, we sometimes observed that the brain strains were still increasing at this point in the time record. Accordingly, the data in this thesis represents the peak strains recorded within the 40 ms window of the simulation, but we acknowledge that larger peak strains may have occurred later, beyond the time frame of the simulation. The Beckwith et al. (2018) paper does not present time series data, so it is not clear whether this type of situation may have occurred in their study too.

5.5.2 Maximum Principal Strain

There were limitations as far as the way that we collected and processed the data, and set up for boundary conditions for FEM analysis. MPSs are volatile measures as they are sensitive to local changes in geometry and material properties. We addressed this volatility by calculating average strains over 3x3 element regions of interest, similarly to other researchers (Claeson & Barocas, 2017). As well, another limitation of MPS magnitudes is that they do not consider direction. Accordingly, brain tissues that have a

specific orientation (such as white fiber tracks), may not be best described using MPS magnitudes.

5.5.3 Collection Periods and Type of Head Impacts

This thesis only evaluated purposeful headers during games that were confirmed by video. Although this represents the majority of purposeful heading exposure for youth soccer players, it did not evaluate head impacts from practices. As well, this thesis focused on purposeful headers and did not evaluate head impacts due to player-to-player contact, which are thought to be related to concussions (Zuckerman et al., 2015).

5.5.4 The Single Concussion Case

The field study only captured biomechanical data during the 60 games. The concussion that was used in this study occurred in practice during a crossing drill, therefore only wireless sensor data was available. As such, this head impact only represents one specific example of one mechanism of injury. It is well understood that concussions can occur from a variety of mechanisms of injury depending on factors such as impact direction and the relative magnitude of the linear and angular accelerations (Rowson et al., 2016). Accordingly this thesis does not yield insights that are relevant to other mechanisms of injury.

5.5.5 Number of Variables Assessed

This thesis focused exclusively on quantifying brain responses using MPS. As support, the maximum axonal strain (MAS) was the best parameter based on its receiver operating characteristic compared to other parameters (Giordano & Kleiven, 2014). Furthermore, other models have successfully differentiated between concussive and non-injurious head impacts using MPS (Beckwith et al., 2018; Giordano & Kleiven, 2014), and differentiated between concussions that have LOC compared to those with a LOC (Cournoyer & Hoshizaki, 2019). However, it is important to note that additional variables, such as stresses, might be relevant.

5.5.6 Size of Regions of Interest

This thesis used a small collection of elements to represent the ROI in the various anatomical structures that are related to concussion. The brain regions were identified using imaging studies for reference. This was unlike other literature where all elements in an anatomical region were assessed. The regions assessed in this study may be too minute to characterize the average strains of the whole region. This likely led to higher MPS magnitudes in this thesis compared to studies that used larger anatomical regions. As well, this likely affected our interpretation of the injury thresholds in this thesis.

6 Conclusion

The findings presented in this study offer a unique look into the effects of purposeful headers in soccer on a susceptible youth population. Despite the limitations presented above, this study illustrated increased levels of MPS at specific ROIs in the brain in the single concussion case compared to purposeful headers. It was observed that linear accelerations and angular velocities recorded by head impact sensors were both related to the strains occurring in the brain following head impacts. However, the strength of the relationship varied between ROIs observed, and often predicted a minority of the variance in strain. As well, it was recognized the game scenarios in which a head impact occurs are an important factor related to the magnitude of the MPS in the brain in youth soccer. Based on the findings of this study it is shown that FEM models can provide important insights into the risks associated with purposeful headers, and that ROIs related to concussion warrant further examination.

References

- Alosco, M. L., & Stern, R. A. (2019). Youth Exposure to Repetitive Head Impacts From Tackle Football and Long-term Neurologic Outcomes: A Review of the Literature, Knowledge Gaps and Future Directions, and Societal and Clinical Implications. *Seminars in Pediatric Neurology*, *30*, 107–116.
<https://doi.org/10.1016/j.spen.2019.03.016>
- Banks, S. D., Coronado, R. A., Clemons, L. R., Abraham, C. M., Pruthi, S., Conrad, B. N., ... Archer, K. R. (2016). Thalamic Functional Connectivity in Mild Traumatic Brain Injury: Longitudinal Associations With Patient-Reported Outcomes and Neuropsychological Tests. *Archives of Physical Medicine and Rehabilitation*, *97*(8), 1254–1261. <https://doi.org/10.1016/j.apmr.2016.03.013>
- Basser, P. J., Mattiello, J., & LeBihan, D. (1994). MR diffusion tensor spectroscopy and imaging. *Biophysical Journal*, *66*(1), 259–267. [https://doi.org/10.1016/S0006-3495\(94\)80775-1](https://doi.org/10.1016/S0006-3495(94)80775-1)
- Beckwith, J. G., Zhao, W., Ji, S., Ajamil, A. G., Bolander, R. P., Chu, J. J., ... Greenwald, R. M. (2018). Estimated Brain Tissue Response Following Impacts Associated With and Without Diagnosed Concussion. *Annals of Biomedical Engineering*, *46*(6), 819–830. <https://doi.org/10.1007/s10439-018-1999-5>
- Bernat, J. L., Capron, A. M., Bleck, T. P., Blosser, S., Bratton, S. L., Childress, J. F., ... White, D. B. (2010). The circulatory–respiratory determination of death in organ

donation*: *Critical Care Medicine*, 38(3), 963–970.

<https://doi.org/10.1097/CCM.0b013e3181c58916>

Bernick, C., Banks, S. J., Shin, W., Obuchowski, N., Butler, S., Noback, M., ... Modic, M. (2015). Repeated head trauma is associated with smaller thalamic volumes and slower processing speed: The Professional Fighters' Brain Health Study. *British Journal of Sports Medicine*, 49(15), 1007–1011. <https://doi.org/10.1136/bjsports-2014-093877>

Borich, M., Maken, N., Boyd, L., & Virji-Babul, N. (2013). Combining Whole-Brain Voxel-Wise Analysis with *In Vivo* Tractography of Diffusion Behavior after Sports-Related Concussion in Adolescents: A Preliminary Report. *Journal of Neurotrauma*, 30(14), 1243–1249. <https://doi.org/10.1089/neu.2012.2818>

Bretzin, A. C., Covassin, T., Fox, M. E., Petit, K. M., Savage, J. L., Walker, L. F., & Gould, D. (2018). Sex Differences in the Clinical Incidence of Concussions, Missed School Days, and Time Loss in High School Student-Athletes: Part 1. *The American Journal of Sports Medicine*, 46(9), 2263–2269. <https://doi.org/10.1177/0363546518778251>

Buzzini, S. R. R., & Guskiewicz, K. M. (2006). Sport-related concussion in the young athlete: *Current Opinion in Pediatrics*, 18(4), 376–382. <https://doi.org/10.1097/01.mop.0000236385.26284.ec>

Caccese, J. B., Lamond, L. C., Buckley, T. A., & Kaminski, T. W. (2016). Reducing purposeful headers from goal kicks and punts may reduce cumulative exposure to

head acceleration. *Research in Sports Medicine*, 24(4), 407–415.

<https://doi.org/10.1080/15438627.2016.1230549>

Campbell, K. R., Warnica, M. J., Levine, I. C., Brooks, J. S., Laing, A. C., Burkhart, T. A., & Dickey, J. P. (2016). Laboratory Evaluation of the gForce Tracker™, a Head Impact Kinematic Measuring Device for Use in Football Helmets. *Annals of Biomedical Engineering*, 44(4), 1246–1256. <https://doi.org/10.1007/s10439-015-1391-7>

Claeson, A. A., & Barocas, V. H. (2017). Computer simulation of lumbar flexion shows shear of the facet capsular ligament. *The Spine Journal*, 17(1), 109–119.

<https://doi.org/10.1016/j.spinee.2016.08.014>

Comstock, R. D., Currie, D. W., Pierpoint, L. A., Grubenhoff, J. A., & Fields, S. K. (2015). An Evidence-Based Discussion of Heading the Ball and Concussions in High School Soccer. *JAMA Pediatrics*, 169(9), 830.

<https://doi.org/10.1001/jamapediatrics.2015.1062>

Cortes, N., Lincoln, A. E., Myer, G. D., Hepburn, L., Higgins, M., Putukian, M., & Caswell, S. V. (2017). Video Analysis Verification of Head Impact Events Measured by Wearable Sensors. *The American Journal of Sports Medicine*, 45(10), 2379–2387. <https://doi.org/10.1177/0363546517706703>

Cournoyer, J., & Hoshizaki, T. B. (2019). Biomechanical comparison of concussions with and without a loss of consciousness in elite American football: Implications

for prevention. *Sports Biomechanics*, 1–17.

<https://doi.org/10.1080/14763141.2019.1600004>

Darling, T., Muthuswamy, J., & Rajan, S. D. (2016). Finite element modeling of human brain response to football helmet impacts. *Computer Methods in Biomechanics and Biomedical Engineering*, 19(13), 1432–1442.

<https://doi.org/10.1080/10255842.2016.1149574>

Dekaban, A. S., & Sadowsky, D. (1978). Changes in brain weights during the span of human life: Relation of brain weights to body heights and body weights. *Annals of Neurology*, 4(4), 345–356. <https://doi.org/10.1002/ana.410040410>

Delano-Wood, L., Bangen, K. J., Sorg, S. F., Clark, A. L., Schiehser, D. M., Luc, N., ... Bigler, E. D. (2015). Brainstem white matter integrity is related to loss of consciousness and postconcussive symptomatology in veterans with chronic mild to moderate traumatic brain injury. *Brain Imaging and Behavior*, 9(3), 500–512. <https://doi.org/10.1007/s11682-015-9432-2>

Fraser, M. A., Grooms, D. R., Guskiewicz, K. M., & Kerr, Z. Y. (2017). Ball-Contact Injuries in 11 National Collegiate Athletic Association Sports: The Injury Surveillance Program, 2009–2010 Through 2014–2015. *Journal of Athletic Training*, 52(7), 698–707. <https://doi.org/10.4085/1062-6050-52.3.10>

Giedd, J. N., Raznahan, A., Mills, K. L., & Lenroot, R. K. (2012). Review: Magnetic resonance imaging of male/female differences in human adolescent brain

anatomy. *Biology of Sex Differences*, 3(1), 19. <https://doi.org/10.1186/2042-6410-3-19>

Giordano, C., & Kleiven, S. (2014, November 10). *Evaluation of Axonal Strain as a Predictor for Mild Traumatic Brain Injuries Using Finite Element Modeling*. 2014-22-0002. <https://doi.org/10.4271/2014-22-0002>

Gur, R. C. (2002). Sex Differences in Temporo-limbic and Frontal Brain Volumes of Healthy Adults. *Cerebral Cortex*, 12(9), 998–1003. <https://doi.org/10.1093/cercor/12.9.998>

Gur, R. C., Turetsky, B. I., Matsui, M., Yan, M., Bilker, W., Hughett, P., & Gur, R. E. (1999). Sex Differences in Brain Gray and White Matter in Healthy Young Adults: Correlations with Cognitive Performance. *The Journal of Neuroscience*, 19(10), 4065–4072. <https://doi.org/10.1523/JNEUROSCI.19-10-04065.1999>

Guskiewicz, K. M., Ross, S. E., & Marshall, S. W. (2001). *Postural Stability and Neuropsychological Deficits After Concussion in Collegiate Athletes*. 11.

Gutierrez, G. M., Conte, C., & Lightbourne, K. (2014). The Relationship between Impact Force, Neck Strength, and Neurocognitive Performance in Soccer Heading in Adolescent Females. *Pediatric Exercise Science*, 26(1), 33–40. <https://doi.org/10.1123/pes.2013-0102>

Hanlon, E., & Bir, C. (2010). Validation of a Wireless Head Acceleration Measurement System for Use in Soccer Play. *Journal of Applied Biomechanics*, 26(4), 424–431. <https://doi.org/10.1123/jab.26.4.424>

- Hanlon, E. M., & Bir, C. A. (2012). Real-Time Head Acceleration Measurement in Girls' Youth Soccer: *Medicine & Science in Sports & Exercise*, 44(6), 1102–1108.
<https://doi.org/10.1249/MSS.0b013e3182444d7d>
- Harmon, K. G., Clugston, J. R., Dec, K., Hainline, B., Herring, S. A., Kane, S., ... Roberts, W. O. (2019). American Medical Society for Sports Medicine Position Statement on Concussion in Sport: *Clinical Journal of Sport Medicine*, 29(2), 87–100. <https://doi.org/10.1097/JSM.0000000000000720>
- Harriss, A., Johnson, A. M., Walton, D. M., & Dickey, J. P. (2019a). Head impact magnitudes that occur from purposeful soccer heading depend on the game scenario and head impact location. *Musculoskeletal Science and Practice*, 40, 53–57. <https://doi.org/10.1016/j.msksp.2019.01.009>
- Harriss, A., Johnson, A. M., Walton, D. M., & Dickey, J. P. (2019b). The number of purposeful headers female youth soccer players experience during games depends on player age but not player position. *Science and Medicine in Football*, 3(2), 109–114. <https://doi.org/10.1080/24733938.2018.1506591>
- Harriss, A., Walton, D. M., & Dickey, J. P. (2018). Direct player observation is needed to accurately quantify heading frequency in youth soccer. *Research in Sports Medicine*, 26(2), 191–198. <https://doi.org/10.1080/15438627.2018.1431534>
- Hinkley, L. B. N., Marco, E. J., Findlay, A. M., Honma, S., Jeremy, R. J., Strominger, Z., ... Sherr, E. H. (2012). The Role of Corpus Callosum Development in Functional

Connectivity and Cognitive Processing. *PLoS ONE*, 7(8), e39804.

<https://doi.org/10.1371/journal.pone.0039804>

Hootman, J. M., Dick, R., & Agel, J. (2007). *Epidemiology of Collegiate Injuries for 15 Sports: Summary and Recommendations for Injury Prevention Initiatives*. 9.

Houck, Z., Asken, B., Bauer, R., Pothast, J., Michaudet, C., & Clugston, J. (2016).

Epidemiology of Sport-Related Concussion in an NCAA Division I Football Bowl Subdivision Sample. *The American Journal of Sports Medicine*, 44(9), 2269–2275. <https://doi.org/10.1177/0363546516645070>

Iwasaki, N., Hamano, K., Okada, Y., Horigome, Y., Nakayama, J., Takeya, T., ... Nose, T. (1997). Volumetric quantification of brain development using MRI.

Neuroradiology, 39(12), 841–846. <https://doi.org/10.1007/s002340050517>

Jiang, B., Cao, L., Mao, H., Wagner, C., Marek, S., & Yang, K. H. (2014). Development of a 10-year-old paediatric thorax finite element model validated against cardiopulmonary resuscitation data. *Computer Methods in Biomechanics and Biomedical Engineering*, 17(11), 1185–1197.

<https://doi.org/10.1080/10255842.2012.739164>

Jin, X., Feng, Z., Mika, V., Li, H., Viano, D. C., & Yang, K. H. (2017). The Role of Neck Muscle Activities on the Risk of Mild Traumatic Brain Injury in American Football. *Journal of Biomechanical Engineering*, 139(10), 101002.

<https://doi.org/10.1115/1.4037399>

Kiernan, J., & Rajakumar, R. (2013). *Barr's The Human Nervous System: An Anatomical Viewpoint* (10th ed.).

King, A. I., Yang, K. H., Zhang, L., Hardy, W., & Viano, D. C. (2003). *0.1 Is Head Injury Caused by Linear or Angular Acceleration?* 12.

Kleiven, S. (2007, October 29). *Predictors for Traumatic Brain Injuries Evaluated through Accident Reconstructions*. 2007-22-0003. <https://doi.org/10.4271/2007-22-0003>

Kumar, R., Saksena, S., Husain, M., Srivastava, A., Rathore, R. K. S., Agarwal, S., & Gupta, R. K. (2010). Serial Changes in Diffusion Tensor Imaging Metrics of Corpus Callosum in Moderate Traumatic Brain Injury Patients and Their Correlation With Neuropsychometric Tests: A 2-Year Follow-up Study. *JOURNAL OF HEAD TRAUMA REHABILITATION*, 12.

Le Bihan, D. (2003). Looking into the functional architecture of the brain with diffusion MRI. *Nature Reviews Neuroscience*, 4(6), 469–480. <https://doi.org/10.1038/nrn1119>

Lebel, C., & Beaulieu, C. (2011). Longitudinal Development of Human Brain Wiring Continues from Childhood into Adulthood. *Journal of Neuroscience*, 31(30), 10937–10947. <https://doi.org/10.1523/JNEUROSCI.5302-10.2011>

Lebel, C., Walker, L., Leemans, A., Phillips, L., & Beaulieu, C. (2008). Microstructural maturation of the human brain from childhood to adulthood. *NeuroImage*, 40(3), 1044–1055. <https://doi.org/10.1016/j.neuroimage.2007.12.053>

- Lenroot, R. K., & Giedd, J. N. (2006). Brain development in children and adolescents: Insights from anatomical magnetic resonance imaging. *Neuroscience & Biobehavioral Reviews*, *30*(6), 718–729.
<https://doi.org/10.1016/j.neubiorev.2006.06.001>
- Ling, H., Morris, H. R., Neal, J. W., Lees, A. J., Hardy, J., Holton, J. L., ... Williams, D. D. R. (2017). Mixed pathologies including chronic traumatic encephalopathy account for dementia in retired association football (soccer) players. *Acta Neuropathologica*, *133*(3), 337–352. <https://doi.org/10.1007/s00401-017-1680-3>
- Luders, E., Thompson, P. M., & Toga, A. W. (2010). The Development of the Corpus Callosum in the Healthy Human Brain. *Journal of Neuroscience*, *30*(33), 10985–10990. <https://doi.org/10.1523/JNEUROSCI.5122-09.2010>
- Mao, H., Gao, H., Cao, L., Genthikatti, V. V., & Yang, K. H. (2013). Development of high-quality hexahedral human brain meshes using feature-based multi-block approach. *Computer Methods in Biomechanics and Biomedical Engineering*, *16*(3), 271–279. <https://doi.org/10.1080/10255842.2011.617005>
- McAllister, T. W., Ford, J. C., Ji, S., Beckwith, J. G., Flashman, L. A., Paulsen, K., & Greenwald, R. M. (2012). Maximum Principal Strain and Strain Rate Associated with Concussion Diagnosis Correlates with Changes in Corpus Callosum White Matter Indices. *Annals of Biomedical Engineering*, *40*(1), 127–140.
<https://doi.org/10.1007/s10439-011-0402-6>

- McCrory, P., Meeuwisse, W., Dvorak, J., Aubry, M., Bailes, J., Broglio, S., ... Vos, P. E. (2017). Consensus statement on concussion in sport—The 5th international conference on concussion in sport held in Berlin, October 2016. *British Journal of Sports Medicine*, bjsports-2017-097699. <https://doi.org/10.1136/bjsports-2017-097699>
- McCuen, E., Svaldi, D., Breedlove, K., Kraz, N., Cummiskey, B., Breedlove, E. L., ... Nauman, E. A. (2015). Collegiate women's soccer players suffer greater cumulative head impacts than their high school counterparts. *Journal of Biomechanics*, 48(13), 3720–3723. <https://doi.org/10.1016/j.jbiomech.2015.08.003>
- Miller, L. E., Pinkerton, E. K., Fabian, K. C., Wu, L. C., Espeland, M. A., Lamond, L. C., ... Urban, J. E. (2019). Characterizing head impact exposure in youth female soccer with a custom-instrumented mouthpiece. *Research in Sports Medicine*, 1–17. <https://doi.org/10.1080/15438627.2019.1590833>
- Miller, L. E., Urban, J. E., Kelley, M. E., Powers, A. K., Whitlow, C. T., Maldjian, J. A., ... Stitzel, J. D. (2019). Evaluation of Brain Response during Head Impact in Youth Athletes Using an Anatomically Accurate Finite Element Model. *Journal of Neurotrauma*, 36(10), 1561–1570. <https://doi.org/10.1089/neu.2018.6037>
- Mukaka, M. M. (2013). *Statistics Corner: A guide to appropriate use of Correlation coefficient in medical research*. 3.

- Munivenkatappa, A., Devi, B. I., Shukla, D. P., & Rajeswaran, J. (2016). Role of the thalamus in natural recovery of cognitive impairment in patients with mild traumatic brain injury. *Brain Injury, 30*(4), 388–392.
<https://doi.org/10.3109/02699052.2015.1089599>
- Ostby, Y., Tamnes, C. K., Fjell, A. M., Westlye, L. T., Due-Tonnessen, P., & Walhovd, K. B. (2009). Heterogeneity in Subcortical Brain Development: A Structural Magnetic Resonance Imaging Study of Brain Maturation from 8 to 30 Years. *Journal of Neuroscience, 29*(38), 11772–11782.
<https://doi.org/10.1523/JNEUROSCI.1242-09.2009>
- Patton, D. A., McIntosh, A. S., & Kleiven, S. (2013). The Biomechanical Determinants of Concussion: Finite Element Simulations to Investigate Brain Tissue Deformations During Sporting Impacts to the Unprotected Head. *Journal of Applied Biomechanics, 29*(6), 721–730. <https://doi.org/10.1123/jab.29.6.721>
- Patton, D. A., McIntosh, A. S., & Kleiven, S. (2015). The Biomechanical Determinants of Concussion: Finite Element Simulations to Investigate Tissue-Level Predictors of Injury During Sporting Impacts to the Unprotected Head. *Journal of Applied Biomechanics, 31*(4), 264–268. <https://doi.org/10.1123/jab.2014-0223>
- Prel, J.-B. du, Hommel, G., Röhrig, B., & Blettner, M. (2009). Confidence Interval or P-Value? Part 4 of a Series on Evaluation of Scientific Publications. *Deutsches Arzteblatt Online*. <https://doi.org/10.3238/arztebl.2009.0335>

- Press, J. N., & Rowson, S. (2017). Quantifying Head Impact Exposure in Collegiate Women's Soccer. *Clin J Sport Med*, 27(2), 7.
- Rodrigues, A. C., Lasmar, R. P., & Caramelli, P. (2016). Effects of Soccer Heading on Brain Structure and Function. *Frontiers in Neurology*, 7.
<https://doi.org/10.3389/fneur.2016.00038>
- Roth, S., Raul, J.-S., & Willinger, R. (2008). Biofidelic child head FE model to simulate real world trauma. *Computer Methods and Programs in Biomedicine*, 90(3), 262–274. <https://doi.org/10.1016/j.cmpb.2008.01.007>
- Rowson, S., Bland, M. L., Campolettano, E. T., Press, J. N., Rowson, B., Smith, J. A., ... Duma, S. M. (2016). Biomechanical Perspectives on Concussion in Sport: *Sports Medicine and Arthroscopy Review*, 24(3), 100–107.
<https://doi.org/10.1097/JSA.0000000000000121>
- Rowson, S., & Duma, S. M. (2013). Brain Injury Prediction: Assessing the Combined Probability of Concussion Using Linear and Rotational Head Acceleration. *Annals of Biomedical Engineering*, 41(5), 873–882.
<https://doi.org/10.1007/s10439-012-0731-0>
- Schmidt, J., Hayward, K. S., Brown, K. E., Zwicker, J. G., Ponsford, J., van Donkelaar, P., ... Boyd, L. A. (2018). Imaging in Pediatric Concussion: A Systematic Review. *Pediatrics*, 141(5), e20173406. <https://doi.org/10.1542/peds.2017-3406>
- Schultz, V., Stern, R. A., Tripodis, Y., Stamm, J., Wrobel, P., Lepage, C., ... Koerte, I. K. (2018). Age at First Exposure to Repetitive Head Impacts Is Associated with

- Smaller Thalamic Volumes in Former Professional American Football Players. *Journal of Neurotrauma*, 35(2), 278–285. <https://doi.org/10.1089/neu.2017.5145>
- Sidaros, A., Engberg, A. W., Sidaros, K., Liptrot, M. G., Herring, M., Petersen, P., ... Rostrup, E. (2008). Diffusion tensor imaging during recovery from severe traumatic brain injury and relation to clinical outcome: A longitudinal study. *Brain*, 131(2), 559–572. <https://doi.org/10.1093/brain/awm294>
- Stewart, W. F., Kim, N., Ifrah, C. S., Lipton, R. B., Bachrach, T. A., Zimmerman, M. E., ... Lipton, M. L. (2017). Symptoms from repeated intentional and unintentional head impact in soccer players. *Neurology*, 88(9), 901–908. <https://doi.org/10.1212/WNL.0000000000003657>
- Stewart, W. F., Kim, N., Ifrah, C., Sliwinski, M., Zimmerman, M. E., Kim, M., ... Lipton, M. L. (2018). Heading Frequency Is More Strongly Related to Cognitive Performance Than Unintentional Head Impacts in Amateur Soccer Players. *Frontiers in Neurology*, 9, 240. <https://doi.org/10.3389/fneur.2018.00240>
- Stiles, J., & Jernigan, T. L. (2010). The Basics of Brain Development. *Neuropsychology Review*, 20(4), 327–348. <https://doi.org/10.1007/s11065-010-9148-4>
- Takhounts, E. G., Craig, M. J., Moorhouse, K., McFadden, J., & Hasija, V. (2013, November 11). *Development of Brain Injury Criteria (BrIC)*. 2013-22–0010. <https://doi.org/10.4271/2013-22-0010>
- Tang, L., Ge, Y., Sodickson, D. K., Miles, L., Zhou, Y., Reaume, J., & Grossman, R. I. (2011). Thalamic Resting-State Functional Networks: Disruption in Patients with

Mild Traumatic Brain Injury. *Radiology*, 260(3), 831–840.

<https://doi.org/10.1148/radiol.11110014>

Van Beek, L., Ghesquière, P., Lagae, L., & De Smedt, B. (2015). Mathematical Difficulties and White Matter Abnormalities in Subacute Pediatric Mild Traumatic Brain Injury. *Journal of Neurotrauma*, 32(20), 1567–1578.

<https://doi.org/10.1089/neu.2014.3809>

van der Knaap, L. J., & van der Ham, I. J. M. (2011). How does the corpus callosum mediate interhemispheric transfer? A review. *Behavioural Brain Research*, 223(1), 211–221. <https://doi.org/10.1016/j.bbr.2011.04.018>

Virji-Babul, N., Borich, M. R., Makan, N., Moore, T., Frew, K., Emery, C. A., & Boyd, L. A. (2013). Diffusion Tensor Imaging of Sports-Related Concussion in Adolescents. *Pediatric Neurology*, 48(1), 24–29.

<https://doi.org/10.1016/j.pediatrneurol.2012.09.005>

Wasserman, E. B., Kerr, Z. Y., Zuckerman, S. L., & Covassin, T. (2016). Epidemiology of Sports-Related Concussions in National Collegiate Athletic Association Athletes From 2009-2010 to 2013-2014: Symptom Prevalence, Symptom Resolution Time, and Return-to-Play Time. *The American Journal of Sports Medicine*, 44(1), 226–233. <https://doi.org/10.1177/0363546515610537>

Wilde, E. A., McCauley, S. R., Hunter, J. V., Bigler, E. D., Chu, Z., Wang, Z. J., ...

Levin, H. S. (2008). Diffusion tensor imaging of acute mild traumatic brain injury

in adolescents. *Neurology*, 70(12), 948–955.

<https://doi.org/10.1212/01.wnl.0000305961.68029.54>

Zhang, L., Yang, K. H., & King, A. I. (2004). A Proposed Injury Threshold for Mild Traumatic Brain Injury. *Journal of Biomechanical Engineering*, 126(2), 226.

<https://doi.org/10.1115/1.1691446>

Zuckerman, S. L., Kerr, Z. Y., Yengo-Kahn, A., Wasserman, E., Covassin, T., & Solomon, G. S. (2015). Epidemiology of Sports-Related Concussion in NCAA Athletes From 2009-2010 to 2013-2014: Incidence, Recurrence, and Mechanisms. *The American Journal of Sports Medicine*, 43(11), 2654–2662.

<https://doi.org/10.1177/0363546515599634>

Appendices

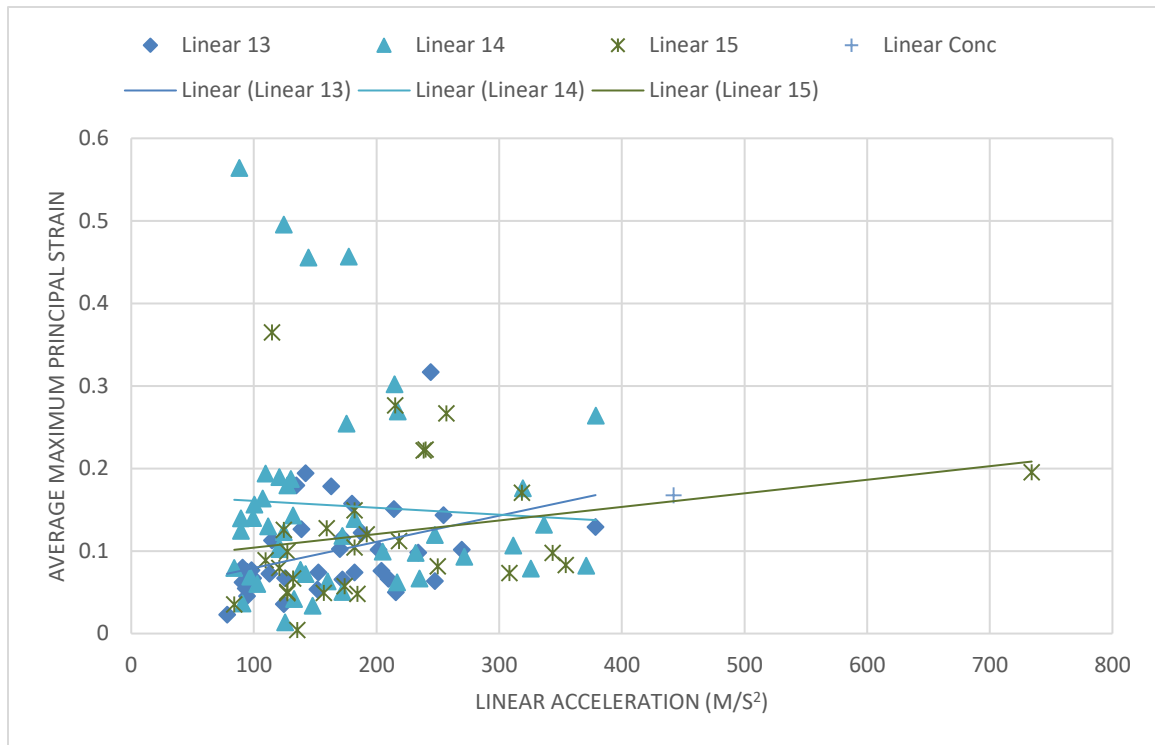
Appendix A

	<i>Practice</i>	<i>Header 1</i>	<i>Header 2</i>	<i>Header 3</i>	<i>Header 4</i>	<i>Header 5</i>
<i>Header</i>	Drill	Goal Kick	Pass Air	Throw	Goal Kick	Throw
<i>Linear (g)</i>	45.07	17.88	12.69	12.79	12.69	10.25
<i>Angular (°/s)</i>	1375	1364	2899	84	1273	660
<i>LCCG</i>	0.168	0.255	0.496	0.014		
<i>RCCG</i>	0.110	0.219	0.390	0.015		
<i>LCCS</i>	0.125	0.180	0.384	0.004		
<i>RCCS</i>	0.186	0.189	0.407	0.005		
<i>LTP</i>	0.079	0.153	0.314	0.006		
<i>RTP</i>	0.162	0.181	0.327	0.007		
<i>LTA</i>	0.082	0.121	0.294	0.006		
<i>RTA</i>	0.066	0.173	0.313	0.005		
<i>LBS</i>	0.095	0.097	0.205	0.006		
<i>RBS</i>	0.103	0.082	0.302	0.007		

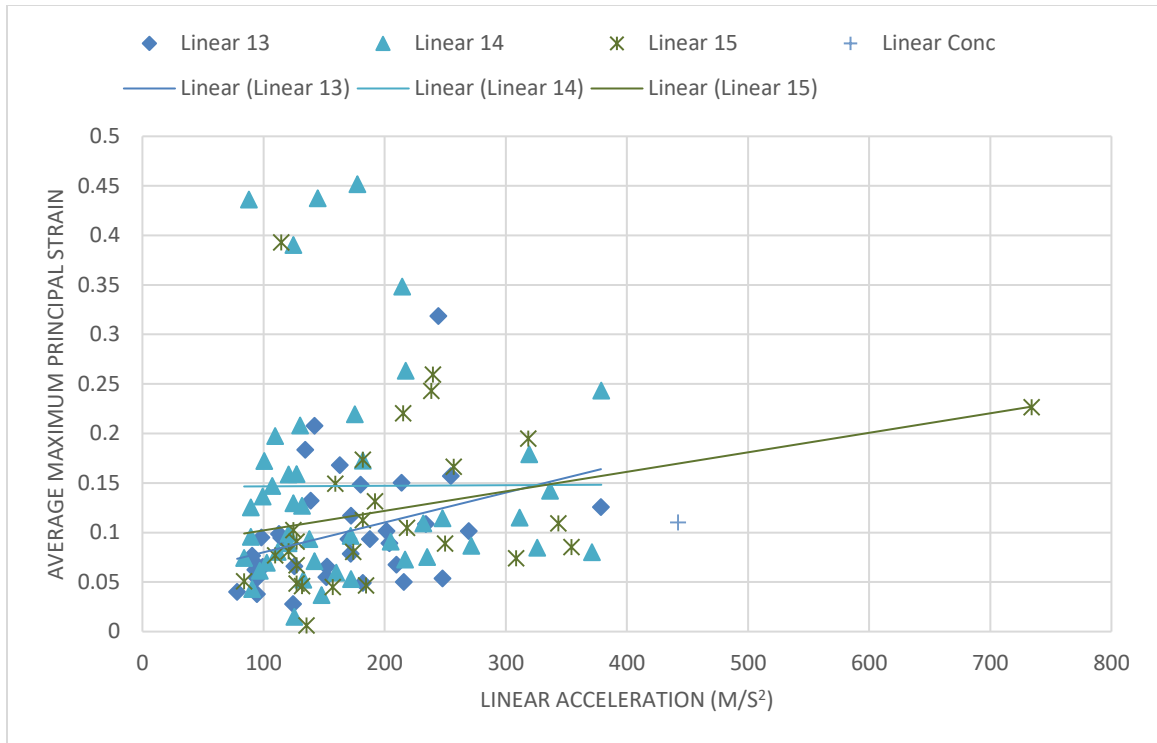
CCG –Genu of Corpus Callosum, CCS – Splenium of Corpus Callosum

TP – Thalamus Posterior, TA – Thalamus Anterior, BS – Brain Stem,

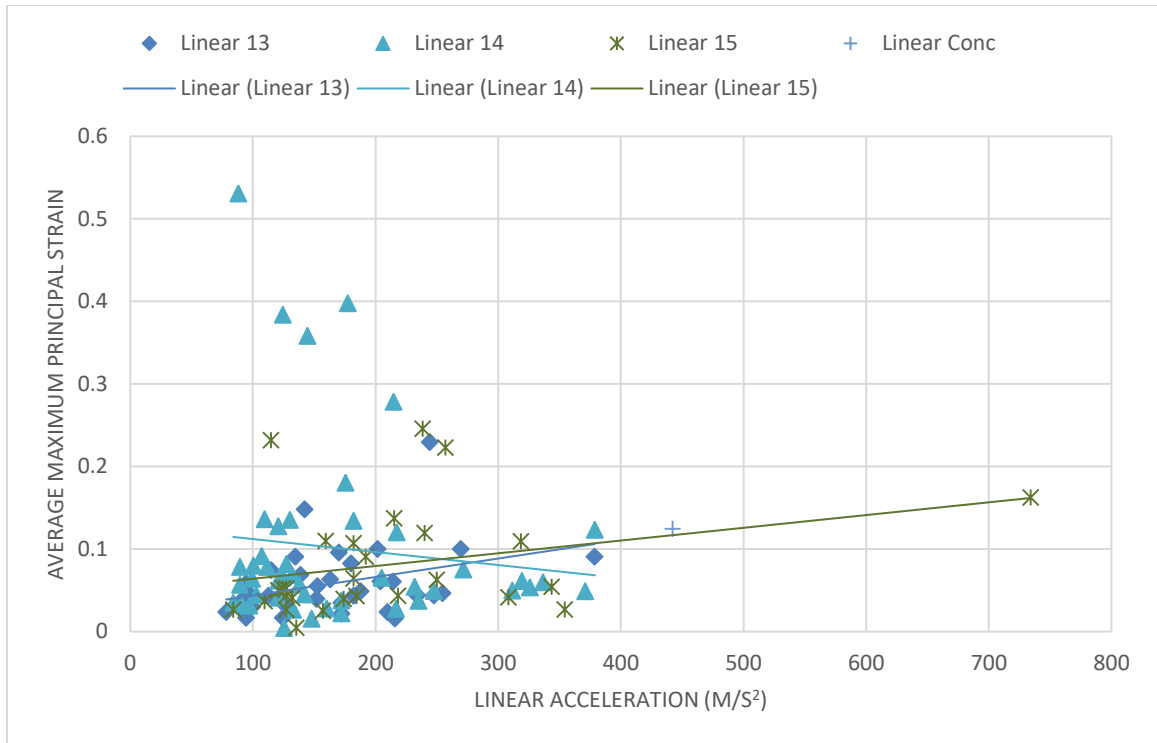
Appendix B



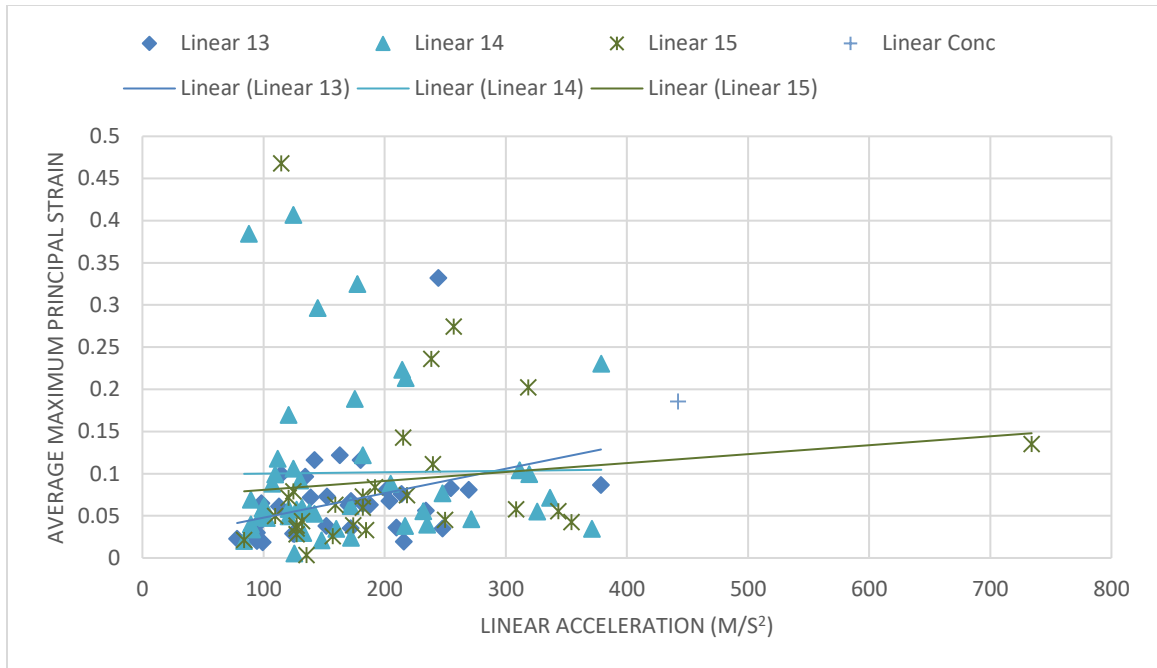
Age differentiated relationship between the peak linear acceleration and resulting APMPS in the genu of the CC on the left side.



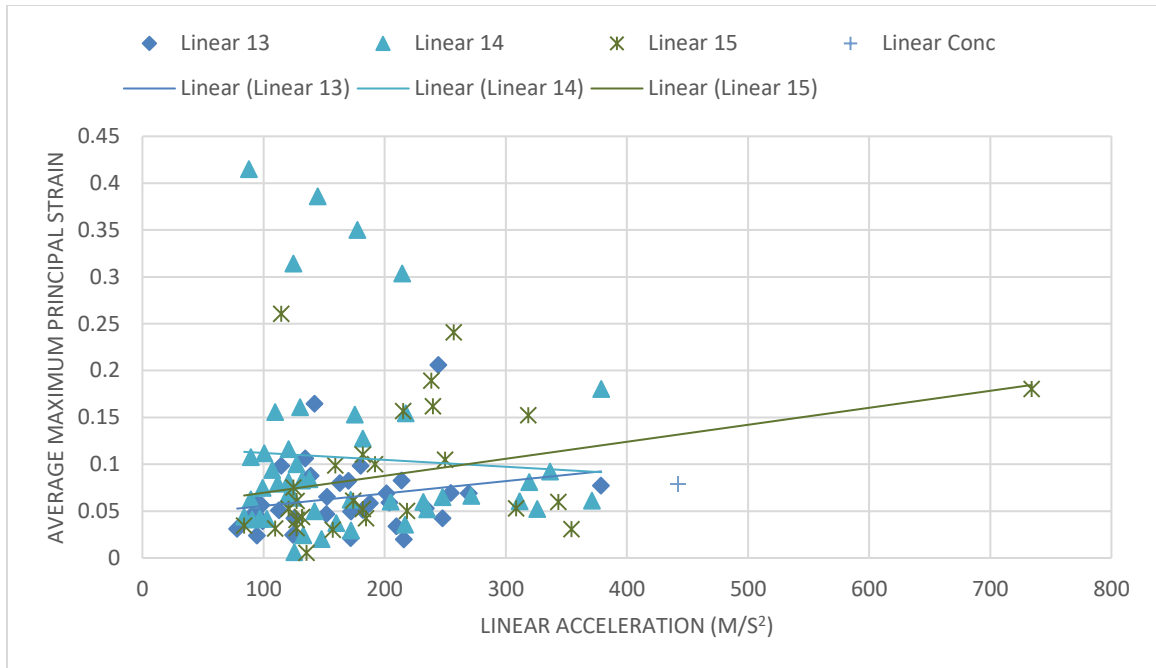
Age differentiated relationship between the peak linear acceleration and resulting APMPS in the genu of the CC on the right side.



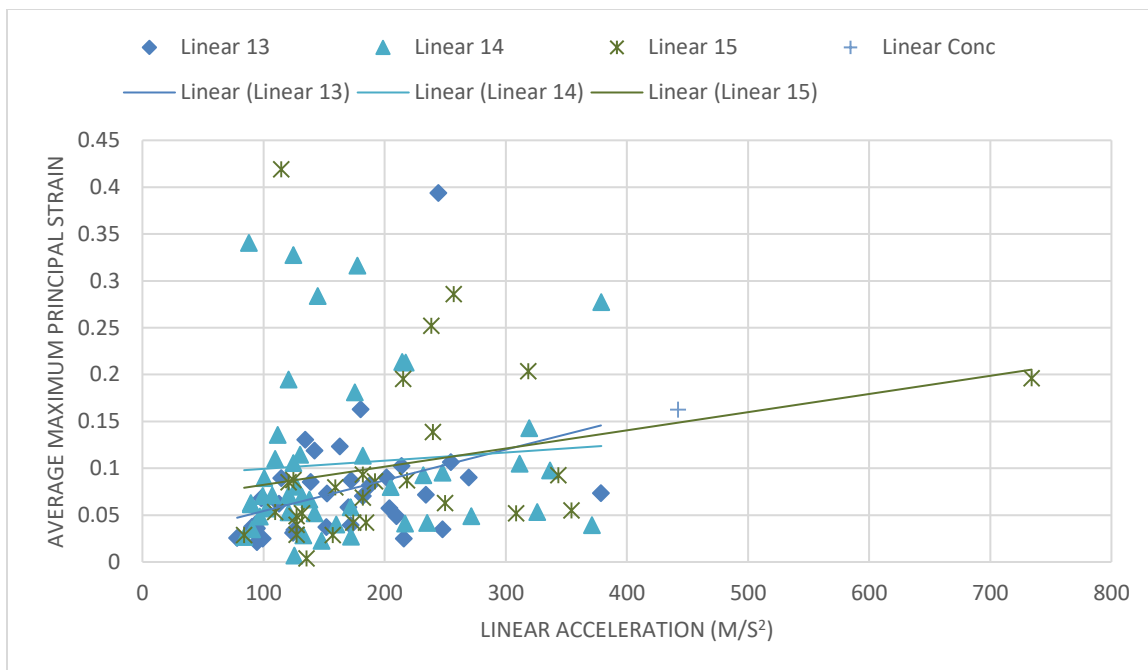
Age differentiated relationship between the peak linear acceleration and resulting APMPS in the splenium of the CC on the left side.



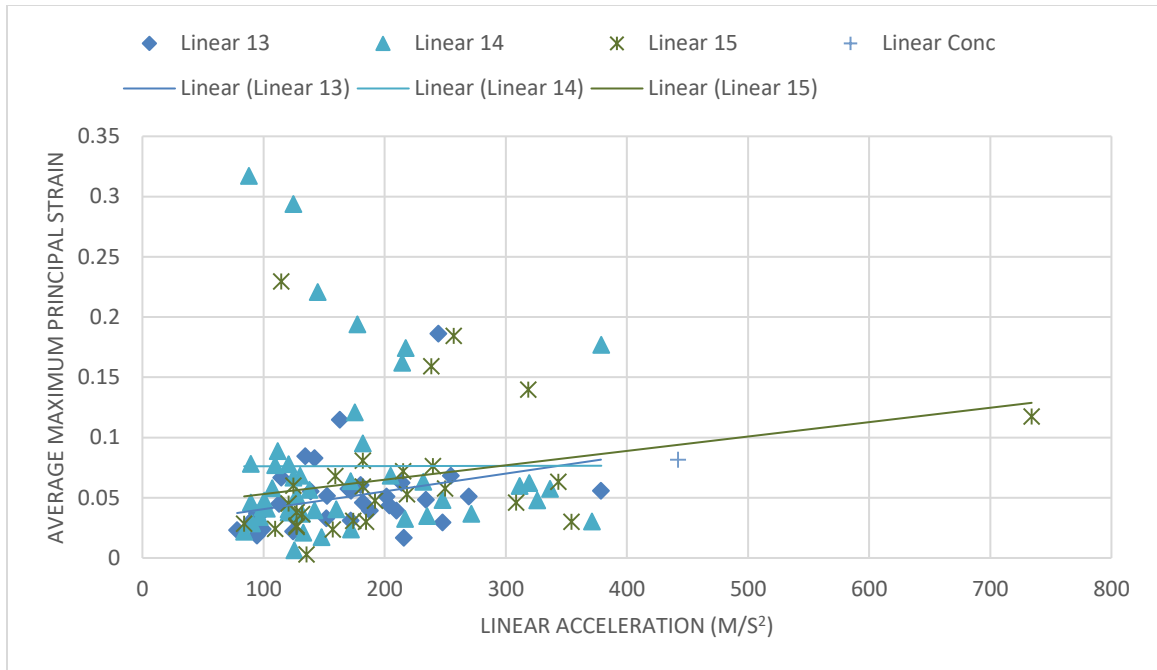
Age differentiated relationship between the peak linear acceleration and resulting APMPS in the splenium of the CC on the right side.



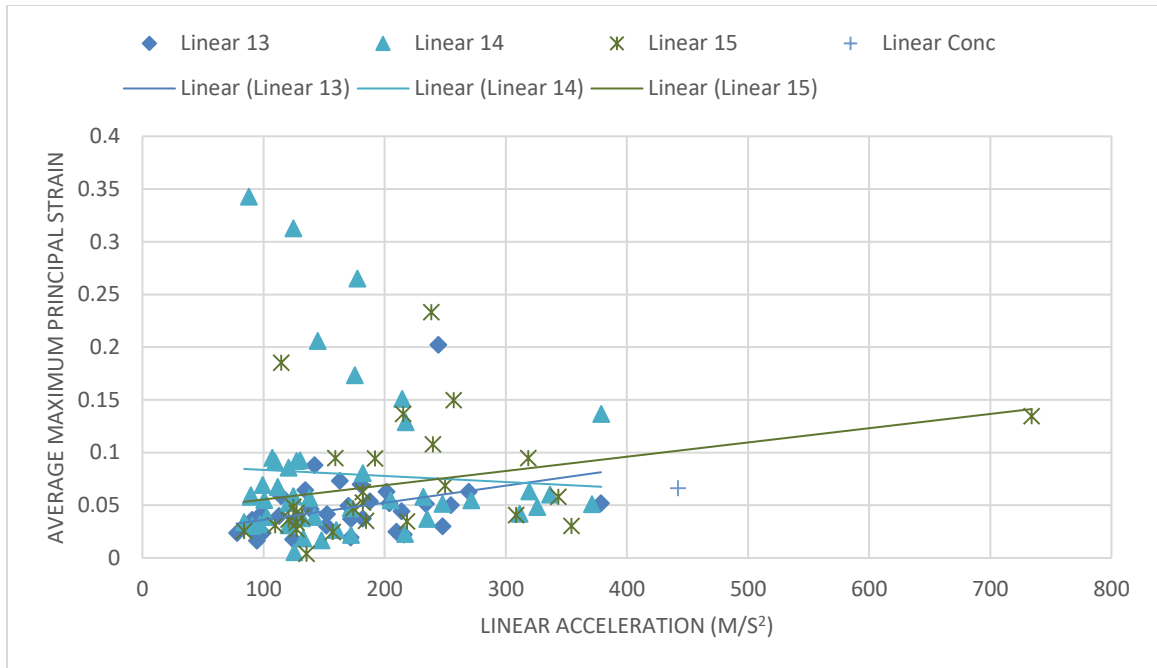
Age differentiated relationship between the peak linear acceleration and resulting APMPS in the posterior thalamus on the left side.



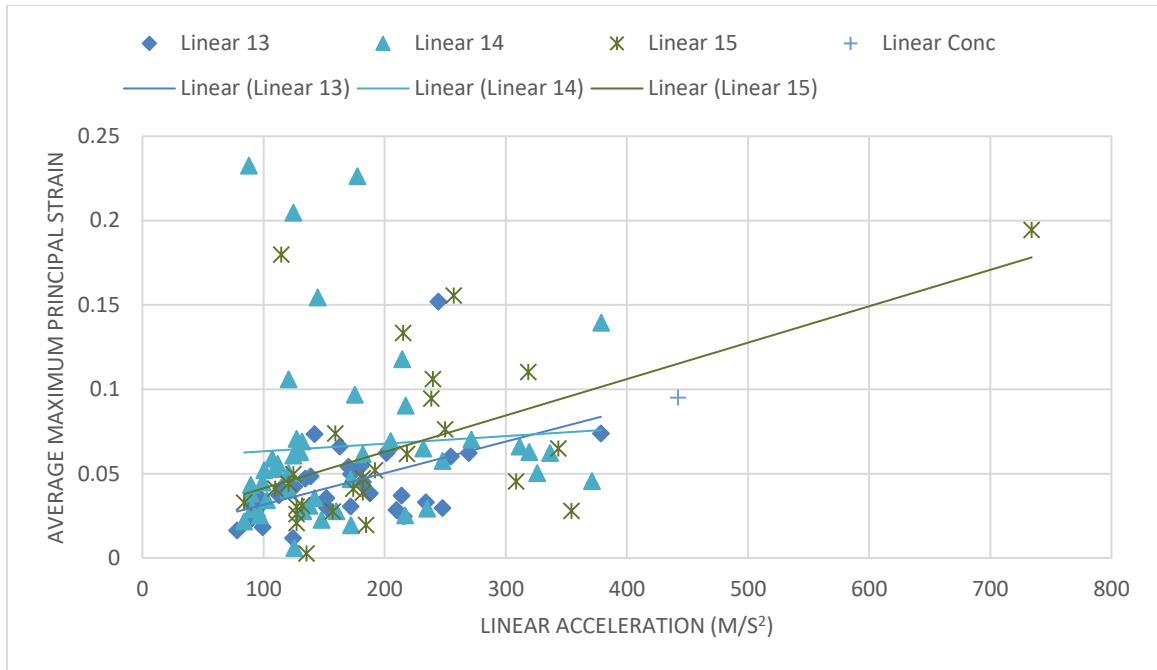
Age differentiated relationship between the peak linear acceleration and resulting APMPS in the posterior thalamus on the right side.



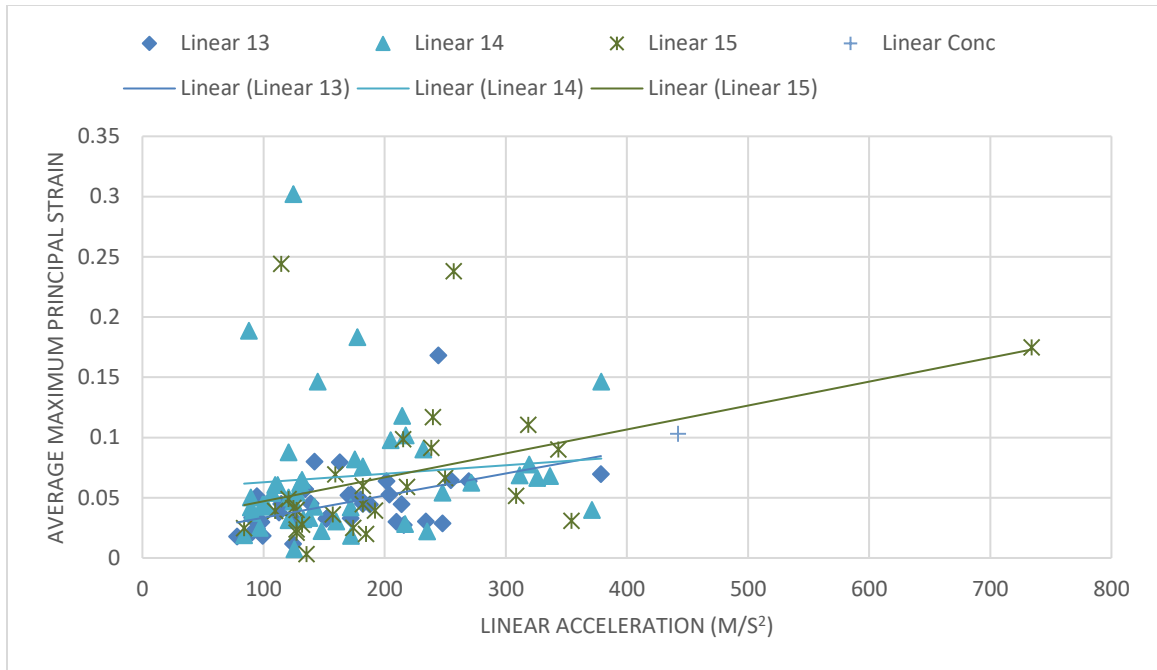
Age differentiated relationship between the peak linear acceleration and resulting APMPS in the anterior thalamus on the left side.



Age differentiated relationship between the peak linear acceleration and resulting APMPS in the anterior thalamus on the right side.

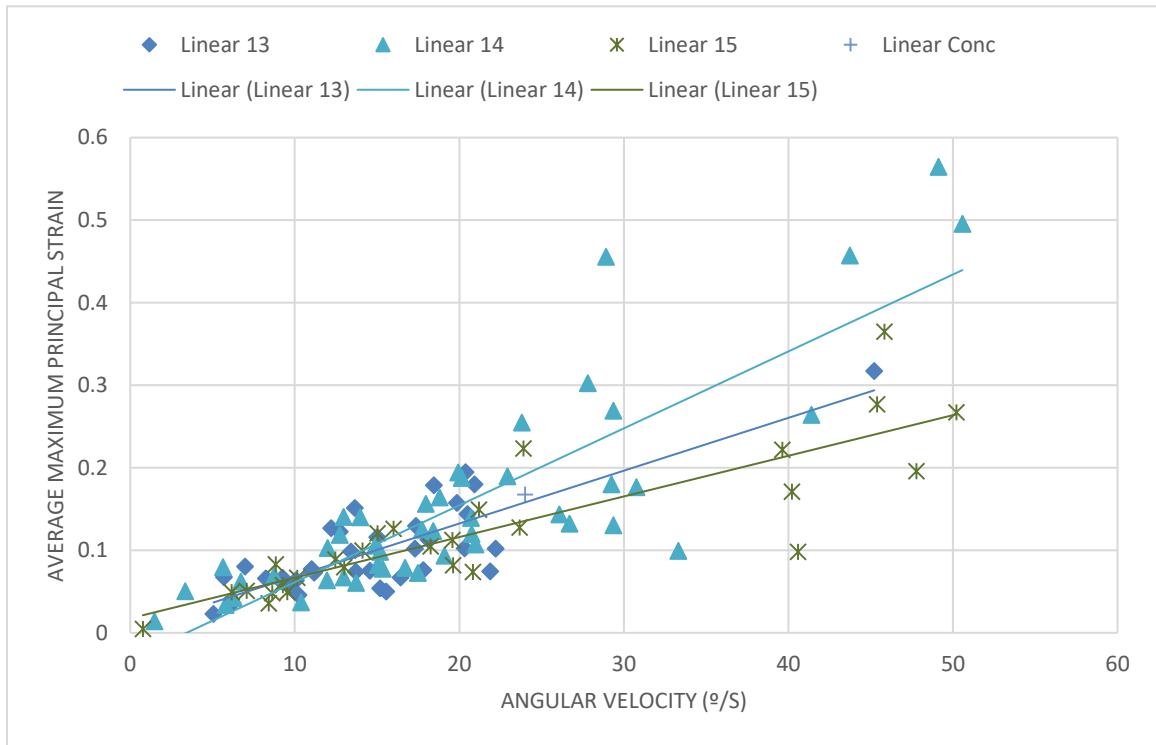


Age differentiated relationship between the peak linear acceleration and resulting APMPS in the lateral posterior brain stem on the left side.

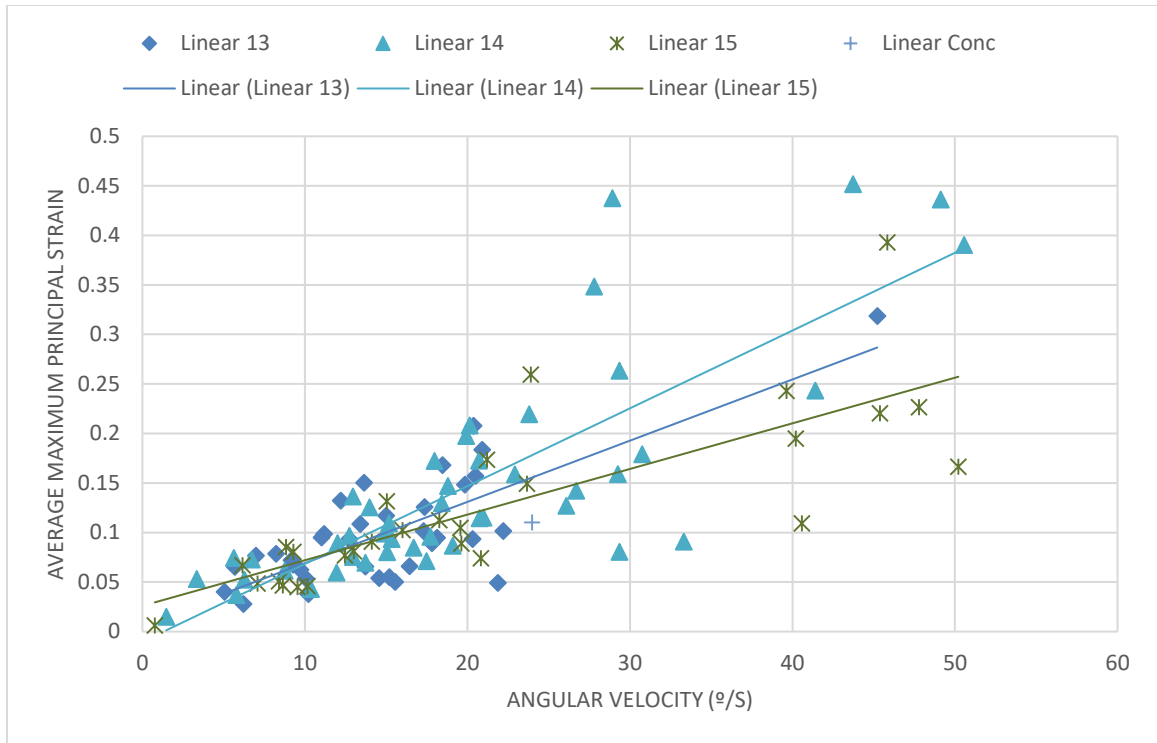


Age differentiated relationship between the peak linear acceleration and resulting APMPS in the lateral posterior brain stem on the right side.

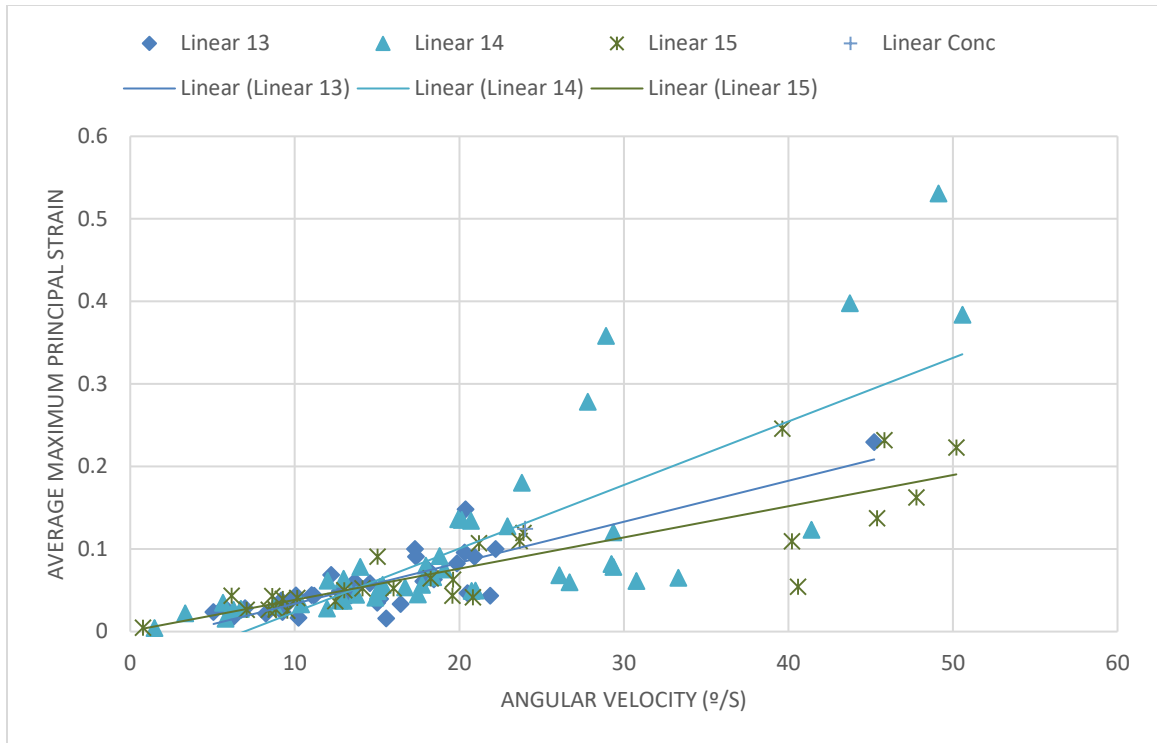
Appendix C



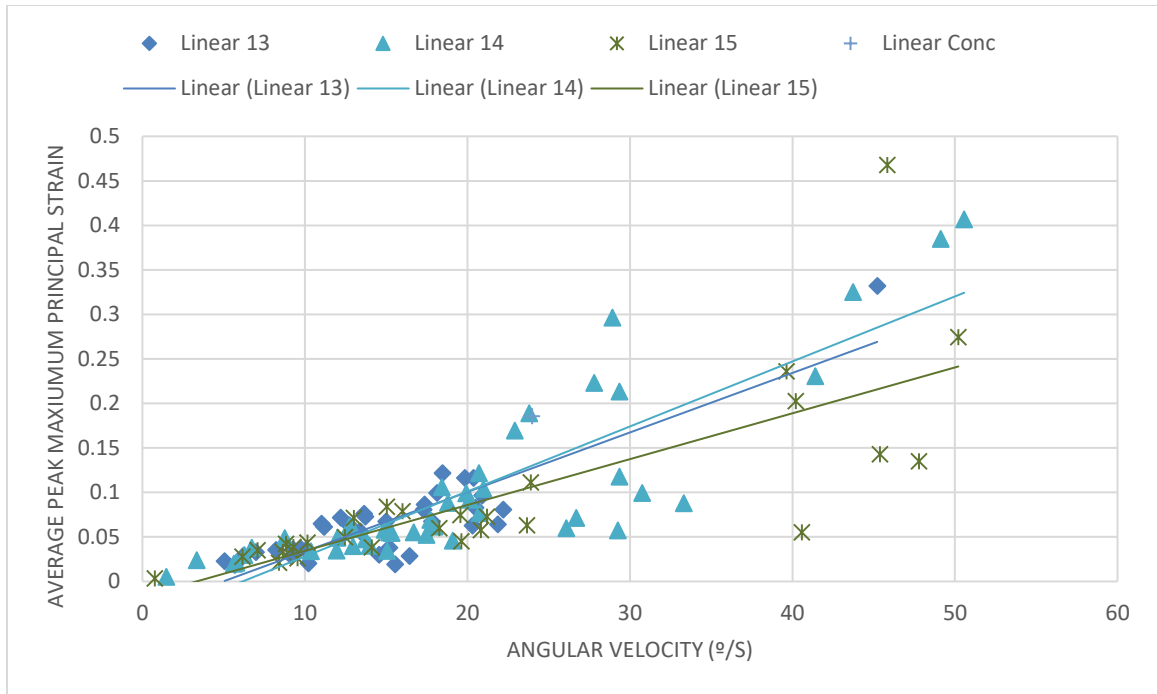
Age differentiated relationship between the peak angular velocity and resulting APMPS in the genu of the CC on the left side.



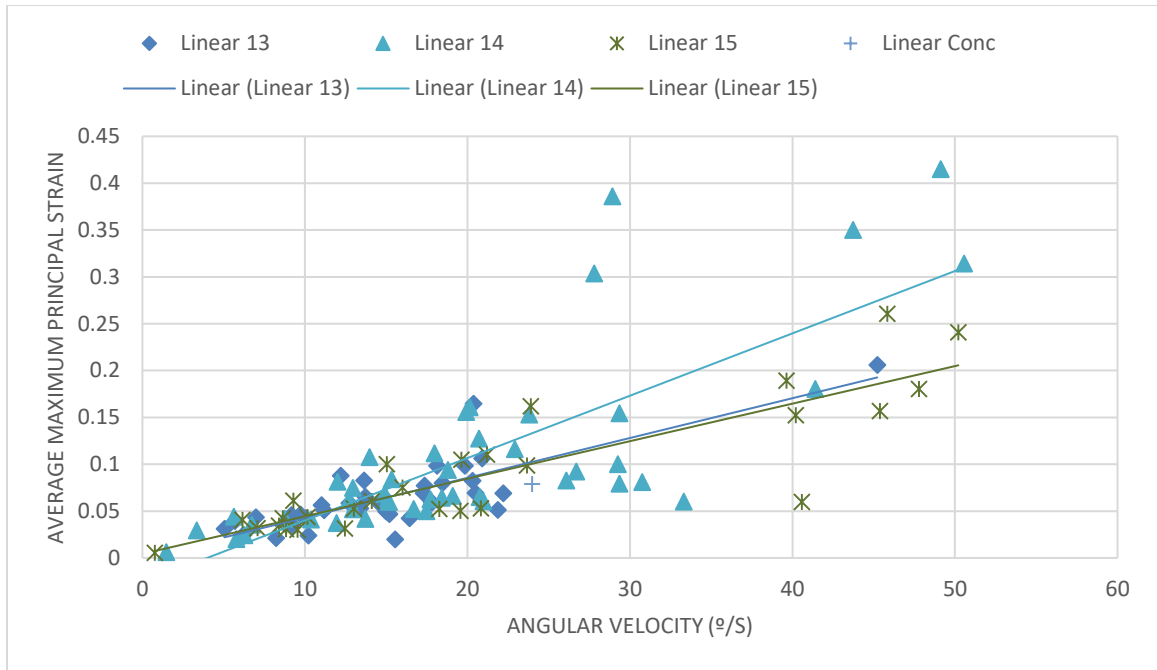
Age differentiated relationship between the peak angular velocity and resulting APMPS in the genu of the CC on the right side.



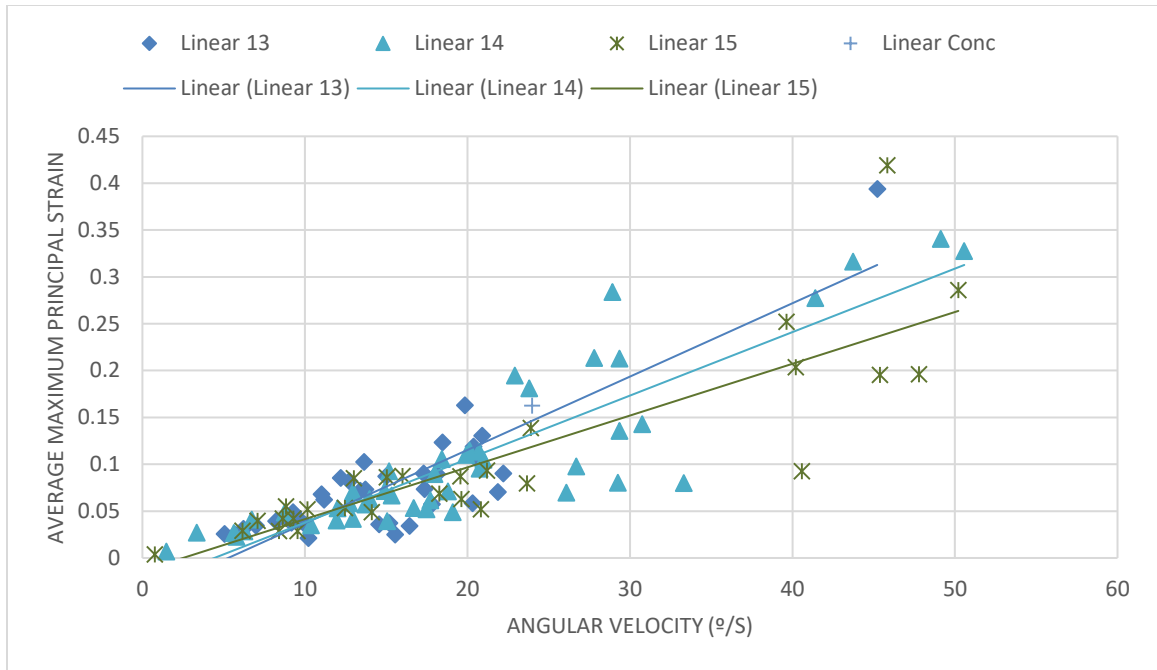
Age differentiated relationship between the peak angular velocity and resulting APMPS in the splenium of the CC on the left side.



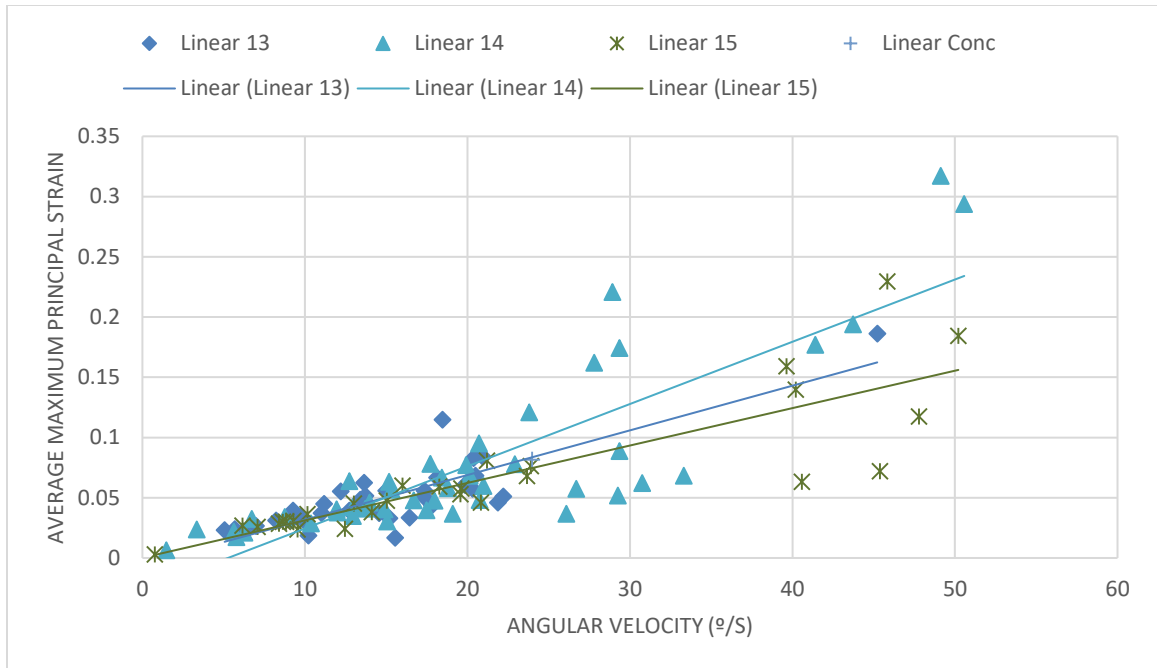
Age differentiated relationship between the peak angular velocity and resulting APMPS in the splenium of the CC on the right side.



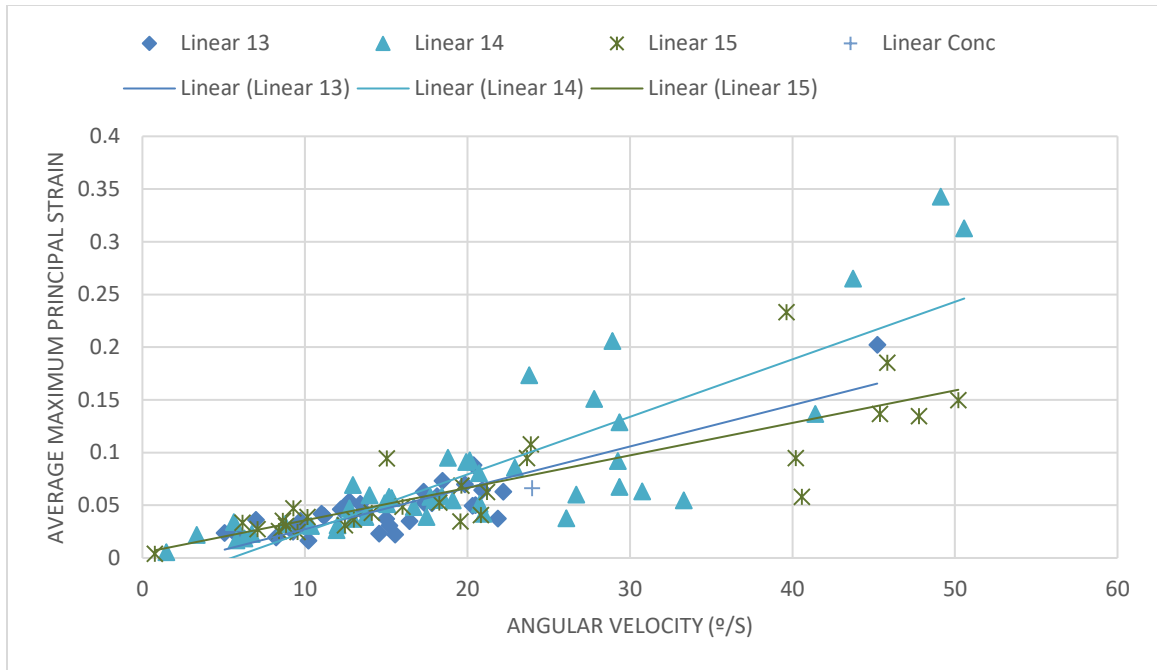
Age differentiated relationship between the peak angular velocity and resulting APMPS in the posterior thalamus on the left side.



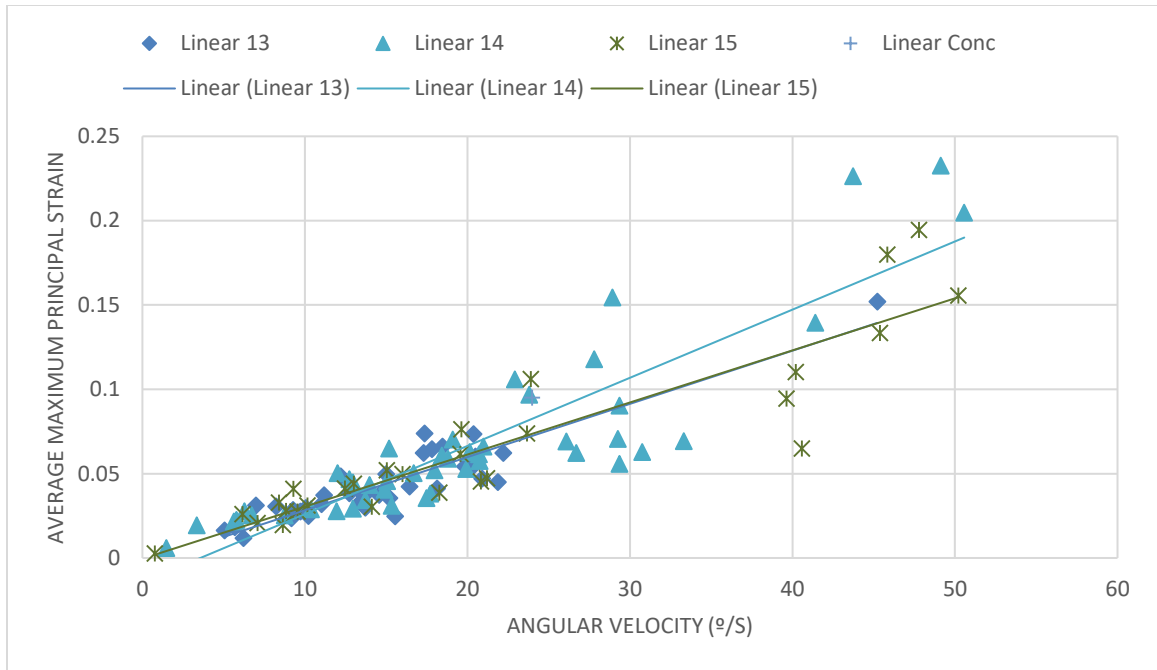
Age differentiated relationship between the peak angular velocity and resulting APMPS in the posterior thalamus on the right side.



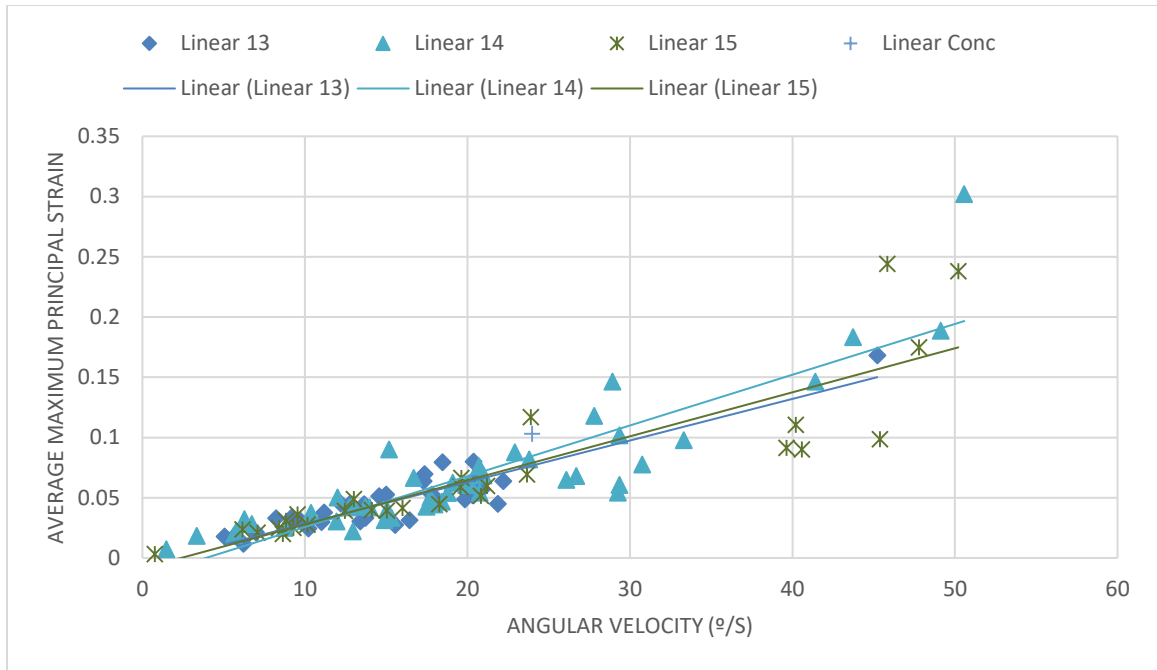
Age differentiated relationship between the peak angular velocity and resulting APMPS in the anterior thalamus on the left side.



Age differentiated relationship between the peak angular velocity and resulting APMPS in the anterior thalamus on the left side.



Age differentiated relationship between the peak angular velocity and resulting APMPS in the lateral posterior brain stem on the left side.



Age differentiated relationship between the peak angular velocity and resulting APMPS in the lateral posterior brain stem on the left side.

Appendix D

Number of purposeful headers simulated in this thesis differentiated by game scenario and age.

	<i>Corner</i>	<i>Deflection</i>	<i>Drop Kick</i>	<i>Goal Kick</i>	<i>Pass Air</i>	<i>Shot Free</i>	<i>Throw</i>	<i>Total</i>
<i>13</i>	0	5	3	0	16	1	10	35
<i>14</i>	0	3	3	2	22	1	16	47
<i>15</i>	3	2	1	0	9	0	13	28
<i>Total</i>	3	10	7	2	47	2	39	110

Curriculum Vitae

Name: Wayne Allison

Post-secondary Education and Degrees: University of Guelph
Guelph, Ontario, Canada
2011-2017 B.Sc.

The University of Western Ontario
London, Ontario, Canada
2017-2019 M.Sc.

Honours and Awards: Western Graduate Research Scholarship
2017-2018, 2018-2019

Related Work Experience Graduate Teaching Assistant
The University of Western Ontario
2017 - 2018

KINESIOL 3341A - Fall 2018
ANATCELL 2221 - Winter 2018, Winter 2019